

FINISHING OF SILICON NITRIDE (Si_3N_4) BALLS
FOR ADVANCED BEARING APPLICATIONS BY
LARGE BATCH MAGNETIC FLOAT POLISHING
(MFP) APPARATUS

By

TEJAS S. KIRTANE

Bachelor of Engineering

Vishwakarma Institute of Technology

University of Pune

Pune, India

1997

Submitted to the Faculty of the
Graduate College of the
Oklahoma State University
in partial fulfillment of
the requirements for
the Degree of
MASTER OF SCIENCE
December, 2004

FINISHING OF SILICON NITRIDE (Si_3N_4) BALLS
FOR ADVANCED BEARING APPLICATIONS BY
LARGE BATCH MAGNETIC FLOAT POLISHING
(MFP) APPARATUS

Thesis Approved:

Dr. Ranga Komanduri

Thesis Advisor

Dr. Hongbing Lu

Dr. C. E. Price

Dr. A. Gordon Emslie

Dean of the Graduate College

SUMMARY

Over the past decade or so, silicon nitride (Si_3N_4) balls have become an important component for advanced bearings. They are currently finished in industry by V-groove lapping. Their manufacturing costs are high due to longer processing time (6 - 16 weeks) and use of expensive diamond abrasive. Furthermore, use of diamond abrasive under heavy loads can result in scratches, pits, and microcracks on the surface of the polished balls. These surface defects can act as nucleation sites for cracks resulting in catastrophic failure by large brittle fracture. Hence, in order to minimize the surface damage, gentle polishing conditions are required, namely, low level of controlled force and abrasives not significantly harder than the workmaterial. This is accomplished by a process known as magnetic float polishing (MFP).

The primary objective of this investigation was to finish large diameter and large batch of Si_3N_4 balls (46 balls of 3/4 in. diameter) for hybrid bearing applications with good sphericity ($0.25 \mu\text{m}$) and surface finish ($R_a, 8 \text{ nm}$) by large batch MFP apparatus. Another aim of this investigation was to reduce the total processing time required to finish a batch.

The original apparatus built for this purpose has been modified to improve its performance. This involves *in-situ* machining of the polishing spindle for improving its roundness and geometric alignment. A fixture was built for *in-situ*

machining of the groove, formed on the bevel of the spindle during polishing. Another fixture was built to fabricate floats to precise dimensions. Polishing was performed in such a way that the chamber was able to self-align with the spindle.

Three important characteristics, namely, ball diameter, sphericity, and surface finish have to be controlled in order to finish balls suitable for bearing applications. The methodology for finishing Si_3N_4 balls by MFP consists of mechanical polishing followed by chemo-mechanical polishing. Boron carbide (B_4C), silicon carbide (SiC), and cerium oxide (CeO_2) are the abrasives used in this investigation.

Three stages are involved in magnetic float polishing of Si_3N_4 balls, namely, 1) roughing to remove maximum material without imparting any damage to the surface, 2) an intermediate stage of semi-finishing to control diameter and improve sphericity, and 3) final finishing to obtain best surface finish and sphericity while maintaining the final diameter.

Taguchi method was applied in the roughing stage to optimize the material removal rate. Level average response analysis indicated that a load of 1.5 N/ball, an abrasive concentration of 20 %, and a speed of 400 rpm would give a high material removal rate. High material removal rates (1 - 1.5 $\mu\text{m}/\text{min.}$) are possible using B_4C (500 grit) abrasive.

A groove is formed on the bevel of the spindle during polishing, which plays an important role in all the three stages. Initially, in the roughing stage, it is preferable to machine the groove, though not essential, in order to obtain high material removal rate using B_4C (500 grit) abrasive. It is, however, necessary to

maintain the groove formed at the end of roughing stage using SiC (600 grit) abrasive, in order to improve sphericity. The sphericity can be significantly improved in the intermediate stage by not machining the groove. SiC (1200 grit) abrasive was found suitable at this stage. This means the groove is beneficial for improving the sphericity at this stage. Further, in the final finishing stage, machining the groove is necessary for rapid improvement in the surface finish. Fine SiC (10,000 grit) abrasive was very effective in improving the surface finish prior to chemo-mechanical polishing with CeO₂ (< 5 μm) abrasive.

An actual polishing time of 20 - 30 hours (10 - 12 polishing runs) is adequate for finishing a batch of Si₃N₄ balls from the as-received condition. Thus, faster processing time and use of abrasives other than diamond would significantly reduce the overall cost of manufacture of Si₃N₄ balls for bearing applications. Also, the variation in diameter, sphericity, and surface finish from ball to ball and within a ball is very small. The large batch magnetic float polishing (MFP) apparatus can be used for finishing Si₃N₄ balls in a wide range of sizes, in a batch size ranging from 50 - 100 balls. This technology is easy to implement in industry and would not require high capital investment.

ACKNOWLEDGEMENTS

I am grateful to my parents and family for their support, guidance, and encouragement.

I would like to thank Dr. Ranga Komanduri, Dr. C. E. Price, and Dr. H. B. Lu for their encouragement and advice. I would also thank Dr. N. Umehara and Dr. Z. B. Hou for their useful discussions.

This project is sponsored by a grant from the Manufacturing Processes and Machines Program (DMI-0000079) of the Division of the Design, Manufacture, and Industrial Innovation (DMII) of the National Science Foundation. The author thanks Drs. W. Devries, G. Hazelrigs, J. Cao, Delcie Durham of DMII and Dr. J. Larsen Basse of the Tribology and Surface Engineering Program for their interest in and support of this work.

The initial development of the experimental set-up and parameter optimization by Taguchi method was jointly conducted with Mr. Robert Gerlick and Mr. Rishiraj Tekawade. I am grateful to them for their valuable discussions and help as research team partners.

I am thankful to Mr. Jerry Dale for his help and discussions. I would like to thank Mr. Anand Uplaonkar, Mr. R. V. Hariprasad, Mr. K. L. Lee, and Mr. J. Mach for their assistance and helpful conversations. I would also thank Mr. Sony Varghese and Mr. Madhan Ramakrishnan for their help. Thanks are also due to all my colleagues at MAERL for their help and friendship.

Finally, I would like to thank the Department of Mechanical and Aerospace Engineering for providing the opportunity to pursue my M.S. at Oklahoma State University.

TABLE OF CONTENTS

Chapter	Page
1. INTRODUCTION.....	1
1.1 Hybrid or Advanced Ceramic Bearings.....	1
1.2 Conventional Finishing of Ceramic Balls.....	4
1.3 Magnetic Float Polishing (MFP).....	5
1.4 Chemo-Mechanical Polishing (CMP).....	6
2. LITERATURE REVIEW.....	8
2.1 Ball Lapping Technology.....	8
2.2 Magnetic Float Polishing.....	18
3. PROBLEM STATEMENT.....	40
4. APPROACH.....	42
4.1 Introduction.....	42
4.2 Salient Features of Magnetic Float Polishing.....	43
4.3 Large Batch Magnetic Float Polishing Apparatus.....	45
4.4 Details of Polishing Spindle.....	51
4.5 Factors affecting Sphericity.....	54
4.6 Silicon Nitride Workmaterial.....	58
4.7 Abrasives.....	60

4.8	Magnetic Fluid.....	61
4.9	Evaluation of Surface Integration.....	63
4.10	Experimental Work.....	66
4.11	Standard Specifications.....	68
5.	METHODOLOGY FOR FINISHING SILICON NITRIDE BALLS.....	69
5.1	Introduction.....	69
5.2	Polishing Procedure and Parameters.....	70
6.	RESULTS AND DISCUSSION.....	73
6.1	Determination of Optimum Polishing Parameters in the Roughing Stage using Taguchi Method.....	73
6.2	Finishing of 3/4 inch Silicon Nitride Balls.....	79
6.3	Discussion.....	91
7.	CONCLUSIONS AND FUTURE WORK.....	93
7.1	Conclusions.....	93
7.2	Future Work.....	95
	REFERENCES.....	98

LIST OF TABLES

Table		Page
Table 1.1	Comparison of properties of silicon nitride and bearing steels.....	2
Table 2.1	Flash times for different flash temperatures.....	31
Table 4.1	Chemical composition of NBD-200 Si ₃ N ₄ ball.....	59
Table 4.2	Mechanical and thermal properties of Si ₃ N ₄ ball.....	59
Table 4.3	Properties of the abrasives used in this study.....	60
Table 4.4	Characteristics of W 40 magnetic fluid used in this study.....	61
Table 4.5	Tolerances by grade for individual balls.....	68
Table 4.6	Tolerances by grade for lots of balls.....	68
Table 5.1	Parameters used in this study.....	72
Table 6.1	Standard L ₉ (3 ⁴) orthogonal array used in Taguchi method.....	74
Table 6.2	Test parameters used and their levels.....	74
Table 6.3	Test run design and results.....	75
Table 6.4	Level average response analysis.....	76
Table 6.5	Test details and results of 3/4 in. silicon nitride balls.....	80

LIST OF FIGURES

Figure		Page
Figure 1.1	Schematic of conventional V-groove lapping apparatus.....	4
Figure 1.2	Schematic of the magnetic float polishing apparatus for finishing advanced ceramic balls.....	5
Figure 1.3	Schematic of the chemo-mechanical action between abrasive, workmaterial, and environment.....	7
Figure 2.1	Plan view of the lapping device.....	9
Figure 2.2	Diagrammatic section along line II - II of Figure 2.1.....	9
Figure 2.3	Plan view of the lapping apparatus.....	11
Figure 2.4	Perspective view of the ball lapping machine.....	12
Figure 2.5	Plan view of the stationary plate in the ball polishing machine...	14
Figure 2.6	One flat surface, one eccentric V-groove lapping.....	15
Figure 2.7	Schematic of the eccentric lapping machine.....	15
Figure 2.8	Schematic of the magnetic float polishing apparatus.....	19
Figure 2.9.1	Variation of polishing load with clearance.....	20
Figure 2.9.2	Variation of stock removal with polishing time.....	21
Figure 2.9.3	Variation of sphericity with polishing time.....	21
Figure 2.10.1	Effect of material of shaft on material removal rate and wear of apparatus.....	22

Figure 2.10.2	Effect of material of float on material removal rate and wear of apparatus.....	23
Figure 2.10.3	Effect of material of guide ring on material removal rate and wear of apparatus.....	23
Figure 2.11	(a) Cell geometry and motions (b) Contact loads, spin moments, and friction forces.....	24
Figure 2.12.1	Magnetic float polishing equipment for ceramic rollers (a) top view (b) side section view through line A-A of (a).....	26
Figure 2.12.2	Assembly of magnet B, float rollers, roller holder, and drive shaft.....	26
Figure 2.13	(a) Calculated temperature rise on the surface along the X-axis (b) Isotherms of temperature contour on the worksurface.....	31
Figure 2.14.1	(a) Plots of the response of each polishing parameter level on the surface finish, Ra (b) Plots of the response of each polishing parameter level on the surface finish, Rt.....	33
Figure 2.14.2	(a) Plot of the S/N ratios showing the effect of each parameter level on the surface finish, Ra (b) Plot of the S/N ratios showing the effect of each parameter level on the surface finish, Rt.....	34
Figure 4.1	Photograph of the machine tool used for polishing.....	47
Figure 4.2	Photographs of the experimental set-up (a) front view (b) side view.....	47

Figure 4.3	Schematic of the experimental set-up (a) front view (b) top view.....	48
Figure 4.4	Photograph showing arrangement of magnets in the chamber base.....	49
Figure 4.5	Magnetic field intensity distribution of chamber base.....	50
Figure 4.6	Photograph of the set-up used for machining the top and side surface of the spindle.....	52
Figure 4.7	Photograph of the set-up used for machining the inner surfaces of the spindle.....	52
Figure 4.8	Photograph of the fixture used for machining the bevel of the spindle.....	53
Figure 4.9	Another photograph of the fixture used for machining the bevel of the spindle.....	53
Figure 4.10	Alignment possibilities of the chamber with respect to the spindle (a) proper alignment (b) spindle axis tilt (c) chamber offset.....	56
Figure 4.11	Photograph of the fixture used for fabricating the floats.....	57
Figure 4.12	Magnetization (M-H) curve of W 40 magnetic fluid used in present study.....	62
Figure 4.13	Least squares reference circle.....	64
Figure 4.14	Minimum zone reference circles.....	64
Figure 4.15	Minimum circumscribed reference circle.....	64
Figure 4.16	Maximum inscribed reference circle.....	64

Figure 4.17	Schematic showing the dimensions of the counterweight arm...67
Figure 5.1	Photograph of the groove formed on the bevel of the spindle during polishing..... 71
Figure 6.1	Level average responses for parameters A, B, and C.....77
Figure 6.2	TalyRond roundness profiles of a 3/4 in. Si ₃ N ₄ ball at various stages of polishing
	(a) As-received.....83
	(b) After polishing with B ₄ C (500 grit) abrasive in Run 1.....84
	(c) After polishing with SiC (600 grit) abrasive in Run 5.....84
	(d) After polishing with SiC (600 grit) abrasive in Run 6.....85
	(e) After polishing with SiC (1200 grit) abrasive in Run 7.....85
	(f) After polishing with SiC (10,000 grit) abrasive in Run 14.....86
	(g) After polishing with CeO ₂ (< 5 μm) abrasive in Run 16.....86
Figure 6.3	TalySurf surface roughness profiles of a 3/4 in. Si ₃ N ₄ ball at various stages of polishing
	(a) As-received.....87
	(b) After polishing with B ₄ C (500 grit) abrasive in Run 1.....87
	(c) After polishing with SiC (600 grit) abrasive in Run 5.....88
	(d) After polishing with SiC (1200 grit) abrasive in Run 7.....88
	(e) After polishing with SiC (10,000 grit) abrasive in Run 12.....88
	(f) After polishing with SiC (10,000 grit) abrasive in Run 14.....89
	(g) After polishing with CeO ₂ (< 5 μm) abrasive in Run 16.....89
Figure 6.4	Photograph of 3/4 in. Si ₃ N ₄ balls finished in this study.....90

CHAPTER 1

INTRODUCTION

1.1 HYBRID OR ADVANCED CERAMIC BEARINGS

Traditional rolling element bearings made from AISI 52100 or M50 high-speed steel are limited in performance for use at very high speeds, high temperatures, and corrosive environments. They need adequate lubrication for satisfactory operation and optimum life. Over the past decade or so, silicon nitride (Si_3N_4) balls have become an important component for advanced bearings. They are most successfully used in hybrid bearings (SNHB). Si_3N_4 is the material of choice because it offers many interesting properties, such as high hardness, high thermal and chemical stability, low density, high Young's modulus, high stiffness, good fatigue life, low friction and high wear properties. Table 1.1 gives a comparison of properties of silicon nitride, AISI 52100 and M50 bearing steels.

It has been reported that [Lynch, 1991] high grade M50 steel bearings and silicon nitride hybrid bearings (SNHB) were tested in air turbine starters under worst-case conditions when the unit restarted a windmilling engine during flight. The starter temperature was raised from zero to 900° F in a few seconds and the turbine speed went up to 95,000 rpm just as quickly. The high grade M50 steel

bearings failed catastrophically after 15 minutes. On the other hand, SNHB remained undamaged when inspected after 45 minutes.

Table 1.1 Comparison of properties of silicon nitride and bearing steels [Wang *et al.*, 2000]

Property	AISI 52100	M50	HIP'ed Si ₃ N ₄ (NBD-200)
Density (kg/m ³)	7800	7800	3160
Hardness (HRC)	66	64	78
Elastic Modulus (GPa)	210	200	320
Poisson's Ratio	0.28	0.28	0.26
Thermal Expansion Coefficient (x 10 ⁻⁶ /°C)	10.9	12.3	2.9
Maximum Use Temperature (°C)	180	320	1000

The lower density of Si₃N₄ balls reduces the gyroscopic slip and centrifugal loading on the outer steel race. This reduces friction, heat, and wear of the bearing elements. Si₃N₄ balls do not react with the steel race and hence micro-welding can be avoided resulting in longer bearing life. SNHB are well suited for applications where marginal lubrication is required and are less sensitive to the lubricant type, lubricant contamination, and lubricant starvation. The higher rigidity, excellent surface finish, and sphericity of Si₃N₄ balls facilitate in reducing noise and vibrations of these bearings, thus enabling higher speeds.

These benefits make SNHB suitable for high speed and high temperature applications, such as turbines, machine tool spindles, dental drills, liquid oxygen pumps, and turbo molecular pumps. The all-ceramic bearings (Si₃N₄ balls in Si₃N₄ races) can operate at temperatures outside the range of SNHB (-40° to +200° Celsius). They perform well in aggressive environments of semiconductor processing, infrared missile seekers, and tidal flow meters. However, their use is

limited mainly due to the difference in thermal expansion coefficient between metal drive shaft and inner ceramic race. Hence, SNHB are preferable for most of the applications.

The failure mode of Si_3N_4 balls is by fatigue flake-off, which is similar to metallic rolling elements due to its higher fracture toughness. The performance and reliability of ceramic rolling element bearings depend on the quality of the resulting surface. Ceramics have high hardness and inherent brittleness. They are sensitive to defects resulting from grinding and polishing processes. Fatigue failure begins at regions of surface irregularities, such as scratches, pits, and microcracks. Hence, it is important to produce superior quality and finish with minimum defects in order to obtain reliability in performance.

In general, compared to traditional steel bearings, SNHB can more easily meet the requirements of higher efficiency, higher reliability, higher accuracy, higher speed, greater stiffness, longer life, lower friction, corrosion resistance, marginal lubrication, and less maintenance action [Wang *et al.*, 2000]. As the environmental friendly processing grows, the use of permanently lubricated and sealed bearings will also increase, and many of these will likely feature Si_3N_4 balls [Katz, 1999].

1.2 CONVENTIONAL FINISHING OF CERAMIC BALLS

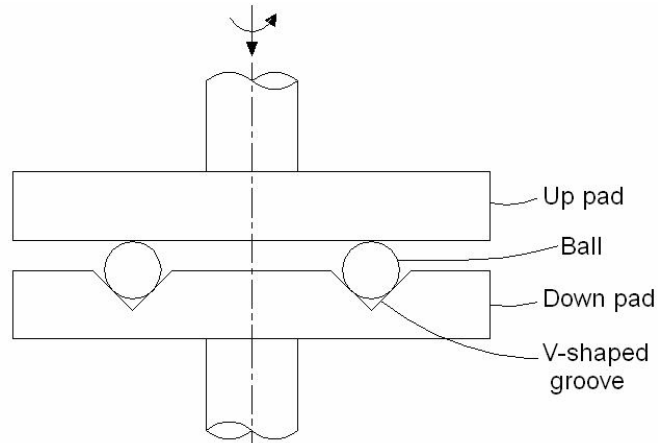


Fig. 1.1 Schematic of conventional V-groove lapping apparatus
[Yuan *et al.*, 2002]

Ceramic balls are finished in industry by grinding followed by V-groove lapping. This is essentially the same technique used for finishing steel balls. The schematic of this process is shown in Figure 1.1. The balls are in 3-point contact running in the V-groove. The balls revolve around the pad, at the same time they rotate continuously, and glide and roll relatively against the contacting surfaces of the pad [Yuan *et al.*, 2002]. The process uses high loads (~ 10 N per ball), low polishing speeds (~ 50 rpm), and diamond abrasive. Due to lower speeds, considerable time (6 - 16 weeks) is required for finishing a batch of ceramic balls from the as-received condition to the finished condition. Thus, long processing time and use of expensive diamond abrasive result in high processing costs. Furthermore, use of diamond abrasive under heavy loads can result in scratches, pits, and microcracks on the surface of the polished balls. These surface defects can act as nucleation sites for cracks resulting in catastrophic failure by large brittle fracture.

In order to prevent such failures, it is necessary to minimize the surface damage as much as possible. For this purpose “gentle” polishing conditions are required, namely, low level of controlled force and abrasives not significantly harder than the workmaterial. High material removal rates and shorter polishing times can be obtained using high polishing speeds. This is accomplished by a process known as magnetic float polishing (MFP).

1.3 MAGNETIC FLOAT POLISHING (MFP)

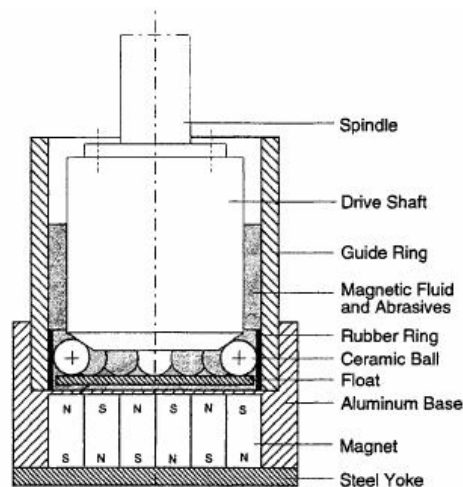


Fig. 1.2 Schematic of the magnetic float polishing apparatus for finishing advanced ceramic balls [Jiang and Komanduri, 1998c]

MFP involves fine mechanical polishing followed by chemo-mechanical polishing (CMP). This technique is based on magneto-hydrodynamic behavior of a magnetic fluid that can levitate all non-magnetic materials suspended in it. Figure 1.2 is a schematic of the magnetic float polishing apparatus. The magnetic fluid is a colloidal dispersion of extremely fine (100 to 150 Å) sub-domain ferromagnetic particles, usually magnetite (Fe_3O_4), in a carrier fluid, such as water or kerosene. The ferrofluids are made stable against particle agglomeration by the

addition of surfactants. When the magnetic field is applied, the Fe_3O_4 particles are attracted down towards the area of higher magnetic field and an upward buoyant force is exerted on all the non-magnetic materials, namely, the abrasive grains, the ceramic balls, and the acrylic float to push them towards the area of lower magnetic field. The drive shaft is fed down to exert the desired force on the balls. A three-point contact is obtained, namely, with the shaft at the top, the chamber on the side, and the float at the bottom. The balls are polished by the abrasives under the action of magnetic buoyancy force when the spindle rotates.

MFP uses low loads (~ 1 N per ball), high speeds (~ 2000 rpm for 2.5 in. diameter shaft in small batch apparatus and ~ 400 rpm for 12.2 in. diameter spindle in large batch apparatus), and abrasives such as boron carbide, silicon carbide, and cerium oxide. An actual polishing time of about 20 hours is adequate to finish a batch from the as-received condition [Komanduri *et al.*, 1999b]. The number of balls required to finish a batch of 3/4 inch balls is 6 for small batch apparatus and 46 for large batch apparatus.

1.4 CHEMO-MECHANICAL POLISHING (CMP)

In CMP, a chemical reaction takes place between the abrasive, the workmaterial, and the environment. The reaction products formed on the surface of the workmaterial is subsequently removed by the mechanical action of the abrasive, since this is weaker than the abrasive as well as the workmaterial. The chemo-mechanical action depends on the availability for a short duration of time a certain threshold pressure and temperature at the contact zone [Figure 1.3] [Yasunaga *et al.*, 1978, Komanduri *et al.*, 1997].

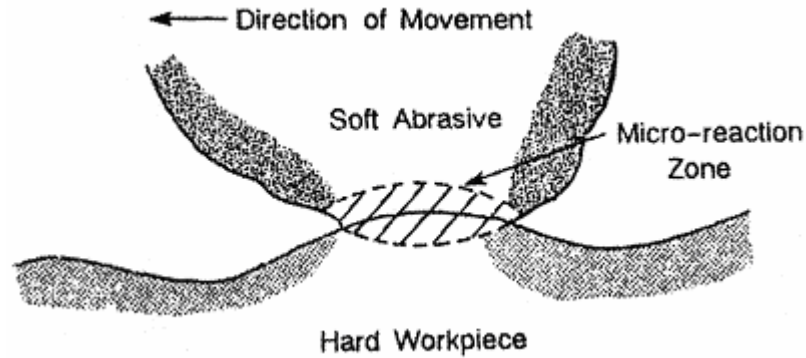


Fig. 1.3 Schematic of the chemo-mechanical action between abrasive, workmaterial, and environment [Yasunaga *et al.*, 1978, Komanduri *et al.*, 1997]

Since the material removal by this mechanism does not depend on the hardness but on the chemical potentials, it is possible to remove material by abrasives that are substantially softer than the workmaterial. Consequently, no scratching, microcracking, or pitting is expected with these abrasives resulting in a very smooth surface finish.

However, if chemo-mechanical reaction products remain on the surface or diffuse into the workmaterial, they may affect the performance and reliability of the product in subsequent use. Hence, it is necessary to ensure that the reaction products are completely removed from the surface as well as subsurface.

Chapter 2 contains the literature review on ball lapping and magnetic float polishing process. Chapters 3 and 4 deal with problem statement and the approach, respectively. Chapter 5 deals with the methodology used for finishing silicon nitride balls in this investigation. Chapter 6 covers the results and discussion. Chapter 7 deals with conclusions and future work.

CHAPTER 2

LITERATURE REVIEW

2.1 BALL LAPPING TECHNOLOGY

Finishing ball blanks requires precise and controlled removal of material from the surface. The ball motion plays an important role in the lapping process. The balls are generally lapped under load between two parallel plates having a relative rotational motion. The plates can be arranged horizontally, vertically or inclined depending upon the design of the apparatus. Further, they can be concentric or eccentric with respect to each other. The plates are generally made of cast iron or steel. The important process parameters are lapping load, lapping speed, abrasive type, size, and concentration, slurry used for lapping, and duration of lapping. In the following section, some selected patents and papers related to lapping of balls are discussed.

Messerschmidt (1972) built a lapping device for polishing balls. As shown in Figures 2.1 and 2.2, two superimposed lapping discs are spaced by a working gap and are rotated relative to each other. The upper disc is held stationary and the lower disk is rotated. The lower disc has in its side facing the upper disc three concentric grooves for lapping balls by relative rotation of the two disks. The discs are encompassed by a rotary magazine including a circular guide path for

balls to be lapped. A radial recess in the stationary disc connects the working gap with the guide path.

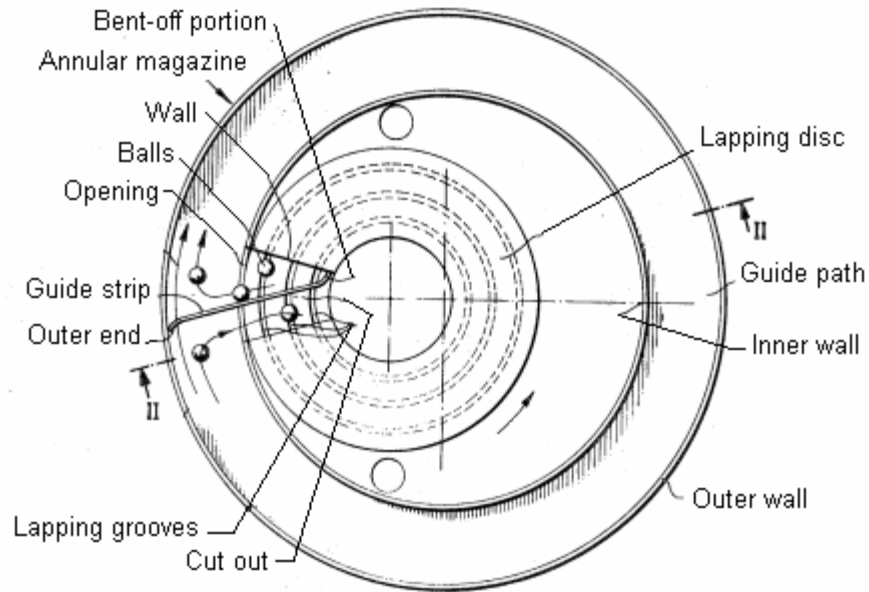


Fig. 2.1 Plan view of the lapping device [Messerschmidt, 1972]

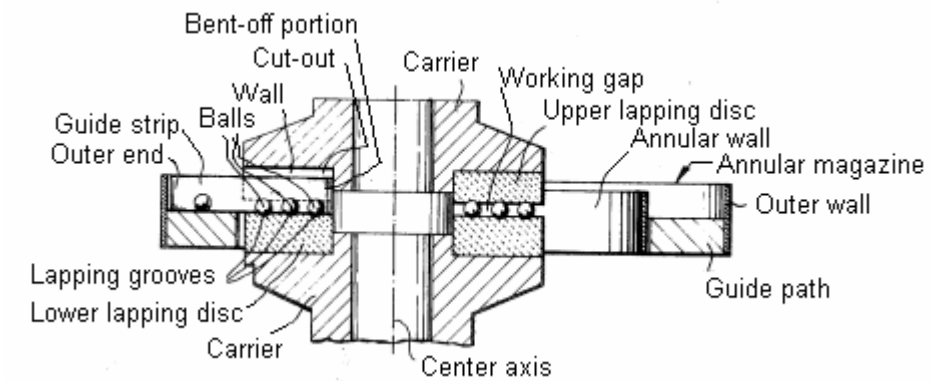


Fig. 2.2 Diagrammatic section along line II – II of Fig. 2.1 [Messerschmidt, 1972]

The balls are fed to the recess and received from the recess and guided, after each rotation between the discs, through the magazine. As the balls roll along the surface of the grooves and disks, a sliding movement of varying magnitude is set up which constitutes the lapping force. This lapping force, in combination with suitable abrasive slurry, causes gradual altering of non-round shape of the balls. When the balls are substantially identical in size and shape, the connection between the sector-shaped recess and the magazine is interrupted and the balls are caused to rotate continuously between the lapping discs until they have maximum required surface finish [Messerschmidt, 1972].

London (1990) developed an apparatus for low stress polishing of spherical balls as shown in Figure 2.3. The apparatus includes a hard ceramic plate mounted on a metal backing plate which is rotated by a motor. Facing the ceramic plate is a transparent glass plate, which is made stationary during operation. This enables visual monitoring of the balls during operation. Both the plates have smooth facing surfaces. Magnets are positioned on the top surface of the glass plate to magnetically limit the path of travel of the balls and preventing them from getting ejected from the polishing surfaces. Etched grooves are formed on the inner surface of the glass plate, which facilitates mixing of the balls during polishing.

Use of magnetic fields enables rotation of ball around an infinite number of axis, which improves the diameter uniformity. The polishing process allows the system to be tolerant of balls that are divergent from the norm (e.g. larger, smaller, or non-symmetrical). Initially, polishing action is more on balls that are

larger in diameter, which is continued till all the balls are of same diameter. Thus, a uniform polishing takes place resulting in superior degree of sphericity.

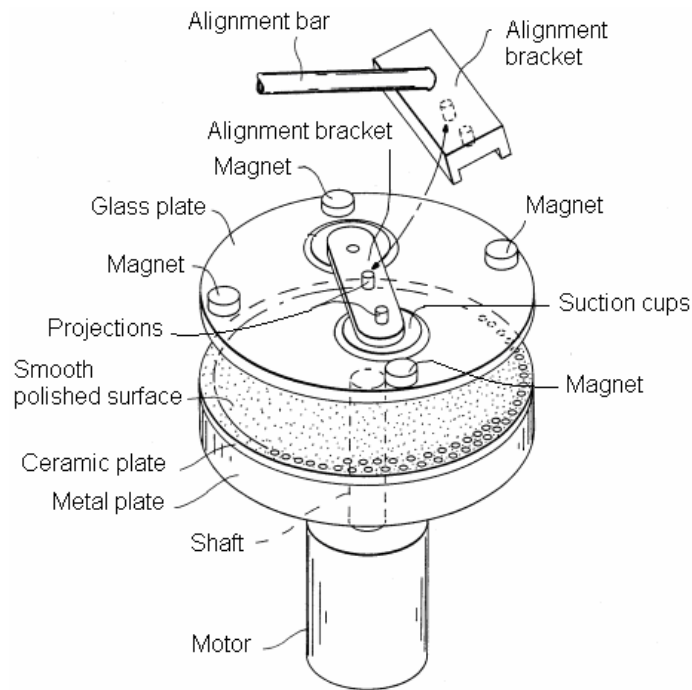


Fig. 2.3 Plan view of the lapping apparatus [London, 1990]

This apparatus can polish steel balls by using slurry consisting of glycol mixed with fine diamond particles. The polishing load of few hundred grams is applied on the balls and the rotational speeds are also low, ranging from 5 - 60 rpm. The quantity of balls can vary from 500 - 3000 per polishing lot depending on the ball blank diameter. Thus, the combination of smaller abrasives, less load acting on the balls, reduced speed of rotation, and enhanced random motion results in more uniform stock removal at a reduced rate of removal. The polishing process can be carried out continuously for 24 hours without the continuous presence of human operator. In this way, the average time to complete a lot reduces from 23 to 10 days.

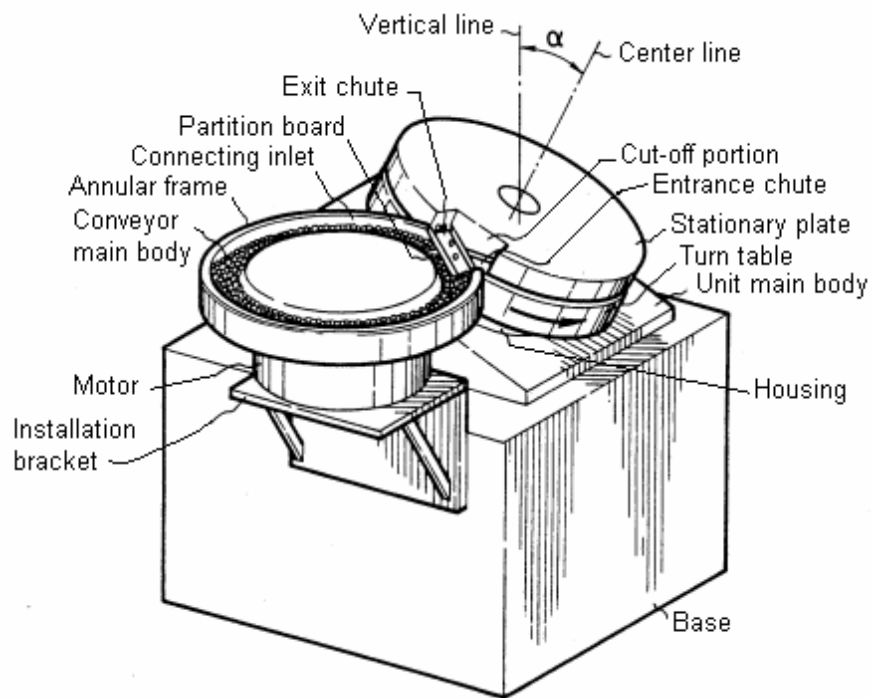


Fig. 2.4 Perspective view of the ball lapping machine [Sato, 1994]

Sato (1994) developed a ball lapping machine, which has several advantages over conventional ball lapping machines. Figure 2.4 shows the perspective view of the ball lapping machine. The machine has a central shaft having a common center line with a sleeve, which rotates around the central shaft. Housing is provided to support the sleeve rotation. A stationary plate is mounted on the central shaft and a turn table is mounted on the sleeve. The stationary plate is vertically movable and hence load can be applied on the ball blanks during lapping. The axial center of the housing is allowed to incline at an appropriate angle to the vertical.

The center line of the shaft is held vertical while loading and unloading the balls and is inclined when the ball blanks are to be machined. Since the center lines are the same and the support portions for both discs are on the same side of each of the discs, the concentricity and parallelism of the grooves on both discs are maintained constant. Also, there is no effect caused by heat generation by the rotating spindle on the turn table side and the temperature rise of lapping liquid. As a result, the sphericity, surface roughness, and dimensional accuracy for the finished balls are enhanced, whereas the operability of loading and unloading the balls is improved. Moreover, the circulation of ball stocks during lapping becomes smooth. It is also possible to prevent scratches on the finished balls due to accumulation of the abrasive particles in the groove of the discs [Sato, 1994].

Tonooka *et al.* (1999) developed a ball polishing machine by modifying the stationary plate of conventional ball lapping machines. As shown in Figure 2.5, relief grooves are formed on the guide groove portions of the stationary plate. The positions and the lengths of the relief grooves are so determined that whenever the ball passes through them, the inclination of the axis of rotation of the ball is changed. As the inclination of the axis of rotation changes, the portion of the ball, which contacts the guide groove of rotary plate, namely, the polishing locus is changed. Hence, the surface of the ball is uniformly polished in one polishing operation. As a result, the number of polishing operations per ball can be decreased, which results in high efficiency.

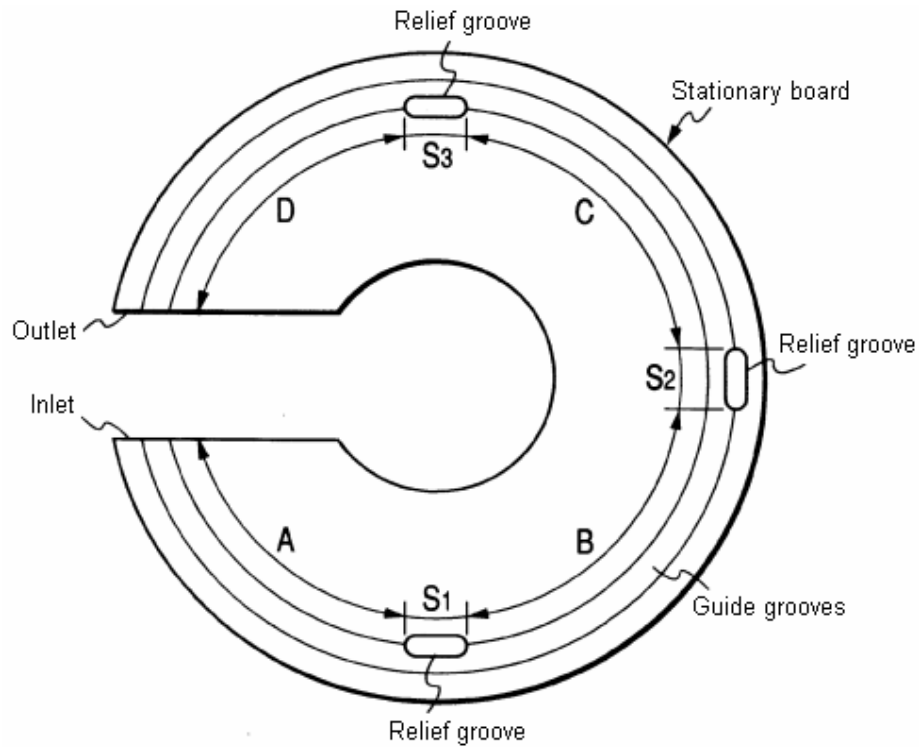


Fig. 2.5 Plan view of the stationary plate in the ball polishing machine [Tonooka *et al.*, 1999]

Kang *et al.* (2000) developed an eccentric lapping machine for finishing advanced ceramic balls. Figure 2.6 shows the schematic of one flat surface, one eccentric V-groove lapping and Figure 2.7 shows the schematic of the eccentric lapping machine. The top plate has a flat surface and is held stationary, whereas the bottom plate is rotational having an eccentric V-groove. The load is applied to the top plate by a spring loaded unit. Ceramic balls are lapped in between the two lapping plates while a mixture of diamond paste and lubricating fluid is supplied.

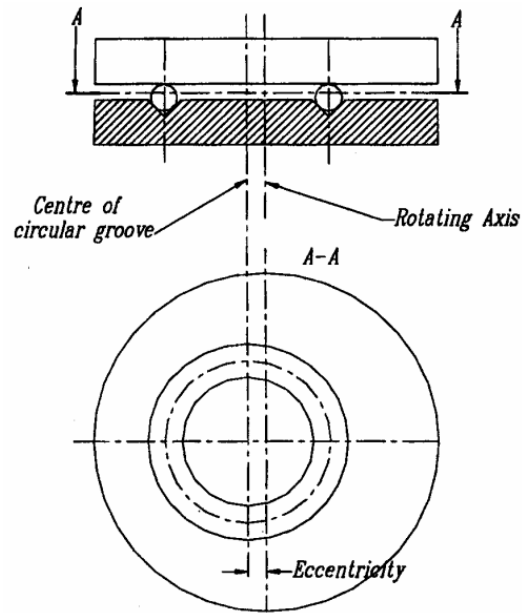
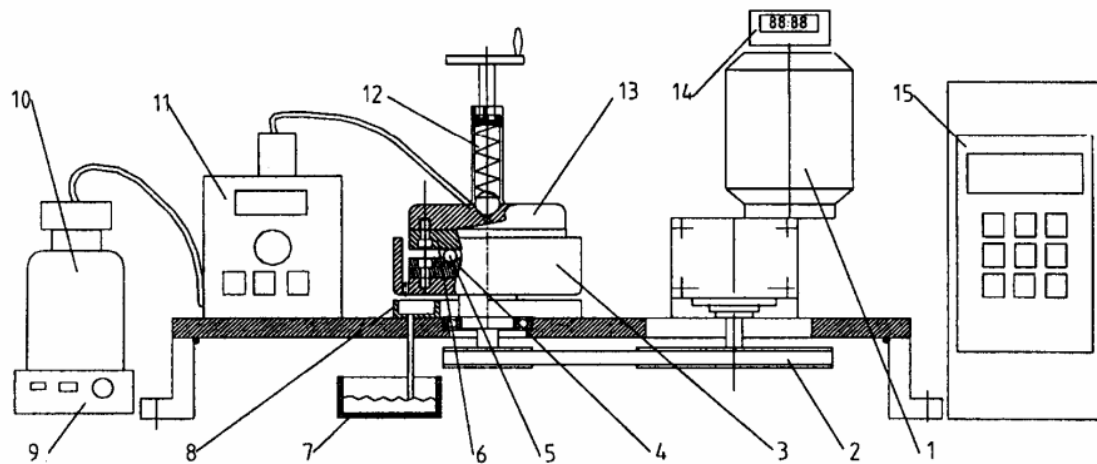


Fig. 2.6 One flat surface, one eccentric V-groove lapping [Kang *et al.*, 2001b]



- 1, a.c. motor and gearbox combination; 2, pulleys and belt; 3, flange shaft; 4, lower plate; 5, ceramic ball; 6, top plate; 7, lubricant fluid collection tank; 8, lubricant fluid tray; 9, magnetic stirrer; 10, lubricant fluid; 11, pump; 12, spring loading unit; 13, backing plate; 14, time counter; 15, microinverter

Fig. 2.7 Schematic of the eccentric lapping machine [Kang *et al.*, 2001b]

High speed, high load aggressive lapping tests were conducted on half inch silicon nitride ball blanks. At first, the material removal rate increased with the lapping load reaching a maximum, 68 $\mu\text{m}/\text{h}$, at a load of 4.37 kg/ball. At higher loads, the material removal rate decreased to 55 $\mu\text{m}/\text{h}$ at 6 kg/ball, 25 $\mu\text{m}/\text{h}$ at 7.95 kg/ball, and 20 $\mu\text{m}/\text{h}$ at 10.87 kg/ball. At the two highest loads (7.95 kg/ball and 10.87 kg/ball), the lapped ball roundness was in the range of 3 - 4 μm with some individual ball measuring 6 μm . However, at load 6 kg/ball or less the roundness was in the range of 1 - 2 μm . It was anticipated that the improper rolling motion of the ball at higher loads resulted in decrease in the material removal rate and increase in the ball roundness. The difference in the material removal rate was not significant at lapping speeds of 270 rpm and 500 rpm.

After lapping, the balls were inspected for surface damage using dye penetrant testing as well as optical microscopy. Surface spalls and sub-surface damage were found on balls after lapping at an average load of 10.87 kg/ball. No substantial surface or sub-surface damage was found on balls after lapping at an average load of 4.37 kg/ball. Surface spalls were observed after lapping at a speed of 500 rpm. No evidence of lapping induced damage, except for C-cracks, was observed at 270 rpm [Kang *et al.*, 2000].

Kang *et al.* (2001a) used Taguchi methods to optimize four lapping parameters - lapping load, lapping speed, diamond particle size, and paste concentration. The optimum lapping condition was found to be high load, high speed, high paste concentration, and 60 μm diamond particles. The analysis of variance showed that lapping load was the most significant parameter accounting

for 50 % of the total, followed by lapping speed (31 %). The particle size and paste concentration only accounted 12 % and 7 %, respectively.

Kang *et al.* (2001b) conducted lapping tests to investigate the influence of lapping plates on the lapping and polishing process. Cast iron plates were found appropriate for the first step of finishing, i.e. lapping, for achieving maximum material removal rate, whereas steel plates were found suitable for the second step of finishing, i.e. polishing, for achieving roundness, surface finish, dimensional and geometric accuracy. It was found that the surface condition of the V-groove on the lower plate has a significant influence on the sphericity and material removal rate, and the surface condition of top plate has more influence on final surface roughness.

A 90° V-groove angle, 65 mm diameter circular V-groove accommodating 15 ball blanks of diameter 13.4 mm and an eccentricity of 8 mm were the parameters used for obtaining high material removal rate. The maximum material removal rate achieved was under the conditions of average lapping load of 4.37 kg/ball, a lapping speed of 169 rpm, a diamond paste size of 60 µm, and a diamond paste concentration of 1 g/30 ml. A material removal rate of 68 µm/h for ball blank was achieved, which is 15 times higher than conventional concentric lapping. The ball roundness of 0.4 - 1.1 µm was obtained at the lapping step. In the polishing step, the average load varied from 1.1 to 1.5 kg/ball, the speed was 94 rpm and the diamond particle sizes varied from 1 to 0.25 µm. The polished ball surface roughness value, Ra, was 3 nm and ball roundness was in the range of 0.08 - 0.09 µm, which is above grade 5 of precision bearing ball specification.

2.2 MAGNETIC FLOAT POLISHING (MFP)

Magnetic field assisted polishing originated in the U.S. when Coats (1940) applied this technology for polishing interior of barrel shells. In the late 1950's and 1960's this technology was developed in the former U.S.S.R. by Baron and his associates for finishing heavy workpieces [Baron, 1975; Komanduri *et al.*, 1997]. Further in late 1980's, this technology was applied by researchers in Japan [Umehara and Kato, 1990, 1993, 1996; Shinmura *et al.*, 1990] for finishing a wide range of workpieces to a great degree of accuracy and good surface finish. Further advancements in this work were made by Childs *et al.* [1992, 1994a,b, 1995, 2001] in U.K. by concentrating on magnetic fluid grinding cell design and mechanics, and by Komanduri *et al.* [Umehara and Komanduri, 1996; Bhagavatula and Komanduri, 1996; Raghunandan and Komanduri, 1998; Hou and Komanduri, 1998a,b,c; Jiang and Komanduri, 1997, 1998c; Jiang *et al.*, 1998a,b; Komanduri *et al.*, 1996b, 1999a,b,c] in the U.S. by developing methodology for finishing ceramic rollers and balls by magnetic float polishing.

Tani and Kawata (1984) originally developed MFP for finishing soft materials, such as acrylic resin. Figure 2.8 is a schematic of magnetic float polishing after Tani *et al.* [1984]. Material removal occurs due to relative motion between the workpiece and the abrasive under the influence of magnetic levitational force. The polishing pressure is very small as the abrasives are floating in the magnetic fluid. The material removal rate obtained was about 2 $\mu\text{m}/\text{min}$. using silicon carbide (4 μm) abrasive. The surface roughness, R_{max} was improved from 0.5 μm to 0.15 μm . This mode of operation was not suitable for

finishing hard materials, such as steels or ceramics, due to low or negligible material removal rates.

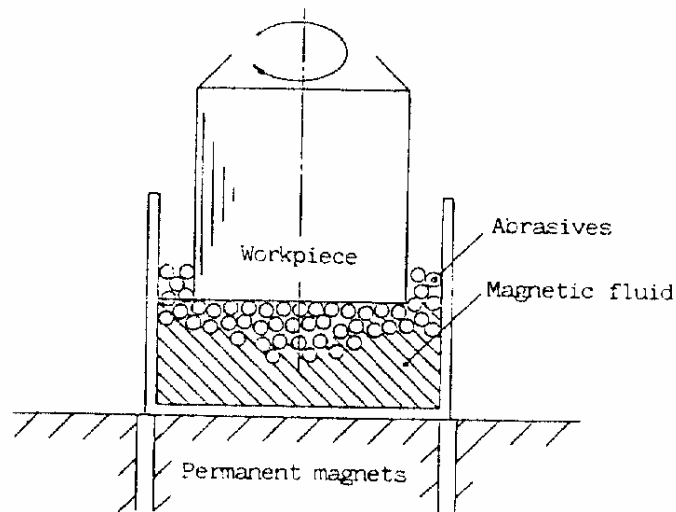


Fig. 2.8 Schematic of the magnetic float polishing apparatus after [Tani and Kawata, 1984]

Umehara and Kato (1990) made a major advancement by introducing a float to the system of workpiece, abrasive grains, magnetic fluid, and magnets to improve the material removal rate and control the shape of the workpiece in polishing. The as-sintered silicon nitride ball having a mean diameter of 7.7 mm, sphericity of 500 μm , and surface roughness, R_{max} of 10 μm was finished to a final size of 7.1 mm, sphericity of 0.14 μm , and surface roughness, R_{max} of 0.1 μm in 180 min. of polishing time.

Figure 2.9.1 shows the variation of polishing load as a function of clearance, h between the surface of the magnets and balls or float. It can be seen that the polishing float can easily produce a large grinding load and this load is found to increase significantly at lower clearance values. Figure 2.9.2 shows the variation of stock removal with grinding time with and without a float at

same clearance of 0.6 mm. The stock removal with a float is significantly larger than without a float. Figure 2.9.3 shows the variation of sphericity with polishing time with and without a float. The sphericity of the balls with a float is found to decrease rapidly with polishing time. Thus, the float was found to be very effective in increasing the material removal rate and for producing a smooth surface with good sphericity.

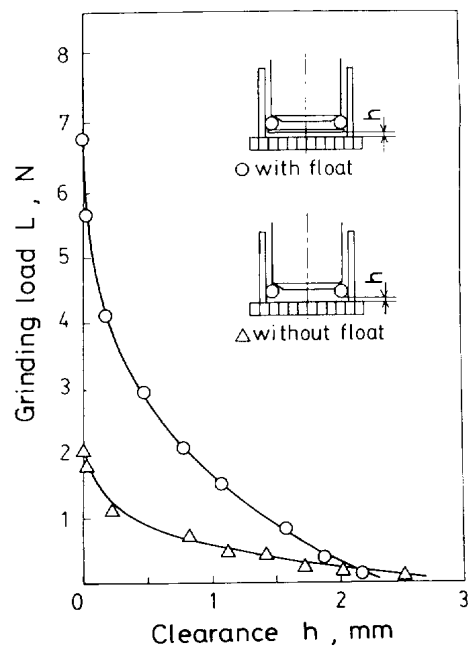


Fig. 2.9.1 Variation of polishing load with clearance [Umehara and Kato, 1990]

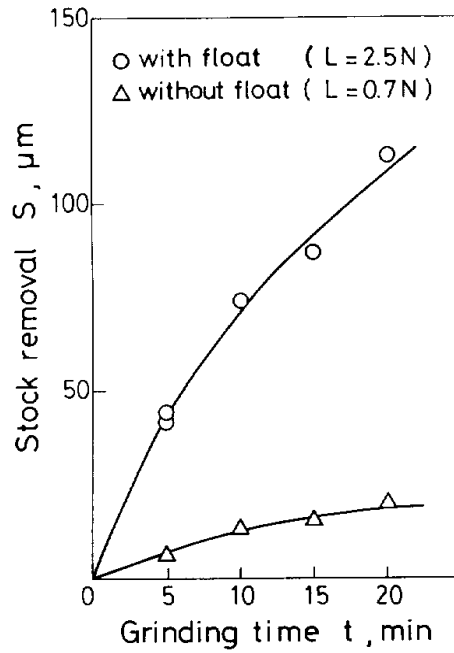


Fig. 2.9.2 Variation of stock removal with polishing time [Umehara and Kato, 1990]

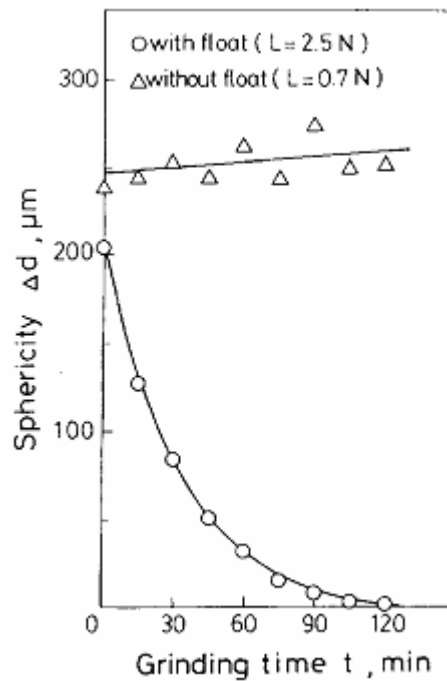


Fig. 2.9.3 Variation of sphericity with polishing time [Umehara and Kato, 1990]

Umehara (1990) studied the effect of material of the shaft, float, and guide ring on the material removal rate and wear of the apparatus. The results are shown in Figures 2.10.1 - 2.10.3. Among different shaft materials including urethane rubber, brass, silicon nitride, aluminum, and stainless steel, the latter gave the highest removable rate and smallest wear. Among the float materials, namely acrylic resin, urethane rubber, and silicon nitride, the removal rates were nearly same but the acrylic resin had the largest wear. For the guide ring, the urethane rubber gave higher material removal rate and lower wear than silicon nitride and stainless steel [Raghunandan, 1996].

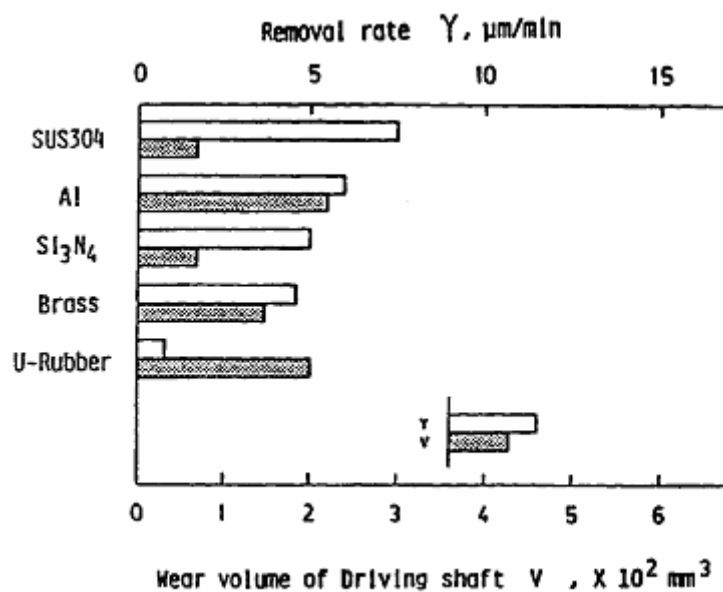


Fig. 2.10.1 Effect of material of shaft on material removal rate and wear of apparatus [Umehara, 1990; Raghunandan, 1996]

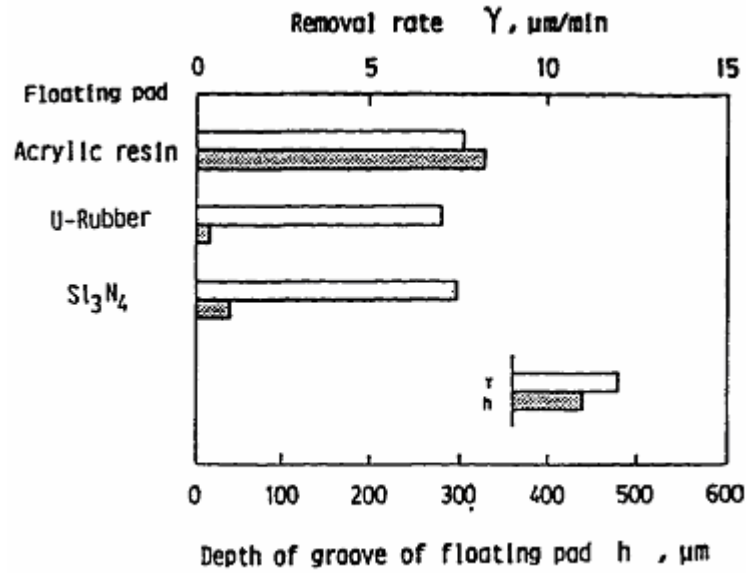


Fig. 2.10.2 Effect of material of float on material removal rate and wear of apparatus [Umehara, 1990; Raghunandan, 1996]

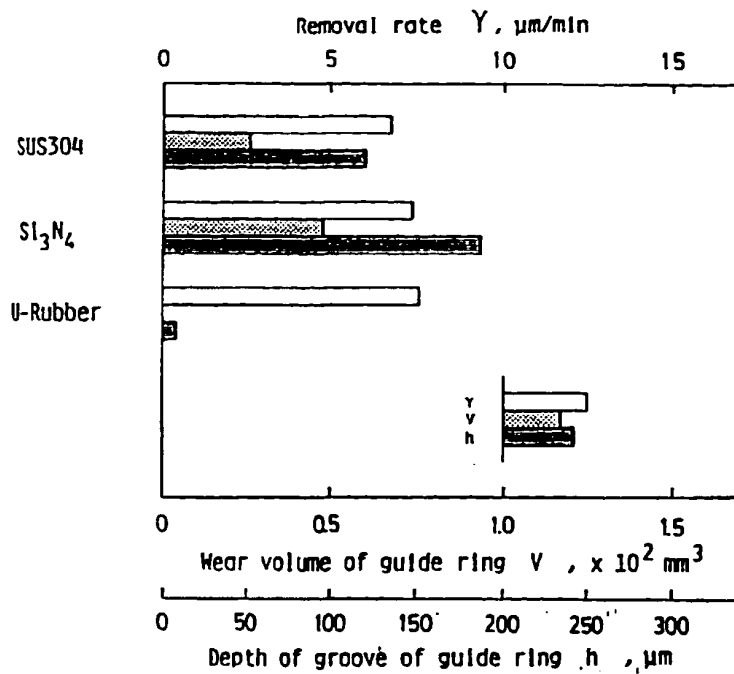


Fig. 2.10.3 Effect of material of guide ring on material removal rate and wear of apparatus [Umehara, 1990; Raghunandan, 1996]

Childs *et al.* (1994a,b) investigated the mechanics of magnetic float polishing of ceramic balls. A model, as shown in Figure 2.11, was developed to calculate sliding speeds and to estimate the wear coefficient.

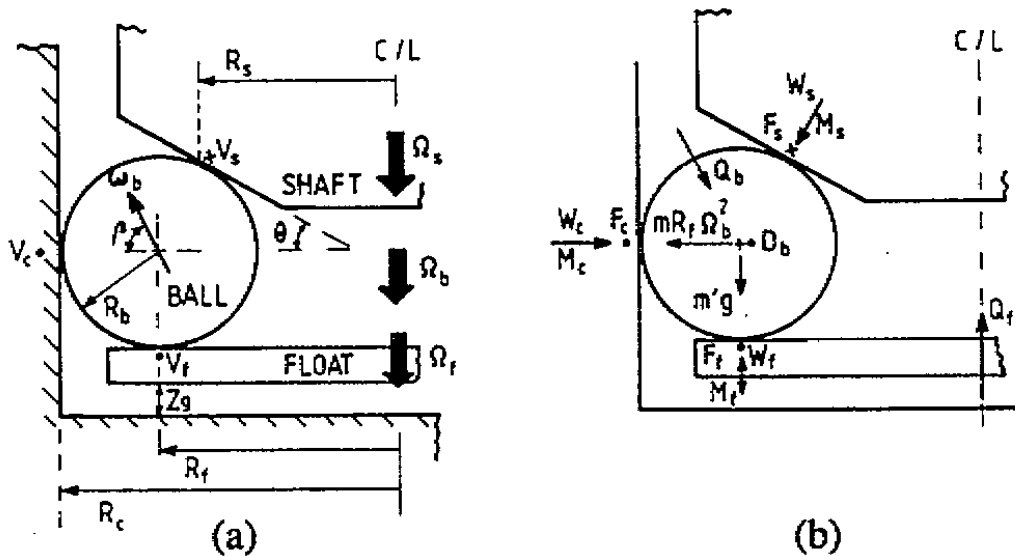


Fig. 2.11 (a) cell geometry and motions (b) contact loads, spin moments and friction forces [Childs *et al.*, 1994b]

Figure 2.11(a) shows a ball of radius R_b driven by a shaft with a conical end of slope θ round a container of inner radius R_c . The ball contacts the float at a radius R_f and the shaft at a radius R_s . The lower face of the float is separated from the bottom of the cell by a gap z_g . The figure also defines the angular speeds Ω_s of the shaft, Ω_b of the ball circulation, and Ω_f of the float, the ball spin angular velocity ω_b , and direction β . Figure 2.11(b) shows the contact loads W_c , W_s and W_f , the spin moments M_c , M_s and M_f and the friction forces F_c , F_s and F_f . The figure also shows the fluid drag moments Q_b and Q_f acting on the ball and float, the centrifugal force $mR_f\Omega_b^2$ acting on the ball, and a drag force D_b acting normal to the plane of the figure due to motion through the fluid.

High material removal rates are found to be due to large skidding velocities between the balls and the drive shaft. The removal rate was found to be proportional to the load acting on the balls and to the skidding velocity at the drive shaft, in a manner expected of an abrasive process. A wear coefficient of 0.07 ± 0.02 for Si_3N_4 balls was estimated from the experiments, which is typical of two-body abrasion.

Childs *et al.* (1995) studied different ball materials and different types of magnetic fluids during finishing of ceramic balls. Based on the results obtained, the material removal process in MFP was considered to be two-body abrasion by the abrasives grits embedded in the drive shaft. It was found that there is an optimum fluid viscosity for getting high material removal rates in MFP process. If the viscosity is too small, skidding does not occur between the balls and drive shaft. On the other hand, if the viscosity is too large, although skidding occurs, there is a reduction in the abrasive efficiency. The reduction of removal rate with operating time was considered probably due to loss of abrasive grits and deterioration of magnetic fluid.

Umehara and Komanduri (1996) finished eight HIP- Si_3N_4 rollers (diameter: 19 mm and length: 26 mm) by magnetic float polishing (also termed as magnetic fluid grinding). Figure 2.12.1 show the top view and exploded side view of the apparatus, respectively. Figure 2.12.2 is an exploded view showing magnetic ring B, float, rollers, roller holder, and drive shaft in the hole of magnetic ring A.

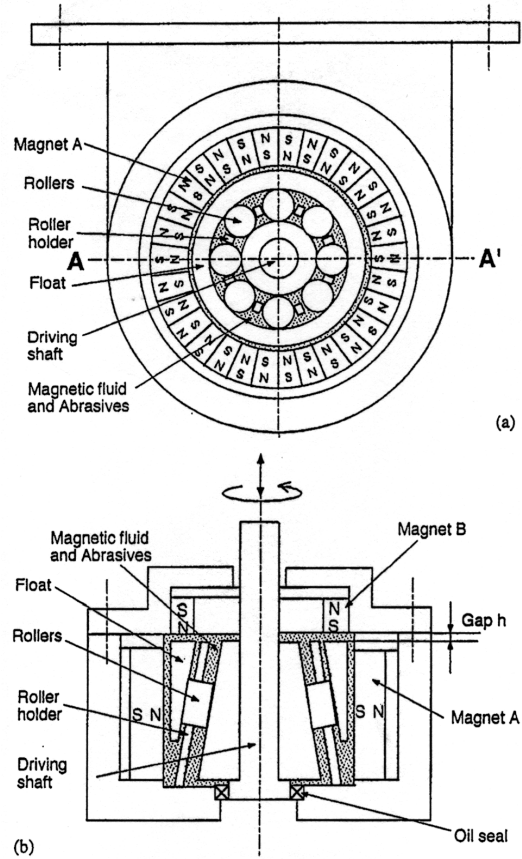


Fig. 2.12.1 Magnetic float polishing equipment for ceramic rollers (a) top view
 (b) side section view through line A-A of (a)
 [Umehara and Komanduri, 1996]

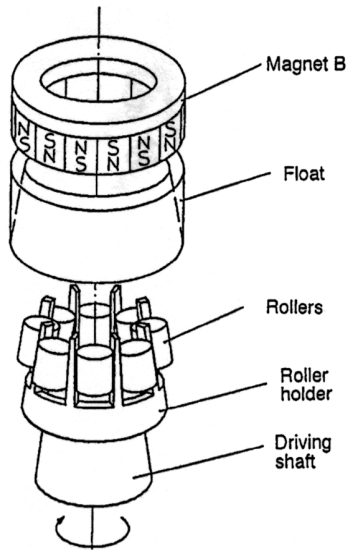


Fig. 2.12.2 Assembly of magnet B, float rollers, roller holder, and drive shaft
 [Umehara and Komanduri, 1996]

Magnetic ring A comprises of 30 individual magnets assembled into one hollow cylindrical magnet. Each magnet is magnetized in the radial direction. Magnetic ring A supports the float in place, as well as facilitates in concentrating the abrasives around the center of the chamber. Magnetic ring B comprises of 16 individual magnets assembled into a ring magnet. Each magnet is magnetized in the longitudinal direction. Magnetic ring B pushes the float in the longitudinal direction with the application of the magnetic buoyant force. The rotation of the rollers along the axis of the shaft is prevented by the roller holder in order to obtain high sliding velocity between the roller and the drive shaft, and consequently higher removal rates. However, the rotation of the rollers around their own axis is facilitated by providing fingers in the roller holder.

The removal rate decreased in the order of decreasing hardness of abrasives used, namely, boron carbide (B_4C), silicon carbide (SiC), and chromium oxide (Cr_2O_3). A high material removal rate ($1.1 \mu\text{m}/\text{min.}$) was obtained with B_4C ($50 \mu\text{m}$). The surface finish was found to improve rapidly with decrease in the grain size. Polishing with Cr_2O_3 ($3 \mu\text{m}$) resulted in the best surface finish (R_a of 5 nm). This was probably due to lower hardness of the abrasive as well as the chemo-mechanical polishing ability of this abrasive with Si_3N_4 workmaterial. The sphericity of the roller improved from $16.65 \mu\text{m}$ to $4.25 \mu\text{m}$. Rollers finished by this technique resulted in slightly rounded edges (crowns), which may be ideal for roller bearing applications.

Komanduri *et al.* (1996b) investigated the possibility of chemo-mechanical action in MFP of Si_3N_4 balls. Aluminum oxide (Al_2O_3) and chromium oxide (Cr_2O_3) abrasives having nearly same hardness were used to investigate mechanical versus chemo-mechanical aspects of polishing. Higher removal rates and a smoother surface texture were obtained with Cr_2O_3 as compared to Al_2O_3 abrasive. This difference was believed to be due to the chemo-mechanical action of Cr_2O_3 abrasive. Higher chemical stability of Al_2O_3 abrasive (compared to Cr_2O_3 abrasive) and the known role of Cr_2O_3 as a catalyst for the oxidation of Si_3N_4 are some of the reasons attributed for this action. It was found that the sliding speed between the drive shaft and the balls with Cr_2O_3 was larger than that with Al_2O_3 at the same drive shaft speed. The difference in shape and friability of these abrasives, which may influence the material removal rates, was also recognized. Formation of pits due to abrasion, brittle fracture, and dislodgement of grains was predominant after polishing with Al_2O_3 abrasive. On the other hand, fewer pits were observed on the surface of Si_3N_4 balls after polishing with Cr_2O_3 abrasive. These were considered to have been generated in the early stages of polishing. Surface finish, R_a of less than 10 nm, was obtained after finishing with Cr_2O_3 abrasive.

Bhagavatula and Komanduri (1996) investigated the chemo-mechanical polishing of Si_3N_4 balls with Cr_2O_3 abrasive. They examined the wear debris generated in the polishing process using a scanning electron microscope with an X-ray microanalyser and a small-angle X-ray diffraction apparatus. The analysis showed conclusively that Cr_2O_3 reacts with the Si_3N_4 workmaterial to form

chromium nitride (CrN) and chromium silicate (Cr₂SiO₄), thus establishing the role of Cr₂O₃ not as a mere catalyst but as actively taking part in the chemical reactions during CMP. A model of CMP of Si₃N₄ workmaterial in air and in water environments with Cr₂O₃ was presented. This model is based of the formation of such reaction products as CrN and Cr₂SiO₄, in addition to the formation of a silica layer (SiO₂) on Si₃N₄ surface as well as gaseous reaction products, such as ammonia (in water) and nitrogen (in air).

Hou and Komanduri (1998a,b) developed a thermal model to calculate minimum flash temperatures and flash durations in magnetic float polishing of ceramic balls. This enables the determination of whether adequate temperatures are generated for a reasonable period of time for chemo-mechanical polishing to occur. The heat source at the area of contact between the balls and the abrasives, where the material removal takes place, is approximated to a disc. A parabolic distribution of heat generation was considered. For a moving disc heat source, the temperature rise at point near and on the moving disc heat source is given by the following solution:

$$\theta_M = \frac{q_{dc} v}{2\lambda a \pi^{3/2} r_o^2} \exp(-XV) \int_0^{r_0} \left(1 - \frac{r_i^2}{r_o^2}\right) r_i dr_i \times \int_0^{v^2 t/4a} \frac{d\omega}{\omega^{3/2}} \exp\left(-\omega - \frac{u_i^2}{4\omega}\right) I_o(p) \dots\dots\dots (2.1)$$

where

$$p = \frac{r_i V^2}{2\omega} \sqrt{\left(X + \frac{2\omega}{V}\right)^2 + y^2}; \quad u_i = R_{hi} V; \quad R_{hi} = \sqrt{r_i^2 + X^2 + y^2 + z^2}$$

a is the thermal diffusivity, m^2/s ; c is the specific heat, $J/gr/^\circ C$; λ is the thermal conductivity, $J/m.s^\circ C$; ρ is the density, gr/cm^3 ; q_{dc} is the rate of heat generation by a disc heat source, J/s ; r_i is the radius of a concentric differential segmental heat source from the disc heat source, $r_i = 0$ to r_o ; r_o is the radius of the moving ring or moving disc heat source, m ; v is the velocity of the moving heat source along X-axis or sliding velocity, m/s ; $V = v/2a$; w is the normal load, $N/particle$, W is the normal load, $N/ball$; x,y,z are the coordinates of the point M in the absolute co-ordinate system; X,y,z are the coordinates of point of interest (point M) in the moving coordinate system; μ is the coefficient of friction; θ_M is the temperature rise at point M; t is the time after the initiation of the moving heat source, s ; τ is the time after the initiation of an instantaneous heat source; ω is a dimensionless number which has its value from 0 to $v^2t/4a$; $I_0(p)$ is the modified Bessel function of the first kind, zero order. A time required for establishing the quasi-steady state (t_{steady}) conditions can be calculated from the relationship:

$$t_{steady} = 20. a / v^2$$

Jiang (1998d), based on this model, calculated the temperature field and the flash temperatures generated at the contact area in magnetic float polishing of silicon nitride balls with cerium oxide (CeO_2) abrasive as shown in Figure 2.13. The flash times for relevant flash temperatures during the polishing process is calculated from the relationship:

$$\text{flash time} = L / v;$$

where L is the length in the X-direction of the region enclosed by the isotherm of a certain critical temperature; v is the velocity of the moving heat source. Table 2.1 gives the flash times for different flash temperatures.

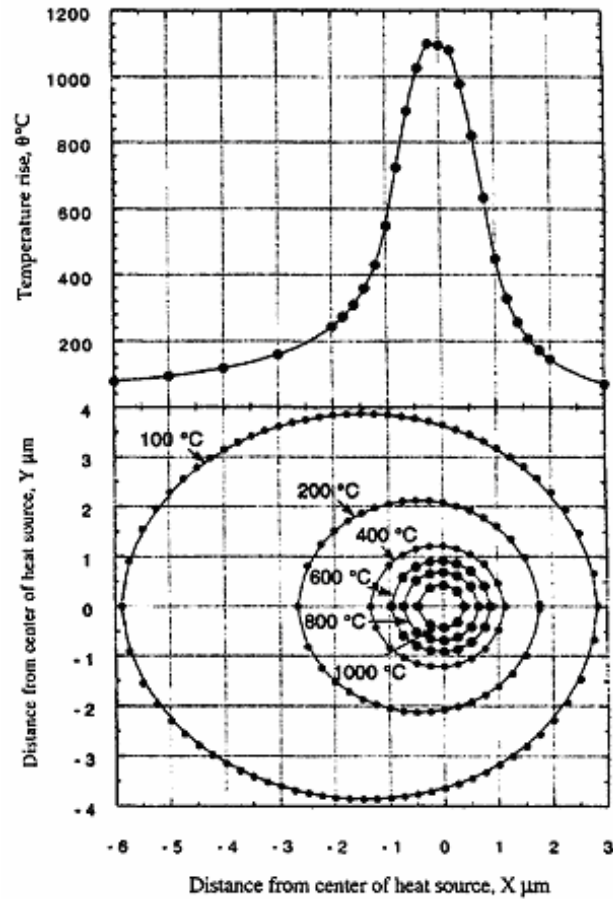


Fig. 2.13 (a) Calculated temperature rise on the surface along the X-axis
 (b) Isotherms of temperature contour on the worksurface
 ($W=1.2$ N/ball, $v = 4$ m/s)
 [Jiang, 1988d; Komanduri *et al.*, 1999a]

Table 2.1 Flash times for different flash temperatures ($v = 4$ m/s, $W=1.2$ N/ball)
 [Jiang, 1998d; Komanduri *et al.*, 1999a]

Flash temperature (°C)	> 100	> 200	> 300	> 400	> 600	> 800	> 1000
Flash time (μs)	2.2	1.1	0.8	0.6	0.4	0.3	0.2

It can be seen that high temperatures can be generated during the polishing process and although the flash times are on the order of a few microseconds, they can be adequate to generate the chemical reactions.

Jiang and Komanduri (1997) applied the Taguchi method for optimization of finishing conditions in the MFP of HIP'ed Si_3N_4 balls. The important parameters that influence the surface quality generated during final mechanical polishing of Si_3N_4 balls, with a suitable abrasive (material and grain size), are polishing load, abrasive concentration, and polishing speed. B_4C (1500 grit) abrasive with a grain size of 1-2 μm was used in this investigation. All the tests were carried out for 45 min. The smallest, standard 3-level orthogonal array (OA) L_9 (3^4) was used to design the experiments. The results are shown in Figures 2.14.1 and 2.14.2. It was found that the polishing load is the most significant parameter for improving the overall surface finish, R_a and R_t . The experimental results also indicated that within the range of parameters evaluated, a high level of polishing load, a low level of abrasive concentration, and a high level of polishing speed are desirable for improving R_a as well as R_t . The best surface finish obtained after polishing with B_4C 1-2 μm abrasive was R_a of about 20 nm and R_t of about 200 nm.

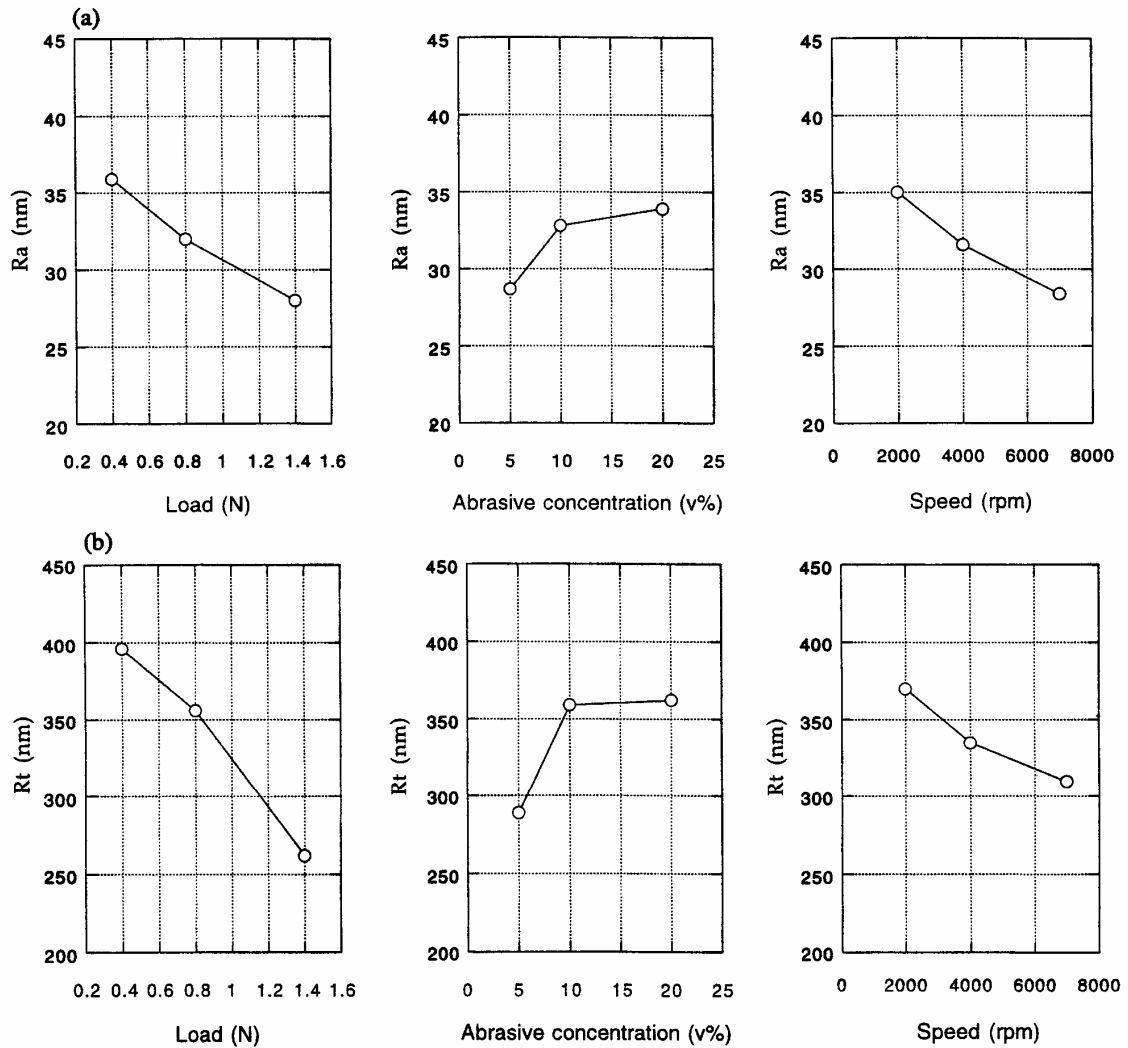


Fig. 2.14.1 (a) Plots of the response of each polishing parameter level on the surface finish, R_a
 (b) Plots of the response of each polishing parameter level on the surface finish, R_t
 [Jiang and Komanduri, 1997]

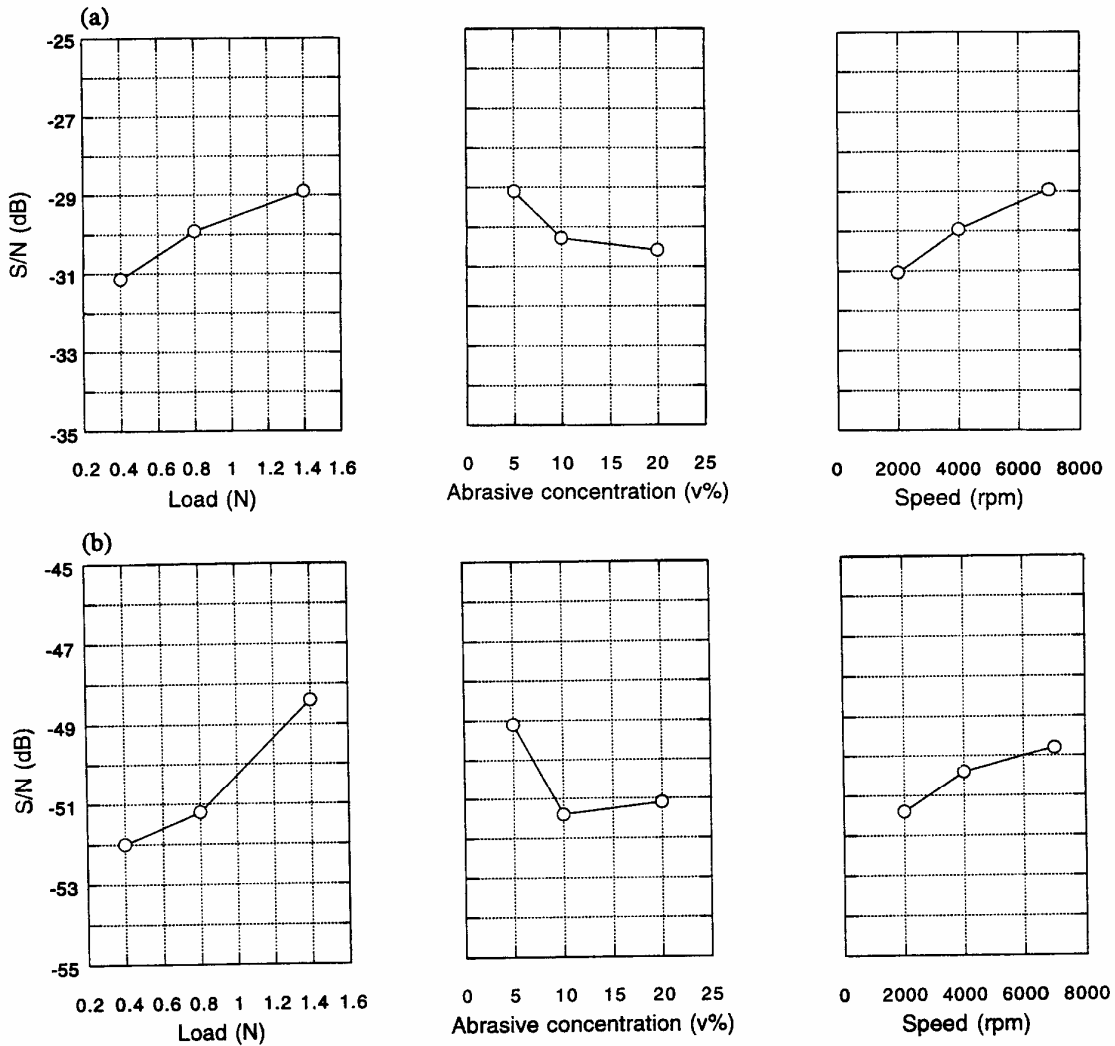


Fig. 2.14.2 (a) Plot of the S/N ratios showing the effect of each parameter level on the surface finish, Ra
 (b) Plot of the S/N ratios showing the effect of each parameter level on the surface finish, Rt
 [Jiang and Komanduri, 1997]

Jiang *et al.* (1998a,b) investigated chemo-mechanical polishing (CMP) of various abrasives in the finishing of HIP'ed Si_3N_4 balls by MFP. Among the abrasives investigated, CeO_2 and ZrO_2 were found to be most effective followed by Fe_2O_3 and Cr_2O_3 . Extremely smooth and damage-free surfaces with a surface finish, Ra of about 4 nm and Rt of about 40 nm were obtained after polishing with either CeO_2 or ZrO_2 abrasive.

A thermodynamic analysis (Gibb's free energy of formation) indicated that CeO_2 participates directly in the chemical reaction with Si_3N_4 workmaterial leading to the formation of a thin SiO_2 layer. The hardness of CeO_2 is closer to the thin layer of SiO_2 formed on Si_3N_4 but significantly lower than Si_3N_4 workmaterial ($\sim 1/3$). Thus, it can remove the thin brittle SiO_2 reaction product effectively without damaging the Si_3N_4 workmaterial. The removal of the reaction product by subsequent mechanical action is very important in CMP. The chemical reaction can proceed only if the passivating layers are removed by mechanical action at the same time. Thus, an extremely smooth and damage-free surface is formed on Si_3N_4 balls.

CMP of Si_3N_4 is particularly effective in a water environment. Water from the water-based magnetic fluid not only facilitates the chemo-mechanical interaction between the abrasive and workmaterial but also participates directly in the chemical reaction with the Si_3N_4 workmaterial, leading to the formation of a SiO_2 layer thereby enhancing CMP. The conductivity and dissolution value of an oil-based polishing fluid is nearly zero and the oil film between the abrasive and

the workmaterial prevents any chemical reaction between them, as well as the removal of reaction layer formed, if any, thus minimizing CMP.

After CMP, the Si_3N_4 ball surface would consist of an outer SiO_2 layer and an intermediate layer of silicon oxynitride ($\text{Si}_x\text{O}_y\text{N}_z$) on Si_3N_4 substrate. This is not much different from the Si_3N_4 workmaterial, which invariably has a natural oxidation layer in air even at room temperature. Also, the reaction products formed after CMP of Si_3N_4 with CeO_2 are much safer than those formed with Cr_2O_3 abrasive, from an environmental point of view [Jiang *et al.*, 1998a,b].

Jiang and Komanduri (1998c) developed a methodology for finishing HIP'ed Si_3N_4 balls from an as-received condition. It involved mechanical removal of material initially using harder abrasives with respect to workmaterial (of different materials of progressively lower hardnesses and grain sizes), followed by final chemo-mechanical polishing using preferably a softer abrasive, for obtaining superior finish with minimum surface or subsurface defects.

Three stages were identified in the MFP of Si_3N_4 balls, namely, roughing, semi-finishing, and final finishing. Initially, in the roughing stage, polishing was aimed at removing as much material as possible without imparting serious damage to the surface. Two coarser abrasives, B_4C 500 grit (17 μm) and SiC 400 grit (23 μm) were used to reach the desired diameter at high removal rates and at the same time improve the sphericity for proper ball motion. An intermediate stage of semi-finishing was introduced where size, sphericity, and surface finish had to be closely monitored. Two harder abrasives with finer grit size, namely, SiC 1000 grit (5 μm) and SiC 1200 grit (3 μm) were chosen at this

stage. The removal rates were much lower and the finish was much better than the roughing stage, but the emphasis was on improvement of sphericity. In the final stage, size, sphericity, and surface finish were closely controlled to meet the final requirements. SiC 8000 grit (1 μm) abrasive was used to approach the required diameter and sphericity and remove all deep valleys from the surface. This was followed by final chemo-mechanical polishing using softer CeO₂ (< 5 μm) abrasive, to produce balls of required diameter, sphericity, and surface finish, which was extremely smooth and damage-free by preferential removal of peaks from the surface.

SEM micrographs of the polishing shaft were taken after polishing with B₄C (500 grit) and B₄C (1500 grit) abrasives. They showed that the abrasives are not always embedded in the shaft, as pointed out by Childs *et al.* (1995), but actually abrade the softer stainless steel polishing shaft. Thus, while the action of abrasives is one of a two-body abrasion (i.e. sliding without rotation) as rightly pointed out by Childs *et al.*, they are not always fixed but sometimes move relative to the shaft [Hou and Komanduri, 1998b].

High material removal rates (1 $\mu\text{m}/\text{min.}$) with minimal subsurface damage were obtained with abrasives, such as B₄C or SiC due to use of flexible support system, small polishing loads (1 N/ball) and fine abrasives but high polishing speeds (~ 2000 - 4000 rpm for a 2.5 in. diameter shaft) due to rapid accumulation of minute amounts of material removed by microfracture. The as-received Si₃N₄ balls had a band (200 μm x 5 mm) at the parting line formed due to HIP'ing process. The initial diameter was 13.4 mm and had to be finished to 12.7 mm.

The actual polishing time was less than 20 hours. The sphericity was improved from an initial value of about 200 μm to less than 0.3 μm . The best sphericity obtained was 0.15 to 0.2 μm and best surface finish obtained was Ra of 4 nm and Rt of 40 nm without scratches or pits on the surface.

Rao (1999) monitored the vibrations generated during polishing of 17/32 - in. Si_3N_4 balls by magnetic float polishing. Mechanical polishing was done initially using B_4C (500 grit) and SiC (800 grit) abrasive with emphasis of material removal. Semi-finishing was done next using SiC abrasive (1000 and 1200 grit) to improve the sphericity without much material removal. Finishing was done with B_4C (1500 grit) with emphasis on sphericity of the balls. Chemo-mechanical polishing was performed next with CeO_2 ($< 5 \mu\text{m}$) abrasive to improve the surface quality of the balls.

The vibrations generated during polishing were recorded using two accelerometer pick-ups and a vibration monitoring device was used to convert the recorded vibrations into frequency spectrum versus time plots. A good set-up was indicated by one dominant frequency, called as excitation frequency in the whole frequency spectrum. During the initial period of the polishing run, more than one frequency would appear. Later, if the polishing set-up was good, only one excitation frequency would be seen with all other frequencies having negligible amplitude. The amplitude of vibration was found to decrease linearly with decrease in the ball sphericity. Any discrepancy would indicate a faulty set-up and the machine could be stopped without further deteriorating the sphericity. This could help to prevent the wastage of material as well as time.

Lakshmanan (2000) polished large diameter and large batch of Si_3N_4 balls using the large batch MFP apparatus. The chamber had to be aligned with the polishing spindle in a similar manner as in small ball polishing apparatus. The three-stage methodology of roughing, semi-finishing, and final finishing developed by Jiang and Komanduri (1998c) was applied. Taguchi method was used to determine the optimum load and speed conditions for polishing 1/2 inch Si_3N_4 balls. A load of 3 N/ball and speed of 200 rpm were found suitable in the roughing stage and a load of 3 N/ball and speed of 300 rpm were found suitable for intermediate stage in terms of good sphericity and uniform material removal.

A large batch consisting of 55, 17/32 in. Si_3N_4 balls was finished with a diametric tolerance of ± 0.001 mm, sphericity of 0.2 - 0.55 μm , surface finish, Ra of 7.2 - 10.4 nm and Rt of 66.3 - 184.3 nm. The total processing time was reduced considerably ($\sim 1/3$) by using the same set-up for more than one polishing run (5 - 6 runs) as compared to the time required for polishing the same batch with different set-ups for each polishing run. Besides this, the non-repeatability of the apparatus alignment was avoided.

The variation in the critical parameters such as sphericity, surface finish, and diametric tolerance among the sample size selected and in a single ball was found out using average and range charts. Based on the results, it was concluded that the process was in controlled variation.

CHAPTER 3

PROBLEM STATEMENT

As discussed under literature review, silicon nitride balls of various sizes have been successfully finished using the magnetic float polishing technology, with small as well as large batch polishing apparatus. However, in the earlier experimental set-ups, the chamber had to be precisely adjusted with the spindle for obtaining good results. In the polishing process, a groove is formed on the bevel of the spindle, which has to be periodically machined. The spindle had to be frequently removed from the polishing machine in order to perform machining on a lathe. This procedure was laborious and time consuming, especially for a large diameter spindle. Furthermore, the alignment of the spindle was crucial for obtaining good repeatability. The number of polishing runs required to finish a batch were quite high. The over-all processing time was significantly reduced by using the same set-up for more than one polishing run. However, the influence of the groove on sphericity was needed to be investigated. Further, to expand the capability of the magnetic float polishing process, finishing large size and large batch of silicon nitride balls were needed. This was accomplished in the present work using following tasks:

1) A new set-up was designed and built by modifying an existing apparatus in order to finish a large diameter and large batch of silicon nitride balls (46 balls of 3/4 in. diameter).

2) *In-situ* machining of the polishing spindle was performed in order to improve roundness and geometric alignment of the spindle.

3) A fixture was built for *in-situ* machining of the groove formed on the bevel of the spindle.

4) Another fixture was built for fabricating floats to precise dimensions.

5) A different technique was used in which the chamber was made to self-align with the spindle during polishing.

6) The main emphasis of this work was on reducing the total polishing runs required to finish a batch in order to reduce the total processing time and cost. This is possible using a sound set-up and right procedure.

7) Polishing parameters were optimized for obtaining high material removal rate using Taguchi method.

8) The effect of the groove formed on the bevel of the spindle was studied in order to improve the sphericity.

9) The previously established methodology was further developed for rapidly finishing a batch from the as-received condition to the finished condition.

CHAPTER 4

APPROACH

4.1 INTRODUCTION

The major emphasis of this investigation was on finishing large size and large batch of silicon nitride balls (46 balls of 3/4 in. diameter) using the large batch magnetic float polishing (MFP) apparatus. The polishing set-up plays a very important role in finishing balls suitable for bearing applications. The set-up was jointly developed with Robert Gerlick. A spindle was made according to the dimensions of a pre-existing chamber. It was machined on the machine tool, which was used for polishing. This resulted in improving the roundness and geometric alignment of the spindle. Polishing was performed in such a way that the chamber was able to self-align with the spindle. A fixture was built for *in-situ* machining of the groove formed on the bevel of the spindle during polishing. This improved the spindle accuracy as well as reduced the processing time and effort. Another fixture was built for fabricating acrylic floats to precise dimensions. The main aim during the initial stage of polishing was to reduce the ball diameter rapidly. Taguchi method was applied to determine optimum conditions for getting a high maximum material removal rate. The three-stage methodology of roughing, semi-finishing, and final finishing was implemented for finishing Si₃N₄ balls from the as-received condition to the final finished condition. The effect of

the groove formed on the bevel of the spindle during polishing was investigated. The characterization of Si_3N_4 balls including ball diameter, sphericity, and surface finish was evaluated using a micrometer, TalyRond, and TalySurf.

4.2 SALIENT FEATURES OF MAGNETIC FLOAT POLISHING TECHNOLOGY

The most prominent characteristics of the magnetic float polishing technology are:

1. High material removal rate
2. Good surface finish
3. Good sphericity

In addition, this technique can handle small as well as large batches. The process does not use diamond abrasives and is considerably faster than conventional V-groove lapping. This process does not require high precision capital intensive machine tools and the experimental set-up is quite simple. Thus, MFP is an efficient and cost-effective process for finishing silicon nitride balls from the as-received condition.

4.2.1 High material removal rate

The main mechanism for material removal in either lapping or magnetic float polishing of ceramic balls is sliding at the contact region between the balls and abrasives embedded in the polishing spindle. The material removal rates in magnetic float polishing are higher than conventional V-groove lapping because there is more sliding involved in the process. This can be accounted in two ways.

(1) The polishing load used in magnetic float polishing is considerably lower than conventional lapping. Hence, the frictional force at the contact region is significantly reduced. Consequently, there is more sliding than rolling.

(2) The polishing speeds used in magnetic float polishing are quite high, as compared to the conventional lapping. The increase in the relative speed also tends to increase the sliding motion [Jiang, 1998d].

4.2.2 Good surface finish

The polishing load applied on the ceramic balls in magnetic float polishing is very low (~ 1 N/ball) and is applied in a controlled manner, by using magnetic buoyancy force of a float. Also, the abrasives used in this process are comparatively softer than the diamond abrasive, which is used in conventional lapping. This helps in minimizing the surface as well as sub-surface damage of the balls. Chemo-mechanical polishing is applied in the final stage to improve the surface finish by using an abrasive, which is softer than the workmaterial. The reaction products formed on the surface of the balls are subsequently removed by frictional action resulting in an extremely smooth and damage free surface.

4.2.3 Good sphericity

The mechanism for obtaining good sphericity in either lapping or magnetic float polishing is that when a ball of larger diameter (or a larger diameter portion of the ball) enters the contact area, the load on the ball is increased and a larger amount of material is removed from this place. This process is continued until all

balls are of uniform diameter, resulting in an improvement of sphericity. In magnetic float polishing, the ball has three contact points resulting in two main ball motions. They are:

- (1) Rotation around the axis parallel to the contact area
- (2) Spinning around the axis vertical to the contact area

The rotation of the ball is the motion for polishing, and the spinning of the ball is the feed for polishing. The combination of the above two ball motions leads to uniform removal of material resulting in an improvement in sphericity [Jiang, 1998d].

4.3 LARGE BATCH MAGNETIC FLOAT POLISHING APPARATUS

Figures 4.1 - 4.2(a)-(b) show photographs of the machine tool and experimental set-up, and Figure 4.3 shows the schematic of the experimental set-up used in this investigation. A 304 L stainless steel spindle having a bevel of 35° is held in the arbor of the machine tool. Linear bearings are used to allow the worktable to move vertically on four columns mounted on the CNC table. An aluminum plate is precisely leveled on top of the worktable. An aluminum chamber has permanent magnets (Nd-Fe-B) in the steel base as shown in Figure 4.4. It consists of several magnets mounted adjacent to each other with alternate N and S poles as shown in Figure 4.5. The magnetic field intensity distribution of the chamber base is also shown in Figure 4.5. The inner surface of the chamber is covered with a urethane liner (Hardness: 90 Shore A, 1 mm thk.), in order to prevent it from wear due to the motion of the balls. An acrylic plate (PMMA) is

fixed (taped) to the chamber bottom in order to have a smooth surface. Another acrylic plate is centrally placed on the aluminum plate and six rolling elements (balls) are equally placed on it. The chamber is then positioned on the top of these balls and is held in place by means of four locking screws. A nylon string is attached, as shown in Figure 4.3 (b) to prevent the rotation of the chamber when the spindle is set into rotation. The arrangement is such that uniform tension is maintained in the string.

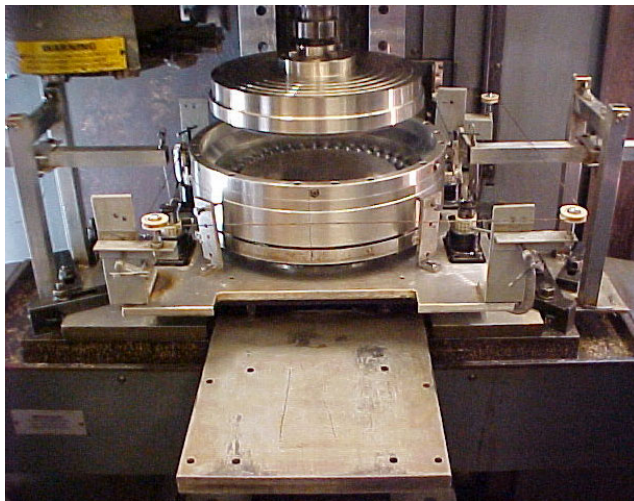
Balls to be polished are placed on top of an acrylic float and the chamber is loaded with a mixture of magnetic fluid and abrasive. The magnetic fluid is subjected to a magnetic field gradient in the vertical direction, and all non-magnetic materials are levitated by the upward buoyancy force. The chamber is moved under the spindle and a balancing weight is applied on the counter-weight system. Additional weights are applied depending upon the load requirement on the balls. The spindle is then brought down inside the chamber and the gap between the spindle and the chamber is kept constant. The spindle is further lowered to contact the balls until the counter-weight arms are flat with the desired level of load applied on the balls.

The balls make a three point contact, namely, with the spindle at the top, urethane liner on the side, and the float at the bottom. The locking screws are loosened and the spindle is set into rotation. As the chamber is free to move in horizontal direction, it self-aligns below the spindle. A gradual increase in the polishing speed is preferable as sudden increase of speed may result in a jerk

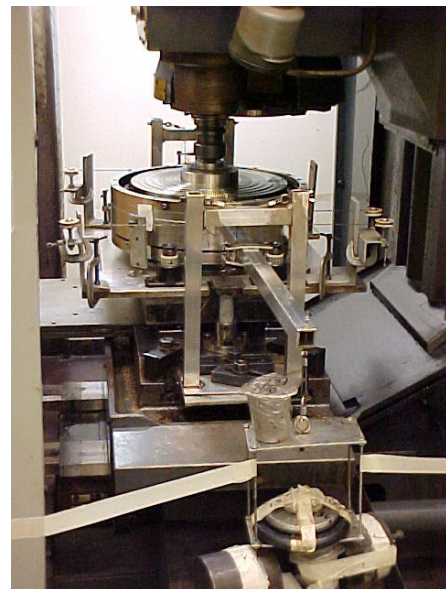
affecting the alignment of the chamber. The locking screws are then set to barely touch the chamber during operation.



Fig. 4.2 Photograph of the machine tool used for polishing



(a)



(b)

Fig. 4.2 Photographs of the experimental set-up (a) front view (b) side view

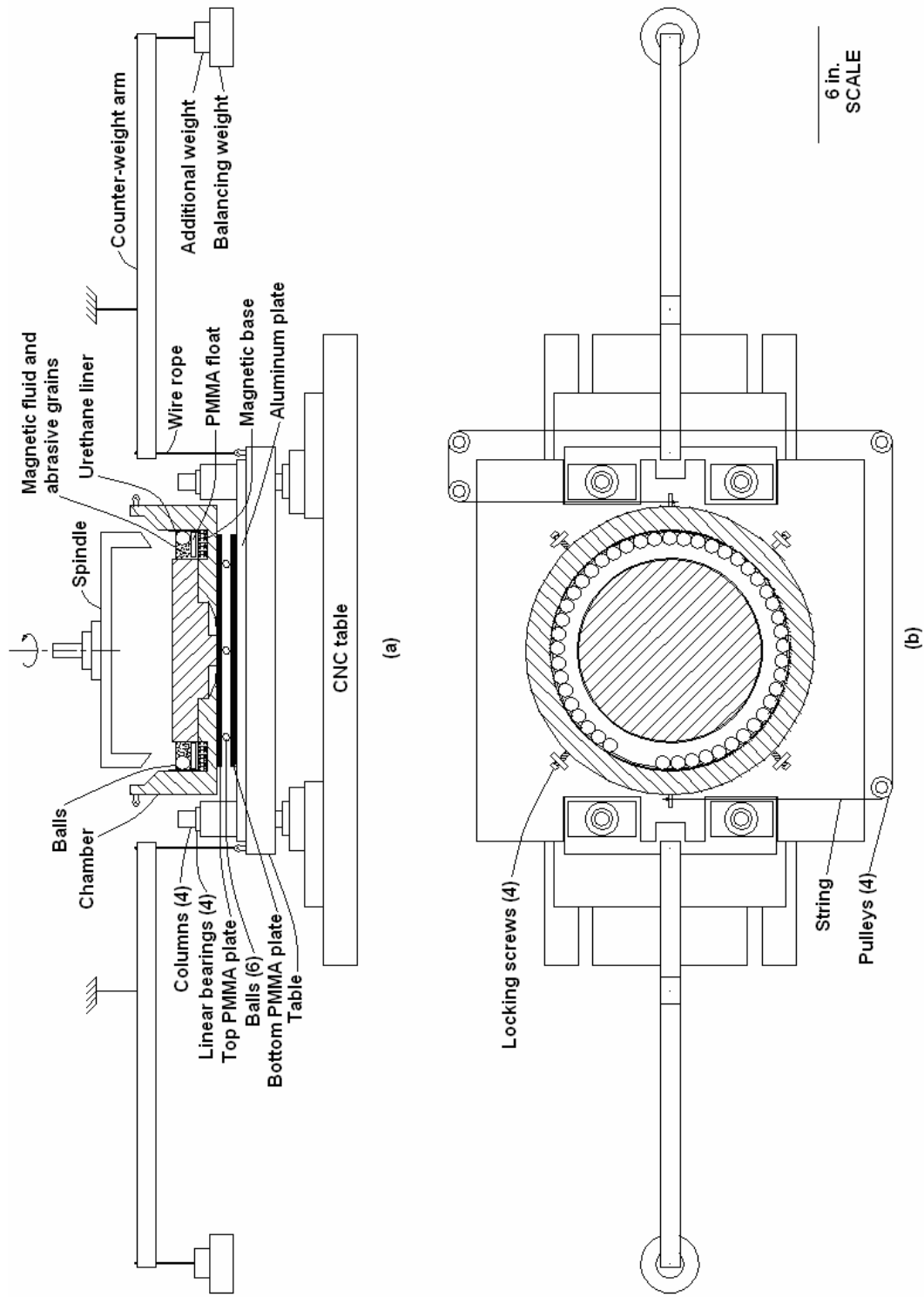


Figure 4.3 Schematic of the experimental set-up (a) front view (b) top view

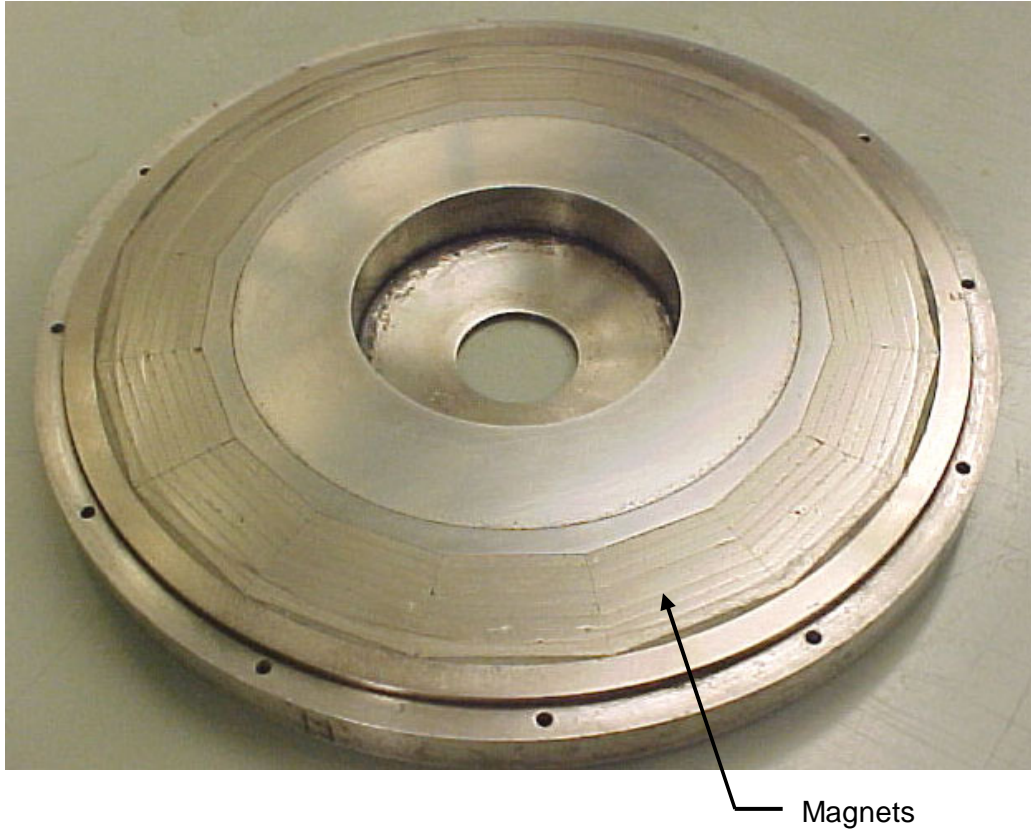


Fig. 4.4 Photograph showing arrangement of magnets in the chamber base

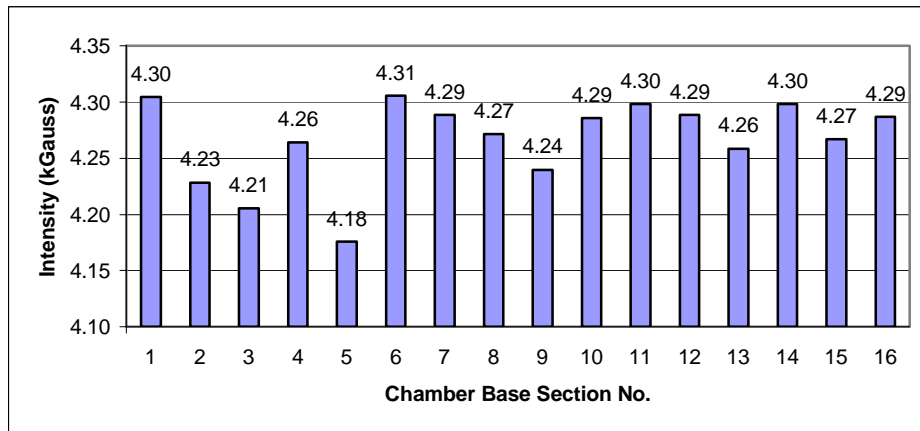
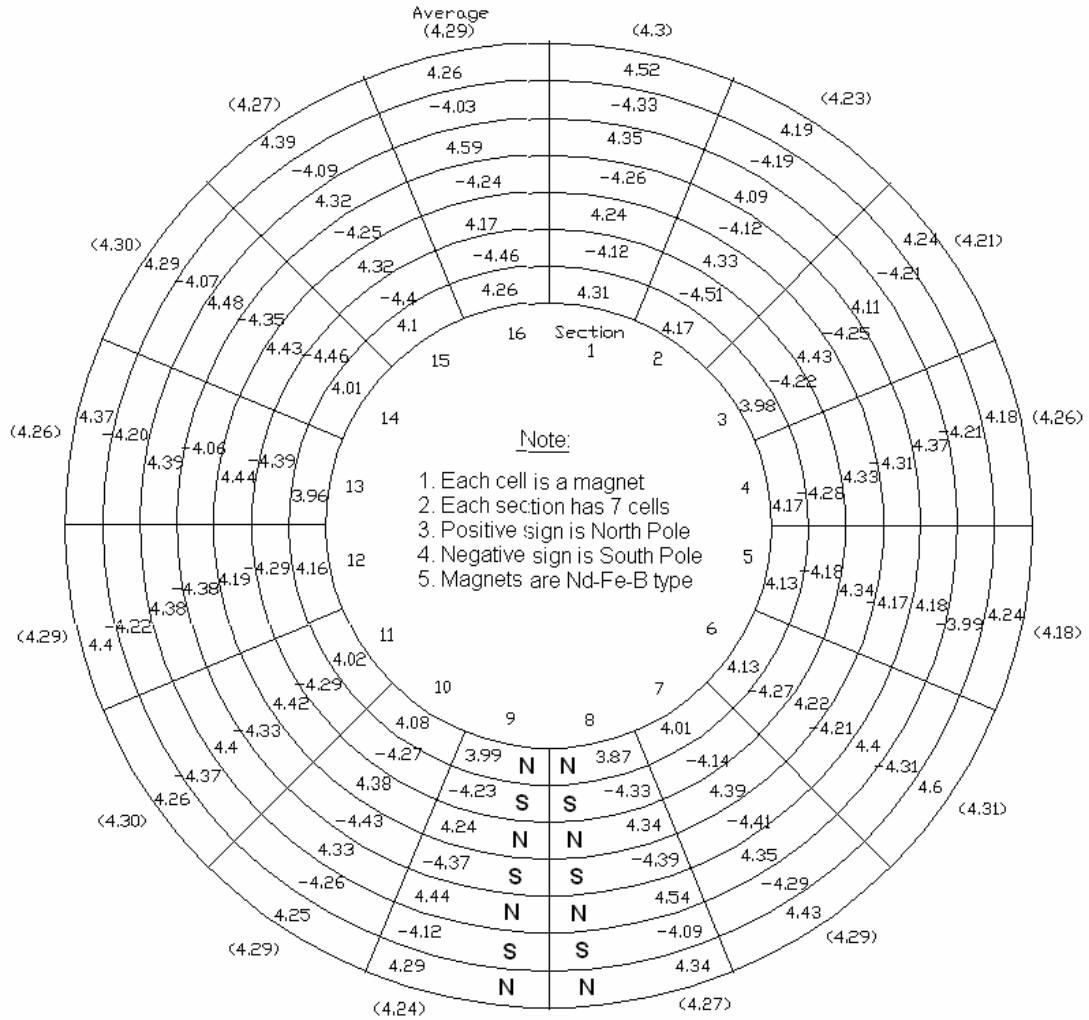


Fig. 4.5 Magnetic field intensity distribution of chamber base (Average intensity: 4.27 kGauss)

4.4 DETAILS OF POLISHING SPINDLE

The spindle was made from S.S 304 L pipe (O.D. 12.75 inch, I.D. 10.8 inch and height 2.6 inch) and S.S 304 L plate (O.D. 11.9 inch and thickness 0.7 inch). A holder was precisely machined and fixed at the center of the plate by means of screws. The plate was then machined in order to make the center of the holder coincide with that of the plate. After making a bevel of 30° on the pipe and plate, they were welded together. The quality of the weld is important as any porosity may result in uneven mass, affecting the motion of the spindle especially at high speeds. The heat affected zone generated due to welding can affect the removal of material during polishing. These problems can be avoided by using a different approach for making the spindle.

The rough machining of the spindle was done on a lathe and the final machining was done on the machine tool, which was eventually used for polishing. The final dimensions of the spindle pipe (O.D 12.2 inch, I.D 10.7 inch and height 2 inch) had to be made according to the chamber dimensions and available space. It is preferable to make the spindle I.D less than 10.7 inch in order to polish balls of larger than 3/4 inch diameter. The lower end of the spindle was beveled at 35°. A gap of 0.15 inch was kept between the spindle O.D and chamber I.D. Figures 4.6 - 4.9 show the set-ups used for machining the spindle. A mirror (not shown) was used for machining the inner surfaces of the spindle.

The *in-situ* machining of the spindle helps in improving the roundness as well as geometric alignment of the spindle with respect to the chamber. This

results in uniform removal of material from the worksurface and consequently leads to improvement in sphericity.

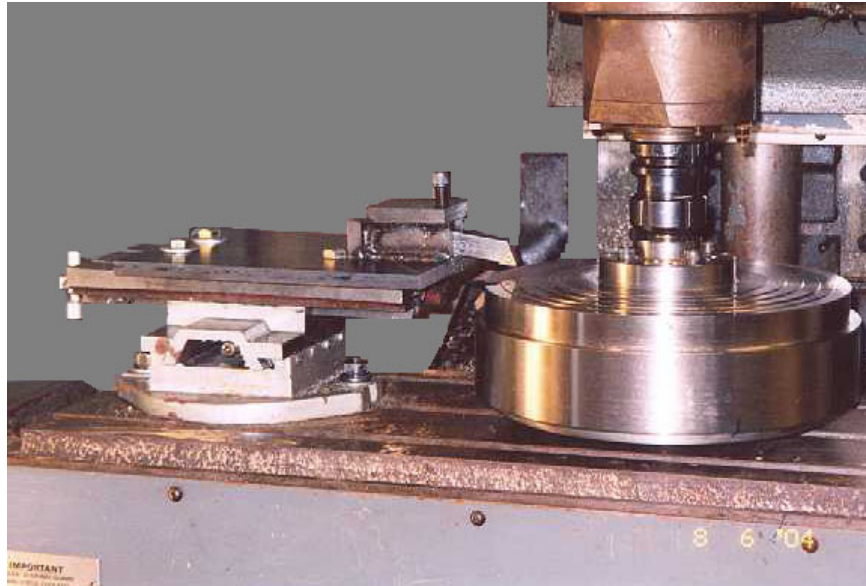


Fig. 4.6 Photograph of the set-up used for machining the top and side surface of the spindle

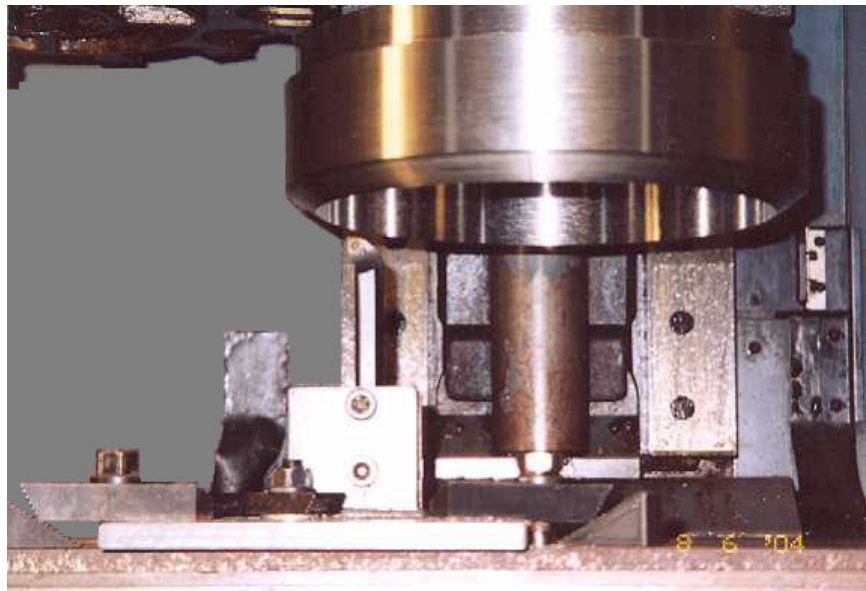


Fig. 4.7 Photograph of the set-up used for machining the inner surfaces of the spindle

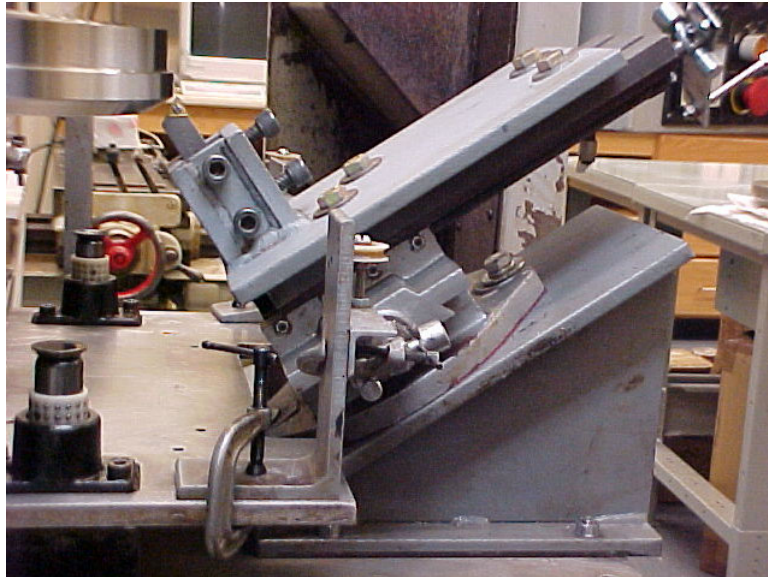


Fig. 4.8 Photograph of the fixture used for machining the bevel of the spindle

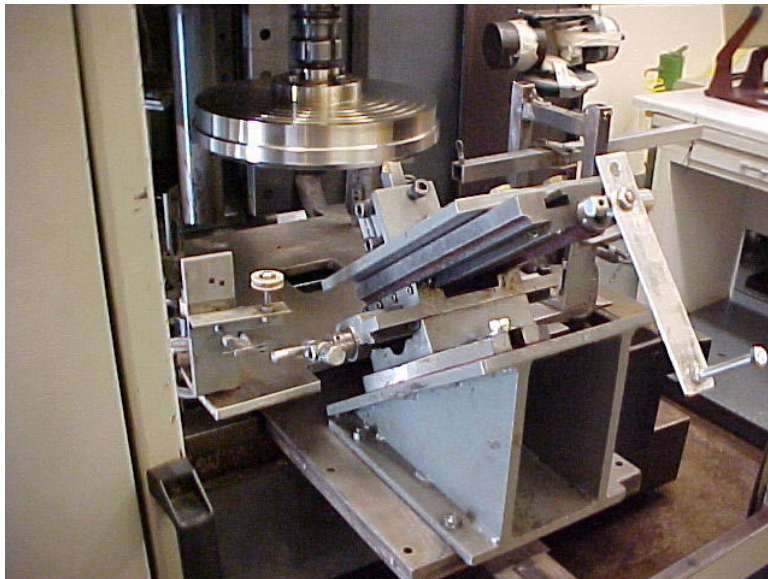


Fig. 4.9 Another photograph of the fixture used for machining the bevel of the spindle

4.5 FACTORS AFFECTING SPHERICITY

Uniform removal of material from the ball surface is essential for getting good sphericity. The apparatus construction and polishing set-up play an important role for obtaining good sphericity.

4.5.1 Factors related to apparatus construction:

1) The dynamic response of the polishing spindle will depend on the bearings and the rigidity of the machine tool spindle. This may affect the amplitude of vibrations of the polishing spindle at high speeds.

2) The coaxiality of the polishing spindle with the machine tool spindle is very important. *In-situ* machining of the polishing spindle improves its roundness and geometric alignment as shown in Figure 4.10(a). However, the spindle can also be balanced in order to improve sphericity further.

3) The axis of the chamber wall should be perpendicular to the chamber bottom. Also, the inner surface of the chamber which comes in contact with the balls should have good roundness. Earlier, a polyurethane resin liner ring was used on the inner surface of the chamber. Continuous use of this ring caused the chamber to become out of round. To solve this problem, the polyurethane resin liner ring was replaced by an aluminum ring and was covered with a replaceable urethane liner.

4) The magnetic field intensity should be consistent all over the chamber base in order to levitate the float uniformly.

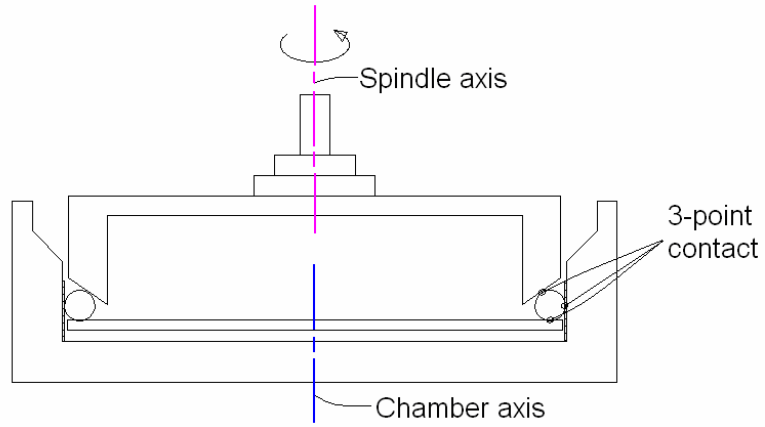
5) The leveling of the plate beneath the chamber is very important and has to be done properly.

6) Friction in the linear bearings may affect the motion of the table supporting the chamber. Periodic lubrication and cleaning of the bearings is necessary for proper motion of the worktable.

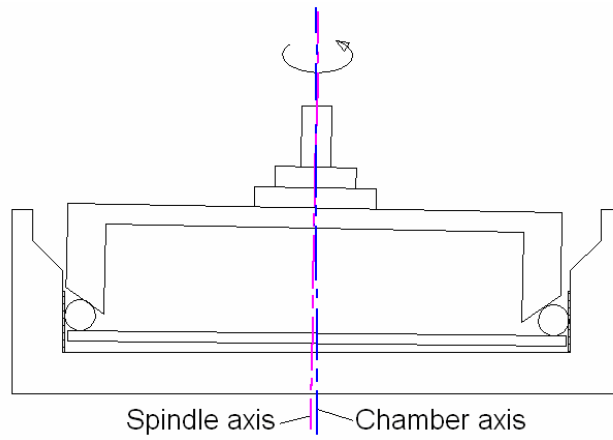
4.5.2 Factors related to polishing set-up:

1) Maintaining the coaxiality between the rotating axis of the polishing spindle and the chamber wall is most important, as shown in Figure 4.10(a). Any mis-alignment between the spindle and chamber axis (as shown in Figures 4.10 (b) - (c)) can lead to non-uniform application of load on the balls, which may consequently lead to non-uniform removal of material resulting in high sphericity values. *In-situ* machining of the spindle and self-aligning method helps to maintain proper alignment of the chamber with the spindle.

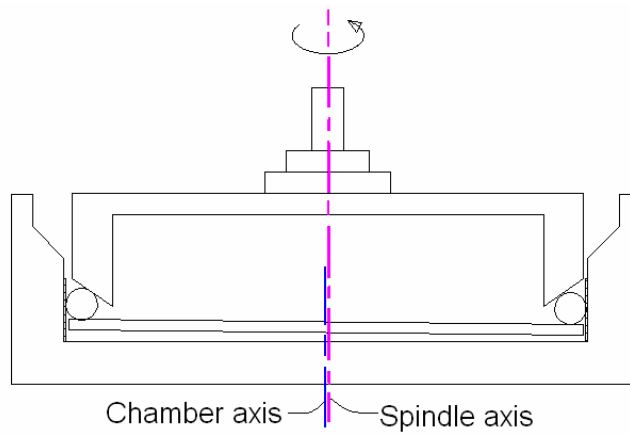
2) Abrasive wear occurs on the polishing spindle, the polishing float, and the polyurethane liner during polishing. The float and the liner can be replaced periodically. A groove is formed on the bevel of the spindle, which has to be periodically machined for obtaining a high material removal rate and good surface finish. Maintaining the groove is favorable for improving the sphericity of the balls. The earlier method was to remove the spindle from the machine tool and machine it on a lathe. However, this was laborious and time consuming. Also, the spindle used to remain out-of-round by 0.0001 to 0.001 inch. *In-situ* machining of the groove is beneficial, which resulted in no deflection on the dial gauge (resolution of 0.0001 inch). This also saved time and effort.



(a) Proper alignment



(b) Spindle axis tilt



(c) Chamber offset

Fig. 4.10 Alignment possibilities of the chamber with respect to the spindle

3) The junction thickness of the polyurethane liner fitted on the inner surface of the chamber has to be closely matched in order to have a proper ball motion.

4) The float was found to be convex on one side and concave on another. The flat surface of the float may be necessary for improving the sphericity further. Figure 4.11 shows the fixture used for making floats. A gap of 1.5 mm was kept between the float and the chamber.

5) The magnetic fluid gets evaporated, especially at higher load and higher speeds. Maintaining the fluid level is important as fluid dry-up may result in degradation of sphericity.

6) Repeatability of the polishing set-up plays an important role in improving the sphericity of the balls.

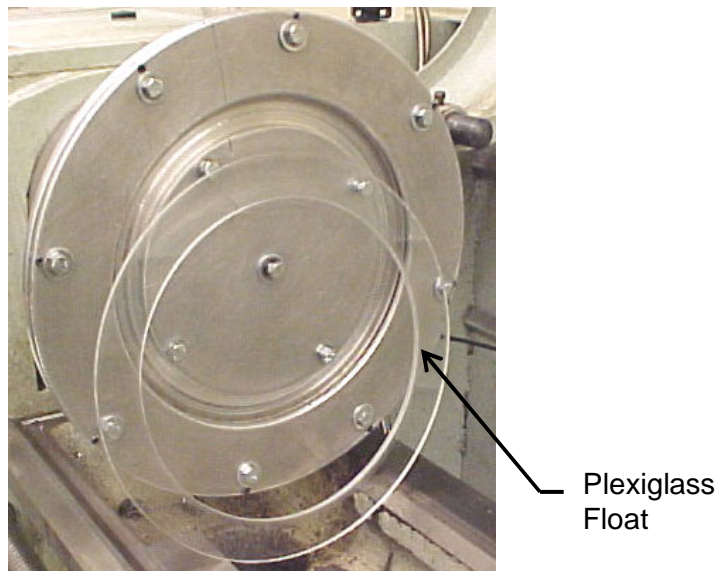


Fig. 4.11 Photograph of the fixture used for fabricating the floats

4.6 SILICON NITRIDE WORKMATERIAL

The ball material used in this investigation is hot-isostatic pressed silicon nitride (HIP'ed Si_3N_4) NBD 200 from Norton Advanced Ceramics. Si_3N_4 is predominantly a covalent material. The microstructure of Si_3N_4 consists of two crystalline phases, namely, a hard α phase and a tough β phase, which are hexagonal in structure. The β - Si_3N_4 phase (a-axis 0.759 - 0.761 nm, c-axis 0.271 - 0.292 nm, $c/a \sim 0.37$) is more elongated than α - Si_3N_4 phase (a-axis 0.775 - 0.777 nm, c-axis 0.516 - 0.569 nm, $c/a \sim 0.7$). The silicon atoms are located in the centre of irregular nitrogen tetrahedral, each nitrogen atom belonging to three tetrahedral [Ziegler *et al.*, 1987]. α - Si_3N_4 is more energy-rich metastable phase. However, it becomes unstable at high temperatures and is converted to β - Si_3N_4 phase.

The manufacture of Si_3N_4 balls generally starts with a Si_3N_4 powder which is milled in either alcohol or water with appropriate sintering aids such as MgO or Y_2O_3 . At the end of milling process, binders are added to the mixture to enhance formability in later operations. The milled slurry is then spray dried to make a flowable, compactable powder. The powder is then pressed into blanks using uniaxial or isostatic methods. The "green" ball blank is then air-fired to remove binders and HIP'ed at extremely high temperatures (>1700 °C) and pressures (>300 MPa) to optimize densification and microstructure [Saint Gobain Ceramics website].

The chemical composition and typical properties of NBD-200 Si₃N₄ ball (β -Si₃N₄, uniaxially pressed with 1 wt. % MgO as main sintering aid) are given in Tables 4.1 and 4.2. Compared to other manufacturing methods, HIP'ing provides a nearly fully theoretically dense product resulting in enhanced mechanical properties. A complex glassy phase is created at the grain boundaries during the high temperature hot pressing of Si₃N₄. It is primarily a magnesium silicate modified by Ca, Fe, Al, and other impurities present in Si₃N₄.

Table 4.1 Chemical composition of NBD-200 Si₃N₄ ball
[Hah *et al.*, 1995, Jiang, 1998d]

Mg	Al	Ca	Fe	C	O	Si ₃ N ₄
0.6 - 1.0	≤ 0.5	≤ 0.04	≤ 0.17	≤ 0.88	2.3 - 3.3	94.1 - 94.7

Table 4.2 Mechanical and thermal properties of Si₃N₄ ball
[Hah *et al.*, 1995, Jiang, 1998d]

PROPERTY	VALUE
Flexural Strength, MPa	800
Weibull Modulus	9.7
Tensile Strength, MPa	400
Compressive Strength, GPa	3.0
Hertz Compressive Strength, GPa	28
Hardness, Hv (10kg), GPa	16.6
Fracture Toughness, K _{1c} , MNm ^{-3/2}	4.1
Density, g/cm ³	3.16
Elastic Modulus, GPa	320
Poisson's Ratio	0.26
Thermal Expansion Coefficient at 20-1000°C, / °C	2.9 x 10 ⁻⁶
Thermal Conductivity at 100° C, W/m-K	29
Thermal Conductivity at 500° C, W/m-K	21.3
Thermal Conductivity at 1000° C, W/m-K	15.5

4.7 ABRASIVES

Table 4.3 gives a list of abrasives used in this study. They are classified into two groups, one for mechanical polishing and the other for chemo-mechanical polishing, depending upon their hardness and chemical activity with respect to the workmaterial. Mechanical polishing was performed using boron carbide (500grit- $\sim 12\mu\text{m}$) and silicon carbide (600grit- $\sim 10\mu\text{m}$, 1200grit- $\sim 2.1\mu\text{m}$, 10,000grit- $\sim 0.5\mu\text{m}$) abrasives with progressively lower hardness and grain sizes, in order to reduce the diameter and improve the sphericity and surface finish. The material removal is predominantly by mechanical micro-fracture with these abrasives, which reduces with the hardness and grain size of the abrasive. The chemo-mechanical polishing was performed with an abrasive softer than the workmaterial, namely, cerium oxide (CeO_2). The main emphasis in using this abrasive was to improve the surface finish with minimal surface or sub-surface damage. The material is removed by the tribo-chemical action of the abrasive with the workmaterial in a suitable environment.

Table 4.3 Properties of the abrasives used in this study [Jiang, 1998d]

Abrasive	Density g/cm^3	Knoop Hardness kg/mm^2	Elastic modulus GPa	Melting point $^\circ\text{C}$
B_4C	2.52	2800	450	2450
SiC	3.2	2500	420	2400
CeO_2	7.13	625	165	2500

* All the abrasives except CeO_2 were obtained from Saint-Gobain Abrasives
 CeO_2 was obtained from Aldrich Chemicals

4.8 MAGNETIC FLUID

The magnetic fluid (also called Ferrofluid) is a colloidal dispersion of extremely fine (100 to 150 Å) sub-domain particles, usually magnetite (Fe_3O_4), in liquid carrier, such as water or kerosene. Ferrofluids are made stable against particle agglomeration by the addition of surfactants. In this investigation, water based magnetic fluid was used. Table 4.4 gives the characteristics of W 40 magnetic fluid.

Table 4.4 Characteristics of W 40 magnetic fluid used in this study

Appearance	Black liquid
Density (g/cm^3) at 25 °C	1.4 ± 0.02
Viscosity (cp) at 25 °C	25 ± 7
Magnetization (gauss) at 10 KOe	380 ± 30
Boiling point (°C)	100
Flash point (°C)	nothing
Applicable thermal range (°C)	10 - 80
Base liquid	water

* The magnetic fluid was obtained from Taiho Industries Co. Ltd., Japan

In the absence of a magnetic field, the magnetic moments of the individual particles are randomly distributed and the fluid has no net magnetization. When a magnetic field is applied to a ferrofluid, the magnetic moments of the particles orient along the field lines almost instantly. The magnetization of the ferrofluid immediately responds to the changes in the applied magnetic field (H), and when the field is removed the moments randomize quickly. The magnetization (M-H) curve of the magnetic fluid used in the present study is given in Figure 4.12.

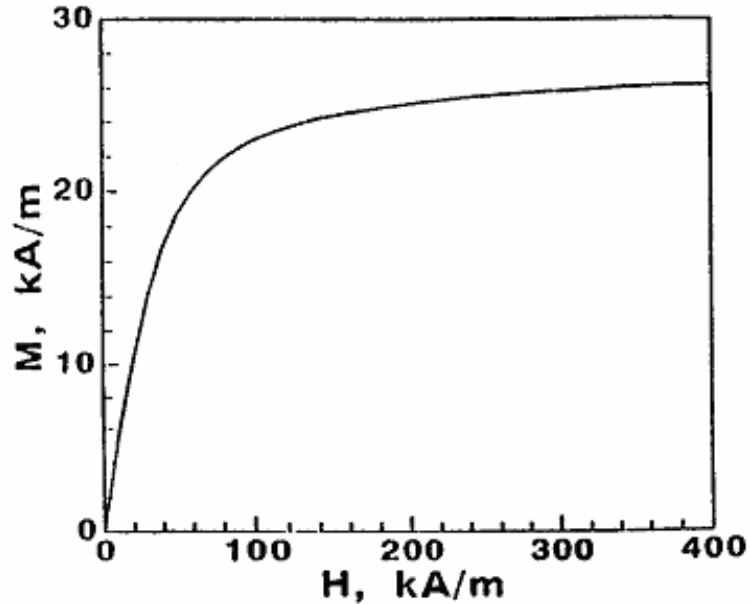


Fig. 4.12 Magnetization (M-H) curve of W 40 magnetic fluid used in present study [Raghunandan *et al.*, 1998]

In a gradient magnetic field, the particles experience a force such that the whole fluid responds as a homogeneous magnetic liquid, which moves to the region of highest flux. Due to this, any non-magnetic material (float, balls, and abrasives in this case) when placed in the ferrofluid experiences a force which tends to push the non-magnetic body in a region of lower flux. This force, called buoyancy or levitational force is proportional to the gradient of the external field and magnetization value of the fluid. Thus, the balls are pushed by the float against the spindle, with an upward buoyant force F_b . The magnetic buoyant force, F_b , can be changed by changing the gap between the magnets and the float, and by changing the magnetic field. This force is utilized for polishing in MFP process.

4.9 EVALUATION OF SURFACE INTEGRATION

4.9.1 Evaluating roundness by number

The out-of-roundness of a part is the difference between the greatest and the least distance of the profile from a centre. Four different reference circles (Figures 4.13 - 4.16) are used to which the measured data can be fitted for assessment. They are: least squares circle (LS), minimum zone circles (MZ), minimum circumscribed circle (MC), and maximum inscribed circle (MI). The least squares reference figure is calculated to be a circle fitted through the data such that the sum of the deviations inside and outside of that circle is at a minimum. The minimum zone reference figure is calculated as the two concentric circles, which totally enclose the data, such that the radial separation between them is a minimum. The minimum circumscribed reference figure is calculated to be the smallest circle that totally encloses the data. The maximum inscribed reference figure is calculated to be the largest circle that totally enclosed by the data [TalyRond User's Handbook]. Least squares circle method is used for measuring roundness in this study.

4.9.2 TalyRond 250

The roundness of the silicon nitride balls was measured using Rank Taylor Hobson's TalyRond 250. This is a computer controlled stylus instrument having a variable inductance pick-up (transducer). It has a worktable and two motorized axes for measurement (the worktable and the vertical straightness unit) and one motorized axis for gauge contact. It is capable of measuring roundness, vertical straightness, squareness, parallelism, flatness, co-axiality, cylindricity,

concentricity, eccentricity, runout, etc. The limit of error for roundness from the worktable and pick-up spindle is about $0.05 \mu\text{m}$ ($0.04 \mu\text{m} + 0.0003 \mu\text{m}/\text{mm}$ height above the worktable).

The stylus tip, a sapphire ball (diameter of 2 mm) contacts the surface of the ball, which is fixed to the rotating worktable (6 rpm). Variable inductance pick-up is used to convert the minute movements of the stylus into proportionate variations of an electrical signal. The signal is amplified and used to operate the recorder. A 2CR filter (2 stage CR networks) with a cut-off of 50 upr (undulations per revolution) is used in the present study.

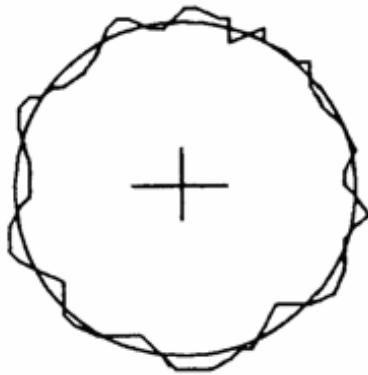


Fig. 4.13 Least squares reference circle
[TalyRond 250 User's Handbook]

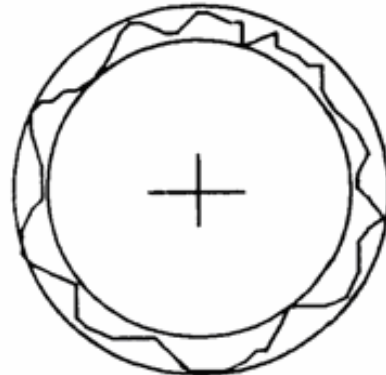


Fig. 4.14 Minimum zone reference circles
[TalyRond 250 User's Handbook]

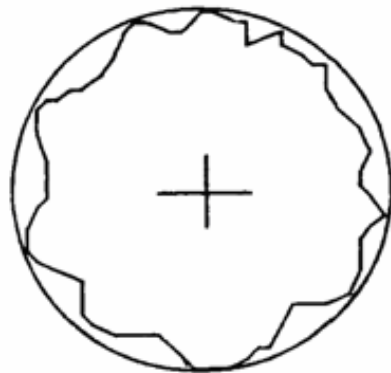


Fig. 4.15 Minimum circumscribed reference circle
[TalyRond 250 User's Handbook]

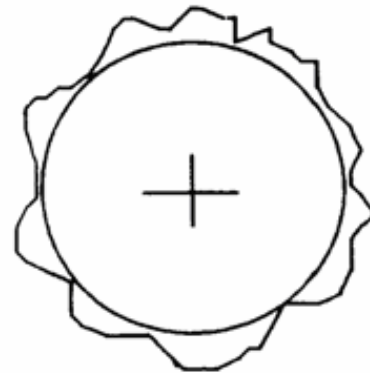


Fig. 4.16 Maximum inscribed reference circle
[TalyRond 250 User's Handbook]

4.9.3 Evaluating surface finish by number

In the magnetic float polishing process, the surface roughness obtained after mechanical polishing generally has a symmetric profile. However, the surface roughness profile can be unsymmetrical after final chemo-mechanical polishing, due to preferential removal of peaks from the surface leaving the valleys intact. The values obtained from the measuring instruments should truly quantify the nature of the surface evaluated. Ra is the arithmetic average value of the departure of the profile from the centre line throughout the sampling length. It represents the average roughness. Any irregularity, such as a non-typical peak or valley is averaged out and has a little influence on the value. Rt is the vertical distance between the highest and lowest points of the roughness profile. This value can directly represent the irregular surface defects present in the surface. Both Ra and Rt values are used to evaluate the surface roughness in this study.

In the stylus type of measuring instruments, the stylus shape and size affects the accuracy of the surface profile. If the stylus tip radius is large compared to the curvature of the surface, the movement of the stylus will not accurately follow the contour of the surface.

4.9.4 TalySurf 120L

The surface finish of the silicon nitride balls was measured by Rank Taylor Hobson's TalySurf 120L. This is a computer controlled stylus instrument having a laser interferometric pick up (transducer) with a 120 mm traverse unit. A straightness datum is used to enable measurements upto 120 mm long without

reference to any external straight line datum. It is capable of measuring the roughness using high frequency band pass filter, and waviness using low frequency band pass filter. It has a vertical resolution of 10 nm and a horizontal resolution of 0.25 μm for using a standard conisphere diamond with a tip radius of 2 μm . The force applied to the sample by the stylus over the full range is 0.7 - 1 mN and the measuring speed is 0.5 mm/sec. An ISO 2 CR (2 stage CR networks) filter with a cut-off of 0.08 mm is used, which suppresses the lower frequencies of waveform. This filter gives a transmission of 75% at its cut-off. This means that the amplitudes of irregularities having a spacing equal to the cut-off length will be reduced to 75% of their true value. The amplitudes of shorter wavelength irregularities will be almost unchanged, while those of longer wavelength will be progressively reduced.

4.10 EXPERIMENTAL WORK

1) The polishing shaft was driven using a vertical machining center (Bridgeport-Interact 412) with a stepped speed regulation in the range of 40 to 4000 rpm.

2) The roundness of the spindle was measured using a dial indicator (resolution: 0.0001 in.).

3) The magnetic field was measured using Gauss/Tesla meter.

4) The material removal rate was calculated by weight reduction in the balls by measuring the weight before and after each polishing run, using a precision balance (resolution: 0.1mg).

5) The polishing load was applied by adding weights on the side arms of the counter-weight system. Initially, the entire set-up was balanced by finding an appropriate weight. The additional weight was calculated depending on the load requirement per ball as shown in Figure 4.17. For example:

For a batch of 46 balls, considering a load of 1 N/ball

Total load on balls = 46 N \approx 10.34 lb

Additional weight on each side arm = $(5.17 \times 7.375) / 14.0625 = 2.71$ lb



Fig. 4.17 Schematic showing the dimensions of the counterweight arm

6) The weights were measured using a Kistler dynamometer (Type 9271 A), a dual mode Kistler amplifier (Type 5004) (range: ± 10 volts) and a digital voltmeter.

7) The ball diameter was measured using a precision micrometer (resolution: 0.0001 in.).

8) The sphericity of the balls was measured using TalyRond 250 (Filter: 2CR, cut-off: 50 upr).

9) The surface finish was measured using TalySurf 120L (Filter: ISO 2CR, Cut-off 0.08 mm, Evaluation length 4 consecutive cut-off).

10) In this investigation, five balls were selected for measuring diameter and sphericity, and three balls were selected for measuring surface finish after each

run. In all the measurements made for diameter, sphericity, and surface finish, the ball was traced in approximately three orthogonal planes.

4.11 STANDARD SPECIFICATIONS

The terminology for anti-friction ball and roller bearings and parts, is given in ABMA STD 1 and ABMA STD 10 is related to metal balls. ASTM specification F 2094 - 03 is related to the standard specification for silicon nitride bearing balls. The tolerances by grade for individual balls and lots of balls are given in Tables 4.5 and 4.6. The letter C indicates silicon nitride ceramic.

Table 4.5 Tolerances by grade for individual balls μm ($\mu\text{in.}$)
[ASTM F2094-03, 2004]

Grade	Allowable Ball Diameter Variation V_D	Allowable Deviation from Spherical Form W	Maximum Surface Roughness Arithmetical Average R_a
2C	0.05 (2)	0.05 (2)	0.004 (0.15)
3C	0.08 (3)	0.08 (3)	0.004 (0.15)
5C	0.13 (5)	0.13 (5)	0.005 (0.20)
10C	0.25 (10)	0.25 (10)	0.006 (0.25)
16C	0.40 (16)	0.40 (16)	0.009 (0.35)
24C	0.61 (24)	0.61 (24)	0.013 (0.50)
48C	1.22 (48)	1.22 (48)	0.013 (0.50)

Table 4.6 Tolerances by grade for lots of balls μm ($\mu\text{in.}$)
[ASTM F2094-03, 2004]

Grade	Allowable Lot Diameter Variation	Nominal Diameter Tolerance	Allowable Ball Gage Deviation	
			High	Low
2C	0.08 (3)	± 0.51 (± 20)	+ 0.51 (+ 20)	- 0.51 (- 20)
3C	0.13 (5)	± 0.51 (± 20)	+ 0.51 (+ 20)	- 0.51 (- 20)
5C	0.25 (10)	± 0.76 (± 30)	+ 0.76 (+ 30)	- 0.76 (- 30)
10C	0.51 (20)	± 2.54 (± 100)	+ 1.27 (+ 50)	- 1.02 (- 40)
16C	0.80 (32)	± 2.54 (± 100)	+ 1.27 (+ 50)	- 1.02 (- 40)
24C	1.22 (48)	± 2.54 (± 100)	+ 2.54 (+ 100)	- 2.54 (- 100)
48C	2.44 (96)	N/A	N/A	N/A

CHAPTER 5

METHODOLOGY FOR FINISHING SILICON NITRIDE BALLS

5.1 INTRODUCTION

In order to produce balls suitable for bearing applications, three important characteristics, namely, diameter, sphericity, and surface finish have to be controlled. The methodology for finishing silicon nitride balls by magnetic float polishing consists of mechanical polishing followed by chemo-mechanical polishing. The mechanical polishing involves mechanical removal of material initially using harder abrasives (with respect to workmaterial) of different materials, namely, B₄C and SiC, with progressively lower hardness and grain size. The mechanism of material removal with these abrasives is by mechanical microfracture due to high hardness and inherent brittleness of the workmaterial. However, due to application of gentle conditions, namely, low level of controlled force, high polishing speeds, and flexible support system, the material removal occurs not by grain pull out, grain fracture or large fracture but by microfracture by cleavage. Thus, high material removal rates (1 - 1.5 μm/min) with minimal surface damage are possible. Chemo-mechanical polishing is carried out using CeO₂ abrasive, which is substantially softer than the workmaterial. The material removal occurs due to tribo-chemical action of the abrasive with the workmaterial

in a suitable environment. The resulting surface is smooth with minimal surface or sub-surface defects, such as scratches or pits.

5.2 POLISHING PROCEDURE AND PARAMETERS

Three stages are involved in magnetic float polishing of Si_3N_4 balls, namely, 1) roughing to remove maximum material without imparting serious damage to the surface, 2) an intermediate stage of semi-finishing to control diameter and improve sphericity, and 3) final finishing to obtain best surface finish and sphericity while maintaining the final diameter. A groove formed on the bevel of the spindle plays an important role in all the three stages of polishing.

Two coarser, harder abrasives, B_4C (500 grit) and SiC (600 grit) (with respect to Si_3N_4 balls) are used in the roughing stage for rapidly reducing the ball diameter and simultaneously improving the ball shape. At this stage, it is preferable, though not essential, to machine the groove in order to obtain high material removal rates ($\sim 1 - 1.5 \mu\text{m}/\text{min}$) using B_4C (500 grit) abrasive. SiC (600 grit) abrasive has material removal rate ($\sim 0.6 \mu\text{m}/\text{min}$.) much lower than B_4C (500 grit) abrasive and hence was suitable at the end of roughing stage to approach the desired diameter. It is, however, necessary to maintain the groove formed with SiC (600 grit) abrasive, in order to improve the sphericity.

Towards the end of roughing stage and in the semi-finishing stage, the sphericity can be significantly improved by not machining the groove. Figure 5.1 shows photograph of the groove formed on the bevel of the spindle, which facilitates in improving the sphericity. Moderate material removal rates are

preferred in the intermediate stage, in order to control the ball diameter. SiC (1200 grit) abrasive was found suitable at this stage.

In the final finishing stage, machining the spindle groove is necessary for rapidly improving the surface finish. Low material removal rates are required at this stage to control the final diameter. Fine SiC (10,000 grit) abrasive is effective in improving the surface finish and was used to approach the final diameter. This was followed by final chemo-mechanical polishing using CeO_2 ($< 5 \mu\text{m}$) abrasive to produce balls of required diameter, sphericity, and surface finish. The parameters used in this investigation are given in Table 5.1.

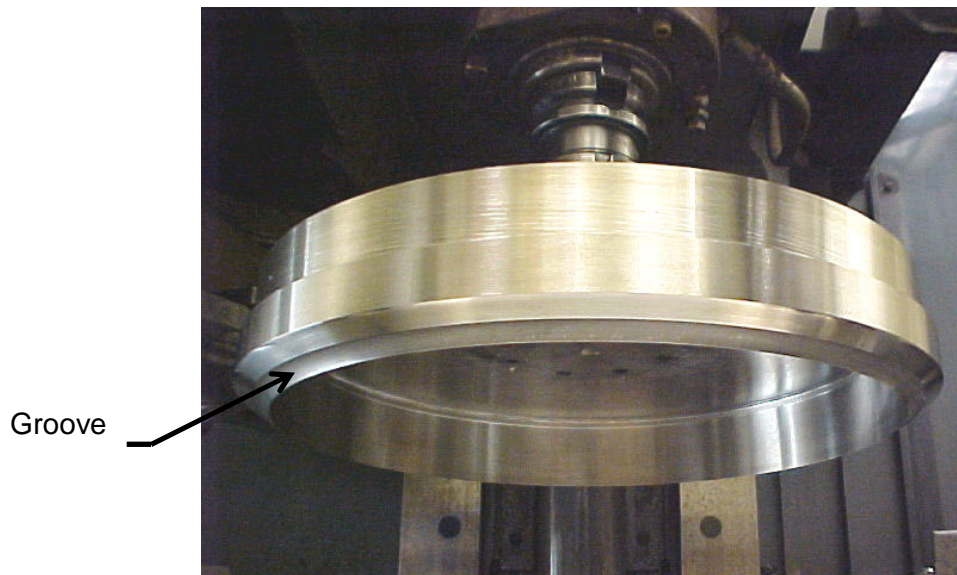


Fig. 5.1 Photograph of the groove formed on the bevel of the spindle during polishing

Table 5.1 Parameters used in this study

Abrasive	Boron carbide (B ₄ C) - 500 grit (12 μm)
	Silicon carbide (SiC) - 600 grit (10 μm), 1200 grit (2.1 μm), 10000 grit (0.5 μm)
	Cerium oxide (CeO ₂) - (< 5 μm)
Abrasive (%)	5, 10, 20
Load (N/ball)	0.5, 0.75, 1, 1.5
Speed (rpm.)	300, 400, 550
Time (min.)	60, 90, 105, 120, 180

~ 300 ml of magnetic fluid was used in each test run. However, the magnetic fluid level drops down with time, especially at higher loads. The fluid level was maintained by addition of water and magnetic fluid. The evaporation of the magnetic fluid was reduced by covering the top of the chamber. Apart from the actual polishing time, a cleaning time of ~ 30 min., spindle machining time of ~ 30 min., characterization time of ~ 60 min. and run set-up time of ~ 30 min. was required.

CHAPTER 6

RESULTS AND DISCUSSION

6.1 DETERMINATION OF OPTIMUM POLISHING PARAMETERS IN THE ROUGHING STAGE USING TAGUCHI METHOD

Taguchi method is used in the roughing stage of polishing to optimize the material removal rate (MRR). It may be noted that Taguchi method can extract information from experiment more precisely and more efficiently. Also, fewer tests are needed even when the number of parameters being investigated is quite large. The smallest, standard Taguchi 3-level L_9 (3^4) orthogonal array (OA) (Table 6.1), which has four 3-level columns available is chosen for this case. The important parameters that influence the MRR generated during mechanical polishing for a given workmaterial and a given abrasive (material and grain size) are (i) the polishing load, (ii) the abrasive concentration, and (iii) the polishing speed. The MRR obtained with B_4C (500 grit) abrasive is quite high and hence was used for this study. Each factor is investigated at three levels to determine optimum conditions for MRR. The factors and their levels are given in Table 6.2

The test run is designated by replacing the level numbers 1, 2, 3 of parameters A, B, C, in the L_9 OA with the chosen parameter level values in Table 6.2. The fourth column (factor D) is not used and designated as an unknown parameter in this investigation. Each row of the array represents a parameter

setting condition in the experiment. Table 6.3 shows the test run design and results. All the tests were carried out for a duration of 60 minutes.

Table 6.1 Standard L_9 (3^4) orthogonal array used in Taguchi method [Jiang and Komanduri, 1997]

Run	Factors Investigated				Results
	A	B	C	D	
1	1	1	1	1	
2	1	2	2	2	
3	1	3	3	3	
4	2	1	2	3	
5	2	2	3	1	
6	2	3	1	2	
7	3	1	3	2	
8	3	2	1	3	
9	3	3	2	1	

Table 6.2 Test parameters used and their levels

Level	Parameters		
	A: Load (N/ ball)	B: Abr. Conc. (%)	C: Speed (rpm)
1	0.5	5	300
2	1	10	400
3	1.5	20	550

Table 6.3 Test run design and results

Test run	Factors Investigated				Results MRR/ball (mg/min.)
	A: Load (N/ball)	B: Abr. Conc. (%)	C: Speed (rpm)	not used	
1	0.5	5	300	-	0.62
2	0.5	10	400	-	1.54
3	0.5	20	550	-	1.09
4	1	5	400	-	1.26
5	1	10	550	-	1.95
6	1	20	300	-	2.03
7	1.5	5	550	-	1.93
8	1.5	10	300	-	1.18
9	1.5	20	400	-	2.91

The level average response analysis is carried out by averaging the experimental results obtained from the three test runs corresponding to each level of each parameter, which is shown in Table 6.4 and plotted in Figure 6.1. It may be seen from Table 6.3 that 1st level of factor A occurs in test runs 1, 2, and 3, all three levels of factors B and C appear once in these three test runs. The 2nd level of factor A occurs in test runs 4, 5, and 6, all three levels of factor B and C also appear once in these three test runs. The 3rd level of factor A occurs in test runs 7, 8 and 9, all three levels of factor B and C also appear once in these three test runs. It means the level conditions of factors B and C with different levels of factor A are the same. Hence, it counteracts the effects of factors B and C on the response of factor A. Thus, from the average data of each of the three test runs wherein one level of factor A occurs, the optimum value of factor A can be determined. By the same way, the optimum values for factors B and C can be determined [Jiang and Komanduri, 1997].

Table 6.4 Level average response analysis

Parameter	Test Run	MRR/ball (mg/min.)	Avg.Response (mg/min.)
A, Load, N/ball			
Level 1, 0.5	1	0.62	1.08
	2	1.54	
	3	1.09	
Level 2, 1	4	1.26	1.75
	5	1.95	
	6	2.03	
Level 3, 1.5	7	1.93	2.01
	8	1.18	
	9	2.91	
B, Abrasive concentration (B ₄ C 500 grit), %			
Level 1, 5	1	0.62	1.27
	4	1.26	
	7	1.93	
Level 2, 10	2	1.54	1.56
	5	1.95	
	8	1.18	
Level 3, 20	3	1.09	2.01
	6	2.03	
	9	2.91	
C, Speed, rpm			
Level 1, 300	1	0.62	1.28
	6	2.03	
	8	1.18	
Level 2, 400	2	1.54	1.90
	4	1.26	
	9	2.91	
Level 3, 550	3	1.09	1.66
	5	1.95	
	7	1.93	

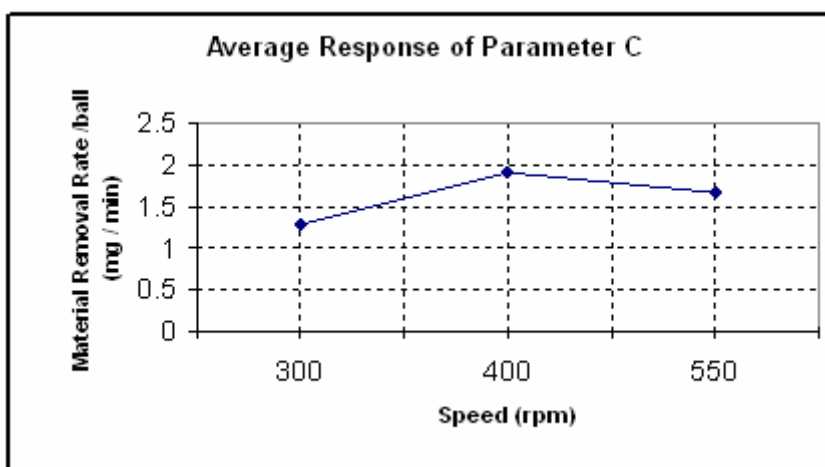
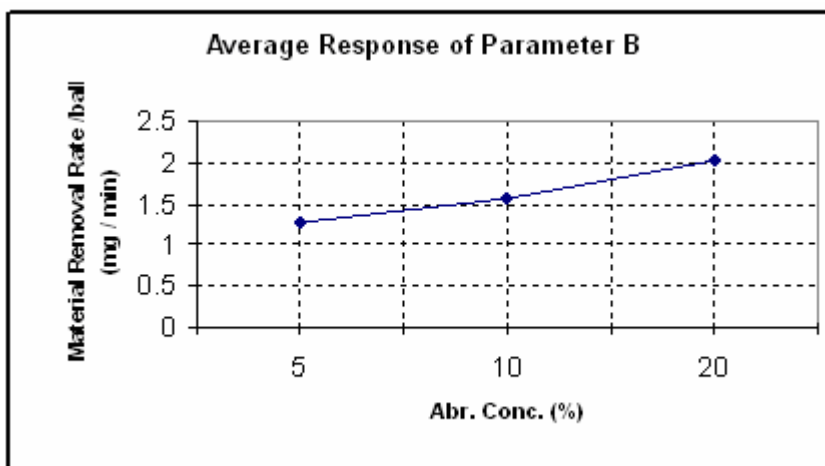
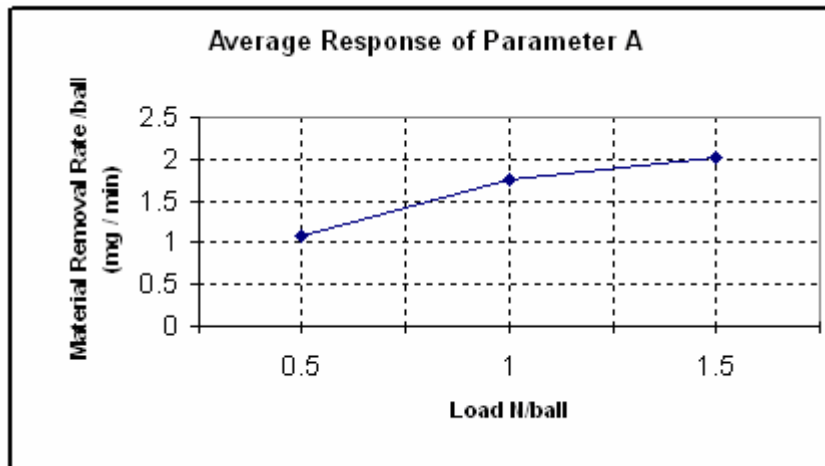


Fig. 6.1 Level average responses for parameters A, B and C

Figure 6.1 shows the influences of polishing parameters on the material removal rate. The material removal rate increases with increase in the polishing load. It increases sharply as the load is increased from 0.5 to 1 N/ball, an increase of 62 %. From 1 to 1.5 N/ball although the load is increased by 50 %, the material removal rate increased only by 15 %.

The material removal rate increases slightly as the abrasive concentration is increased from 5 % to 10 %. However, the material removal rate is found to increase considerably with an abrasive concentration of 20 %.

The material removal rate increases by 48 % with the increase in the speed from 300 to 400 rpm but decreases by 13 % from 400 to 550 rpm. Thus, a speed of 400 rpm was found to be the optimum speed for getting high material removal rate. This speed was also found to be optimum for obtaining good sphericity and surface finish. Hence, it was kept constant throughout this investigation.

Thus, from the level average response analysis it is found that a load of 1.5 N/ball, an abrasive concentration of 20 %, and a speed of 400 rpm would give a high material removal rate. This combination of parameters was used in the roughing stage of polishing.

6.2 FINISHING OF 3/4 INCH SILICON NITRIDE BALLS

A batch of 46 HIP'ed Si_3N_4 balls (CERBEC NBD-200 from Norton Advanced Ceramics) with an initial average diameter of 0.7861 in. (0.7837 - 0.7889 in.) was finished using the large batch magnetic float polishing apparatus. The average sphericity of the as-received ball measured using TalyRond was 24.88 μm (16.90 - 45.25 μm) with a standard deviation of 7.1 μm . The average surface roughness of the as-received ball measured using TalySurf was Ra of 937.14 nm (standard deviation of 173.94 nm) and Rt of 6.30 μm (standard deviation of 0.64 μm). These balls were finished to a final size of 0.7500 in. with an average surface finish, Ra of 8.2 nm (standard deviation of 0.44 nm) and Rt of 0.07 μm (standard deviation of 0.01 μm) and an average sphericity of 0.27 μm (standard deviation of 0.04 μm). The final average sphericity of the 46 balls was as follows: 19 balls were in the range 0.2 - 0.25 μm , 17 balls were in the range 0.25 - 0.3 μm , 8 balls were in the range 0.3 - 0.35 μm and 2 balls were in the range 0.35 - 0.4 μm . The best sphericity obtained was 0.15 μm and best surface finish obtained was Ra of 6.7 nm and Rt of 0.05 μm . The actual polishing time required to finish the batch (not including the set-up time, characterization of balls and cleaning) was less than 30 hours.

Table 6.5 shows test details and results of 3/4 in. Si_3N_4 balls from the as-received condition to the finished condition. Figure 6.2 (a) shows a TalyRond roundness profile (Roundness: 22.5 μm) of an as-received Si_3N_4 ball. Figure 6.3 (a) shows a TalySurf surface roughness profile (Ra, 901.5 nm and Rt, 5.83 μm) of an as-received Si_3N_4 ball.

Table 6.5 Test details and results of 3/4 in. Si₃N₄ balls

Stage	Run Parameters						Results						Remarks	
	Run	Abr. Type	Abr. Size	Abr. %	Load (N/ball)	Speed (rpm)	Time (min.)	Dia. (in.)	Rnd. (μm)	Rnd. Std. Dev. (μm)	S.F. (Ra) (nm)	S.F. (Rt) (μm)		MRR/ball (μm/min.)
	As-received													
I	1	B ₄ C	500	20	1.5	400	120	0.786 1	24.88	7.10	937.14	6.30	1.55	2.66
	2	B ₄ C	500	20	1.5	400	120	0.778 8	1.13	0.14	105.20	0.75	1.29	2.43
	3	B ₄ C	500	20	1.5	400	180	0.772 7	1.63	0.13	87.50	0.66	1.02	1.80
	4	B ₄ C	500	20	1.5	400	180	0.765 5	1.02	0.09	98.50	0.74	1.09	2.11
II	5	SiC	600	10	0.75	400	120	0.755 0	1.04	0.11	59.10	0.50	0.59	0.93
	6	SiC	600	10	1	400	120	0.752 2	0.61	0.11	75.00	0.61	0.59	0.99
	7	SiC	1200	5	0.75	400	120	0.751 5	0.36	0.06	54.90	0.42	0.15	0.28
	8	SiC	1200	5	0.75	400	105	0.751 0	0.38	0.05	59.90	0.45	0.12	0.18
	9	SiC	1200	5	0.75	400	105	0.750 5	0.32	0.07	62.90	0.50	0.12	0.18
	10	SiC	1200	5	0.5	400	90	0.750 3	0.34	0.04	71.20	0.52	0.06	0.15
III	11	SiC	1200	5	0.5	400	60	0.750 2	0.43	0.08	69.30	0.52	0.04	0.20
	12	SiC	10,000	10	0.75	400	60	0.750 2	0.36	0.04	49.60	0.40	-	-
	13	SiC	10,000	10	1	400	105	0.750 1	0.37	0.04	45.00	0.36	-	-
	14	SiC	10,000	10	0.75	400	60	0.750 1	0.35	0.07	14.00	0.13	-	-
	15	CeO ₂	< 5 μm	10	1	400	120	0.750 1	0.29	0.05	8.50	0.08	-	-
	16	CeO ₂	< 5 μm	10	1	400	120	0.750 0	0.27	0.04	8.20	0.07	-	-

Figure 6.2 (b) shows TalyRond roundness profile (Roundness: 0.75 μm) of a Si_3N_4 ball after polishing with B_4C (500 grit) abrasive in Run 1. The average sphericity has significantly improved from 25 μm to 1.13 μm after just one run of 2 hours. Figure 6.3 (b) shows improved TalySurf surface roughness profile (R_a , 107 nm and R_t , 0.82 μm) of a Si_3N_4 ball after polishing with B_4C (500 grit) abrasive in Run 1. A significant improvement in the surface finish can also be observed. The diameter was reduced from 0.7861 in. to 0.7578 in. with B_4C (500 grit) abrasive in Runs 1 - 4. The groove formed on the bevel of the spindle was machined after these four runs. However, the groove can be maintained till the last run of B_4C (500 grit) abrasive with a slight less removal of material.

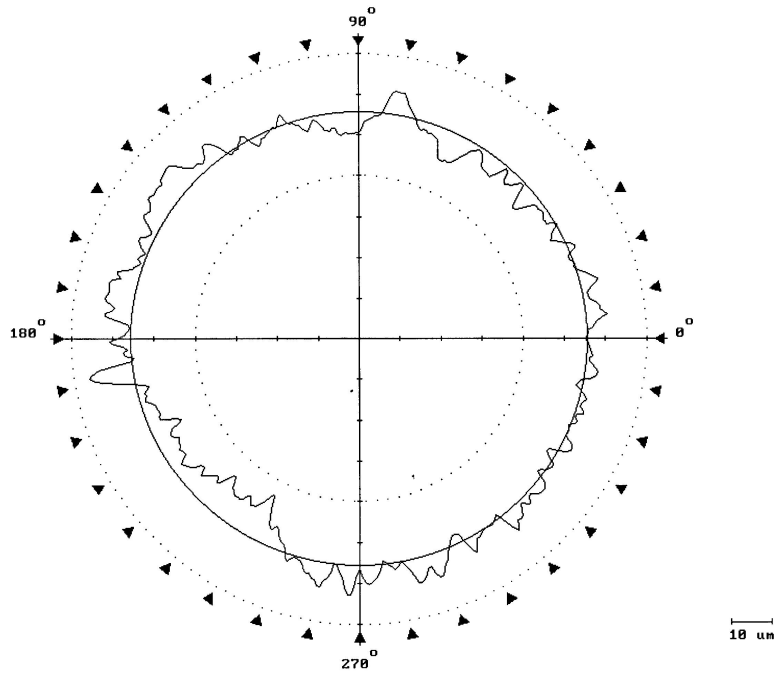
Figure 6.2 (c) shows TalyRond roundness profile (Roundness: 0.85 μm) of a Si_3N_4 ball after polishing with SiC (600 grit) abrasive in Run 5. Figure 6.3 (c) shows improved TalySurf surface roughness profile (R_a , 59.1 nm and R_t , 0.53 μm) of a Si_3N_4 ball after polishing with SiC (600 grit) abrasive in Run 5. In order to improve the sphericity, the groove formed on the bevel of the spindle after Run 5 was not machined. Figure 6.2 (d) shows improved TalyRond roundness profile (Roundness: 0.6 μm) of a Si_3N_4 ball after polishing with SiC (600 grit) abrasive in Run 6. The diameter was reduced to 0.7522 in. with SiC (600 grit) abrasive in Runs 5 - 6.

Figure 6.2 (e) shows improved TalyRond roundness profile (Roundness: 0.35 μm) of a Si_3N_4 ball after polishing with SiC (1200 grit) abrasive in Run 7. Figure 6.3 (d) shows TalySurf surface roughness profile (R_a , 58.8 nm and R_t , 0.38 μm) of a Si_3N_4 ball after polishing with SiC (1200 grit) abrasive in Run 7.

The average sphericity was significantly improved and maintained at $\sim 0.35 \mu\text{m}$ in Runs 7 - 11 without machining the groove formed after Run 5. The diameter was reduced to 0.7502 in. with SiC (1200 grit) abrasive.

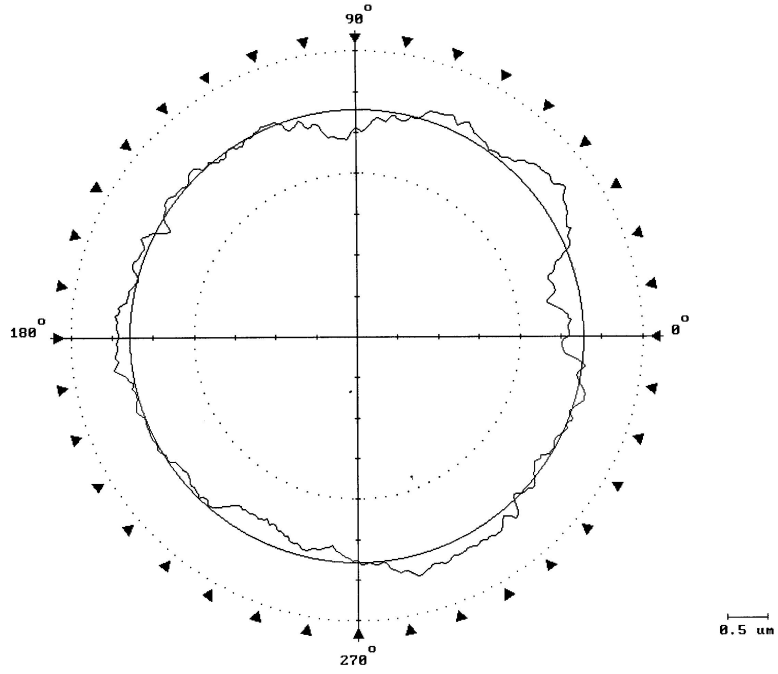
In the final stage, it was difficult to improve the surface finish rapidly while maintaining the groove formed in earlier runs. Figure 6.3 (e) shows TalySurf surface roughness profile (Ra, 45.7 nm and Rt, $0.4 \mu\text{m}$) of a Si_3N_4 ball after polishing with SiC (10,000 grit) abrasive in Run 12. The spindle groove was machined after Run 13, which resulted in significant improvement in the surface finish in further runs. Figure 6.2 (f) shows improved TalyRond roundness profile (Roundness: $0.25 \mu\text{m}$) of a Si_3N_4 ball after polishing with SiC (10,000 grit) abrasive in Run 14. Figure 6.3 (f) shows improved TalySurf surface roughness profile (Ra, 12.6 nm and Rt, $0.12 \mu\text{m}$) of a Si_3N_4 ball after polishing with SiC (10,000 grit) abrasive in Run 14. The diameter was reduced to 0.7501 in. with SiC (10,000 grit) abrasive.

Figure 6.2 (g) shows improved TalyRond roundness profile (Roundness: $0.15 \mu\text{m}$) of a Si_3N_4 ball after polishing with CeO_2 in Run 16. Figure 6.3 (g) shows improved TalySurf surface roughness profile (Ra, 7.9 nm and Rt, $0.06 \mu\text{m}$) of a Si_3N_4 ball after polishing with CeO_2 in Run 16. The balls were finished to a final diameter of 0.7500 in. with an average sphericity of $0.27 \mu\text{m}$ and average surface finish, Ra of 8.2 nm and Rt of $0.07 \mu\text{m}$.



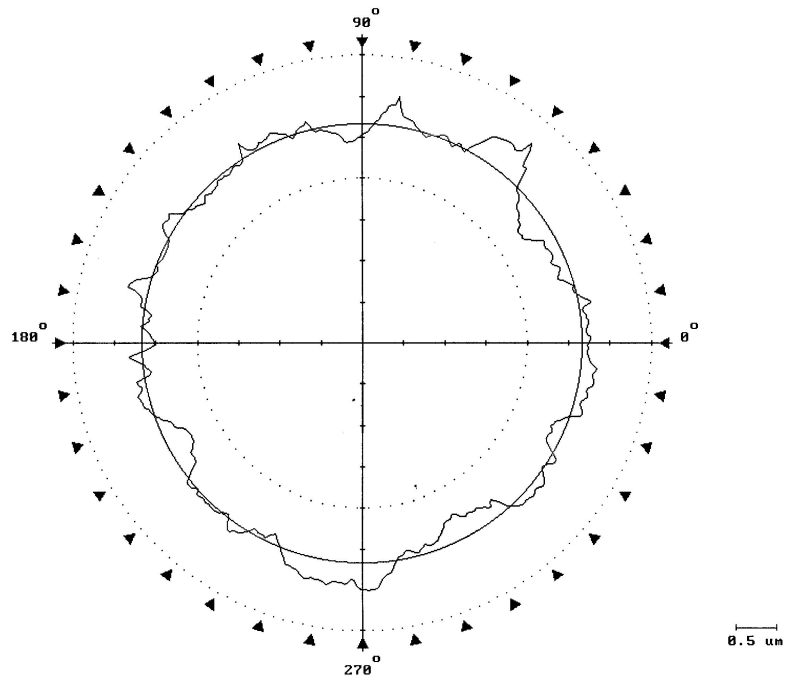
(Roundness: $22.5 \mu\text{m}$)

(a) As-received



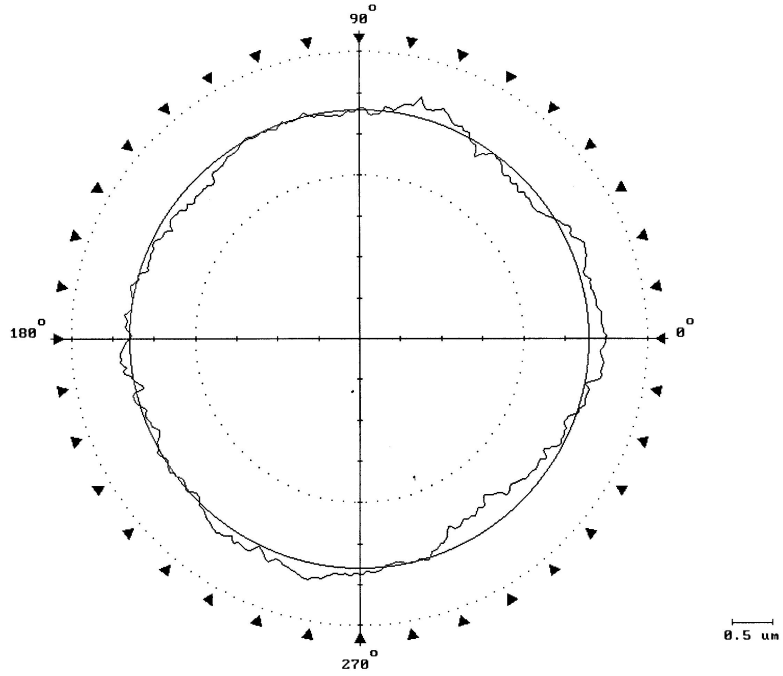
(Roundness: $0.75 \mu\text{m}$)

(b) After polishing with B_4C (500 grit) abrasive in Run 1
(without groove)



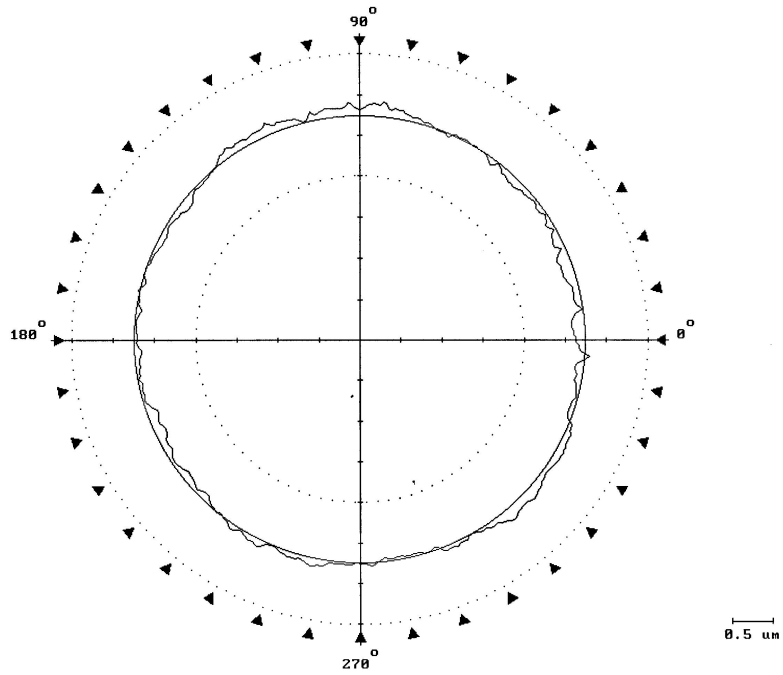
(Roundness: $0.85 \mu\text{m}$)

(c) After polishing with SiC (600 grit) abrasive in Run 5
(without groove)



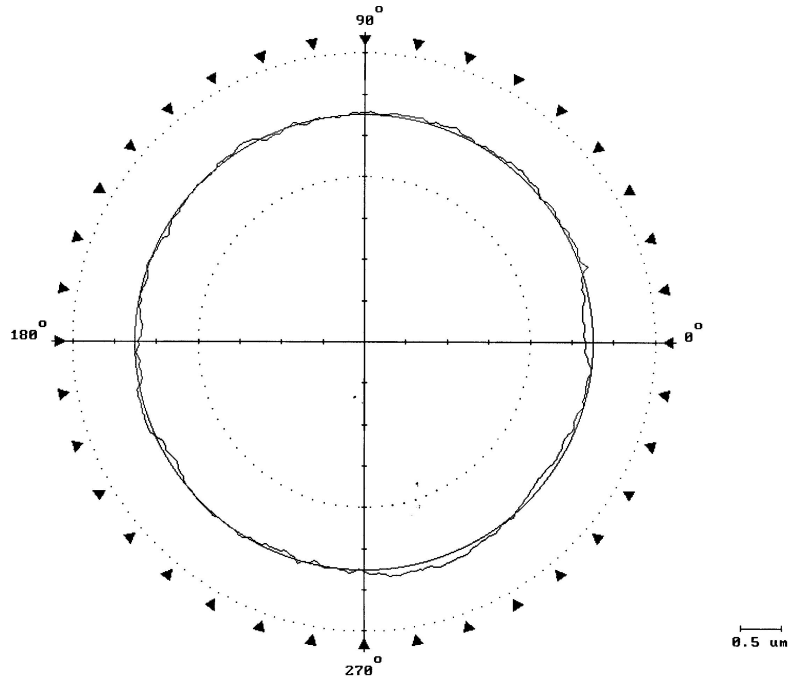
(Roundness: $0.6 \mu\text{m}$)

(d) After polishing with SiC (600 grit) abrasive in Run 6
(with groove)



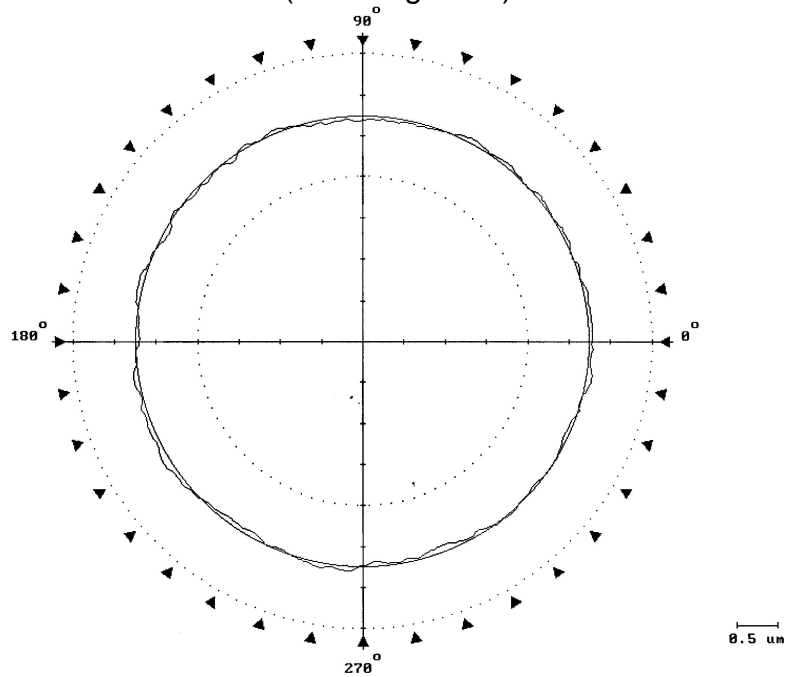
(Roundness: $0.35 \mu\text{m}$)

(e) After polishing with SiC (1200 grit) abrasive in Run 7
(with groove)



(Roundness: 0.25 μm)

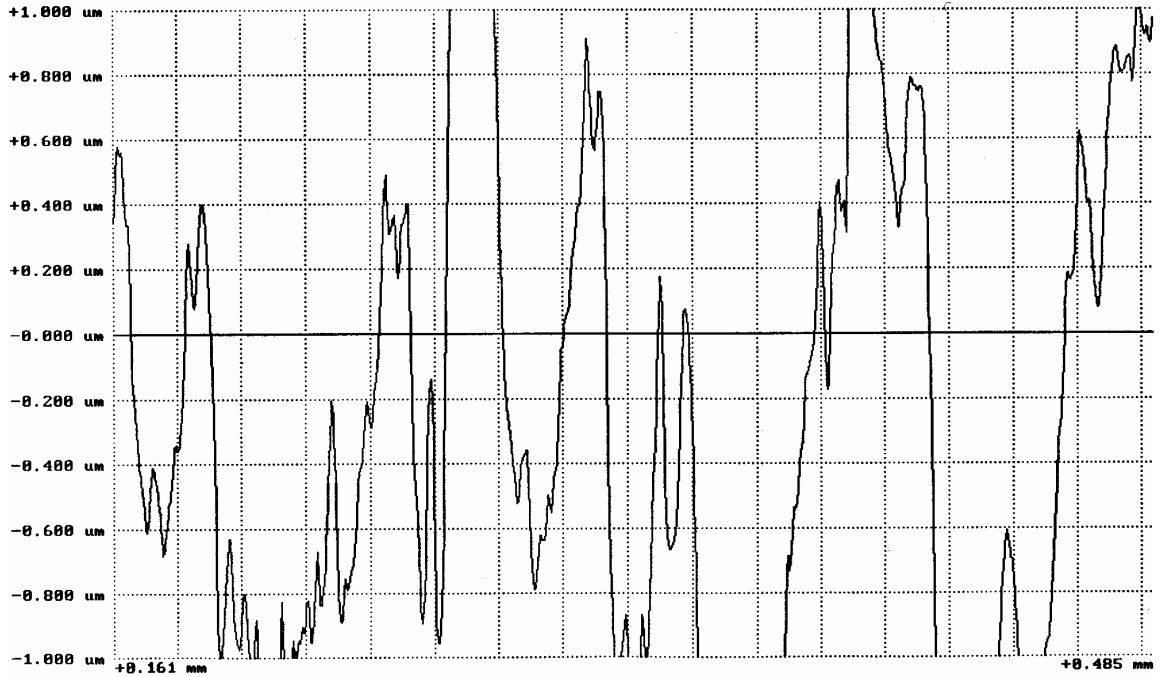
(f) After polishing with SiC (10,000 grit) abrasive in Run 14
(without groove)



(Roundness: 0.15 μm)

(g) After polishing with CeO_2 ($< 5 \mu\text{m}$) abrasive in Run 16
(without groove)

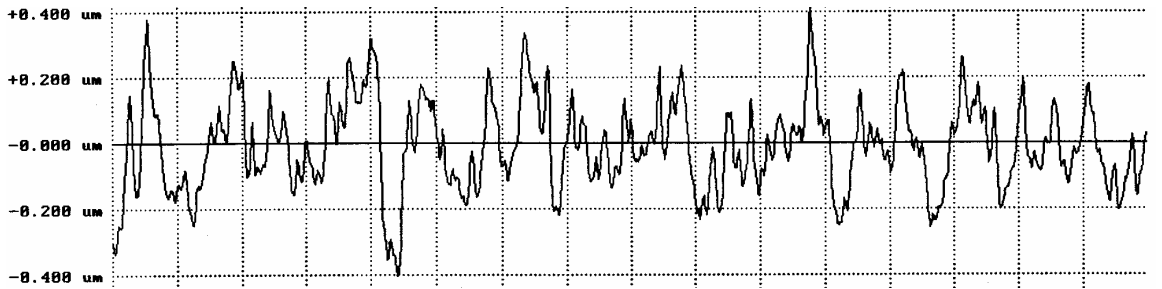
Fig. 6.2 (a) - (g) TalyRond roundness profile of a $\frac{3}{4}$ in. Si_3N_4 ball at various stages of polishing



Horizontal Scale: 20 μm per div.
 Vertical Scale: 0.2 μm per div.

(Ra: 901.5 nm, Rt: 5.83 μm)

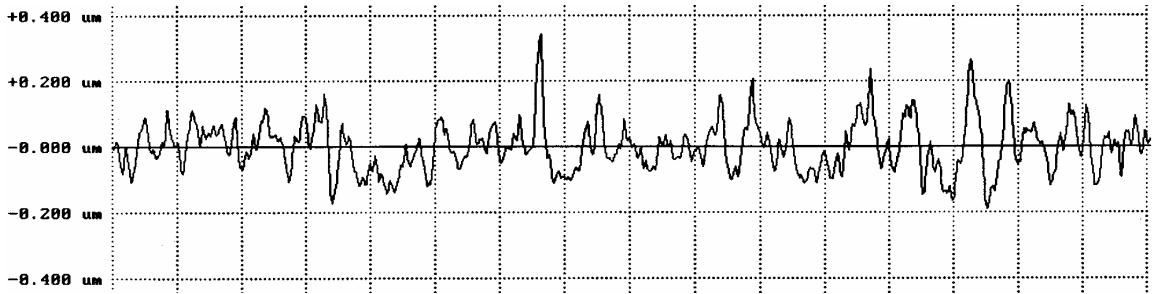
(a) As-received



Horizontal Scale: 20 μm per div.
 Vertical Scale: 0.2 μm per div.

(Ra: 107 nm, Rt: 0.82 μm)

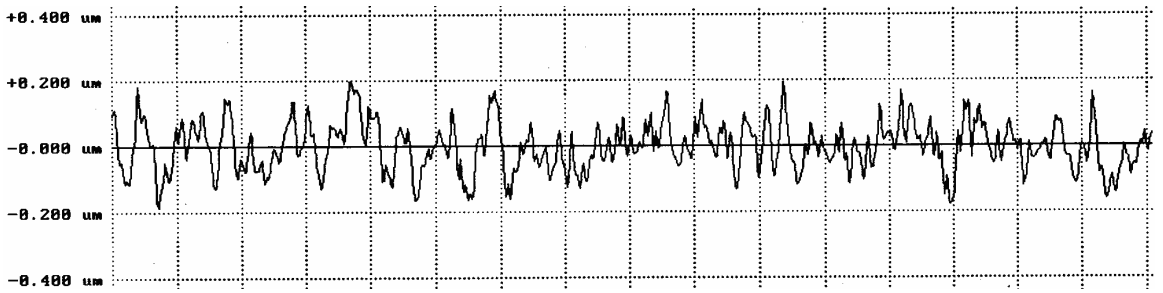
(b) After polishing with B₄C (500 grit) abrasive in Run 1
 (without groove)



Horizontal Scale: 20 μm per div.
Vertical Scale: 0.2 μm per div.

(Ra: 59.1nm, Rt: 0.53 μm)

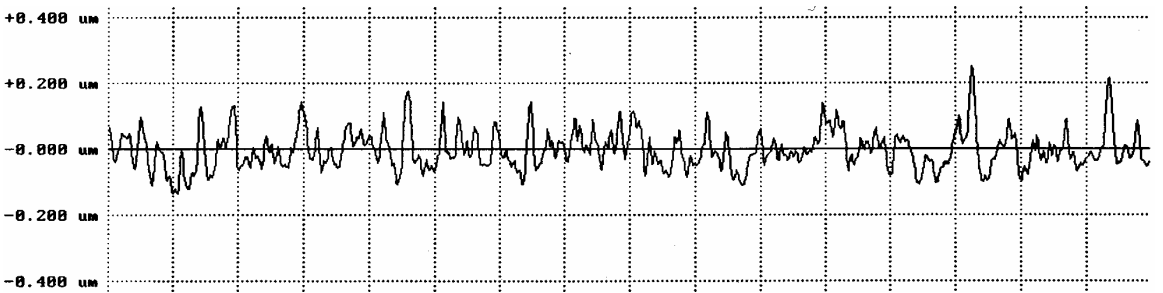
(c) After polishing with SiC (600 grit) abrasive in Run 5
(without groove)



Horizontal Scale: 20 μm per div.
Vertical Scale: 0.2 μm per div.

(Ra: 58.8 nm, Rt: 0.38 μm)

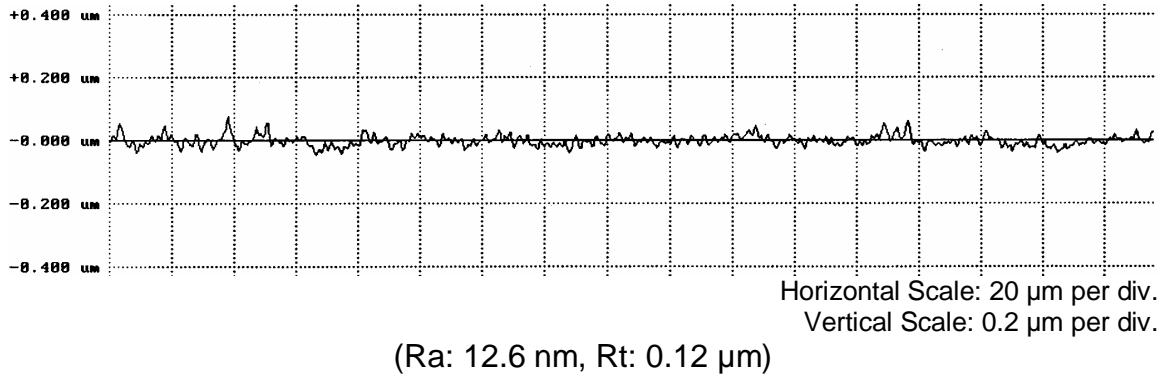
(d) After polishing with SiC (1200 grit) abrasive in Run 7
(with groove)



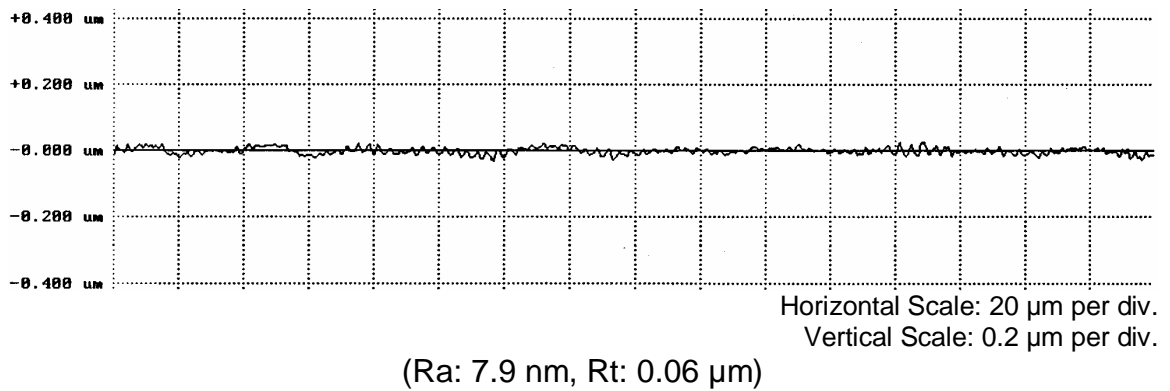
Horizontal Scale: 20 μm per div.
Vertical Scale: 0.2 μm per div.

(Ra: 45.7 nm, Rt: 0.40 μm)

(e) After polishing with SiC (10,000 grit) abrasive in Run 12
(with groove)



(f) After polishing with SiC (10,000 grit) abrasive in Run 14
(without groove)



(g) After polishing with CeO_2 (< 5 μm) abrasive in Run 16
(without groove)

Fig. 6.3 (a) - (g) TalySurf surface roughness profiles of a 3/4 in. Si_3N_4 ball
at various stages of polishing

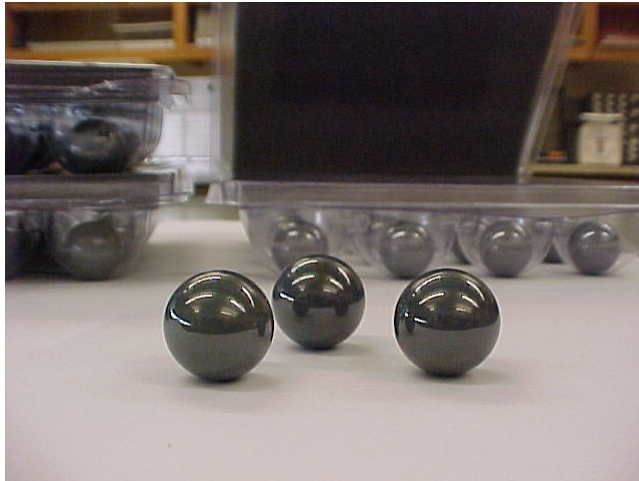


Fig. 6.4 Photograph of 3/4 in. Si₃N₄ balls finished in this study

6.3 DISCUSSION

The three-stage strategy consisting of roughing, semi-finishing, and final finishing was successfully implemented using the large batch MFP apparatus. The three stages are summarized in the following.

(1) Roughing: Here, the emphasis is on obtaining high material removal rate for rapidly reducing the ball diameter and quickly improving the ball shape. Initially, it is preferable, though not essential, to machine the groove formed on the bevel of the spindle for obtaining high removal rate. A load of 1 - 1.5 N/ball, an abrasive concentration of 10 - 20 % and a speed of 400 rpm is suitable for obtaining high removal rates (1 - 1.5 $\mu\text{m}/\text{min}$. on diameter) using B_4C (500 grit) abrasive. The large batch MFP apparatus is also effective in improving the sphericity rapidly. The initial average ball sphericity of $\sim 25 \mu\text{m}$ was significantly improved to $\sim 1 \mu\text{m}$ after just 2 hours of polishing time. At the end of B_4C runs, it is found necessary to machine the bevel of the spindle. This is because the groove formed is quite deep and not quite uniform, as the initial ball size and shape are different. SiC (600 grit) abrasive is suitable at the end of roughing stage to approach the desired diameter. The average ball sphericity of $\sim 1 \mu\text{m}$ was obtained using SiC (600 grit) abrasive by machining the groove. However, it was improved to $\sim 0.6 \mu\text{m}$ without machining the groove. The groove formed on the bevel of the spindle facilitates in improving the sphericity. This may be due to increased rolling motion of the balls resulting in uniform removal of material. Hence, towards the end of roughing stage and in the semi-finishing stage the groove should not be machined. As a result, the total processing time can also be reduced.

(2) Semi-finishing: In this stage, the emphasis is on quick reduction in sphericity with a moderate material removal rate to control the ball diameter. An average ball sphericity of $\sim 0.9 \mu\text{m}$ was obtained using SiC (1200 grit) abrasive by machining the groove formed on the bevel of the spindle. However, it was significantly improved and maintained at $\sim 0.35 \mu\text{m}$ without machining the groove. The number of runs can be reduced at this stage by proper selection of the load, abrasive (material, grain size, and concentration), and polishing time.

(3) Final finishing: Here, the emphasis is to produce best surface finish and sphericity while maintaining the final diameter. Fine SiC (10,000 grit) abrasive is very effective prior to chemo-mechanical polishing. An average surface finish, Ra of about 45 - 50 nm was obtained with this abrasive without machining the groove formed on the bevel of the spindle. However, it was significantly improved to $\sim 14 \text{ nm}$ in just 1 hour of polishing time after machining the groove. This may be due to increased sliding motion of the balls caused by adequate polishing load on the balls. Hence, machining the groove is necessary, in order to improve the surface finish rapidly. Finally, chemo-mechanical polishing with CeO_2 abrasive results in a smooth surface by preferential removal of peaks from the surface.

An average sphericity of $\sim 0.25 \mu\text{m}$ and an average surface finish, Ra of $\sim 8 \text{ nm}$ is obtained in the present study. Also, the variation in ball diameter, sphericity, and surface finish is very small. The polishing time of 20 - 30 hours (10 - 12 runs) is adequate to finish a batch from the as-received condition. However, this can be considerably reduced if the initial diameter is closer to the final requirements.

CHAPTER 7

CONCLUSIONS AND FUTURE WORK

7.1 CONCLUSIONS

1) Magnetic float polishing (MFP) is an efficient and cost effective manufacturing technology for the finishing of large size (3/4 in. diameter), large batch (46) Si_3N_4 balls suitable for bearing applications. It involves fine mechanical polishing followed by chemo-mechanical polishing (CMP). High polishing speed, small and controlled polishing force, and flexible support system used in MFP result in high quality.

2) The large batch MFP apparatus with self-aligning method is effective for finishing bearing grade Si_3N_4 balls in wide range of sizes.

3) A batch of 46, 3/4 inch Si_3N_4 balls was finished to an average sphericity of 0.27 μm (Best value 0.15 to 0.2 μm) and an average surface finish, Ra of 8.2 nm (Best value 6.7 nm) in less than 30 hours of actual polishing time.

4) The variation in diameter, sphericity, and surface finish from ball to ball and within a ball is very small.

5) The initial average ball sphericity of $\sim 25 \mu\text{m}$ can be significantly improved to $\sim 1 \mu\text{m}$ in just 2 hours of polishing time.

6) The three-stage strategy of roughing, semi-finishing, and final finishing was successfully implemented using the large batch MFP apparatus. Mechanical polishing was done using B₄C (500 grit) and SiC (600 grit) abrasives with emphasis on high material removal. Semi-finishing was done next using finer SiC (1200 grit) abrasive to control diameter and improve the sphericity. Finishing was done using SiC (10,000 grit) abrasive followed by softer chemo-mechanical abrasive, namely CeO₂, to improve the surface finish and sphericity while maintaining the final diameter.

7) Taguchi method was applied for parameter optimization in the initial roughing stage of polishing. A polishing load of 1.5 N/ball, an abrasive concentration of 20%, and a speed of 400 rpm were found to be the optimum polishing parameters (within the experimental level ranges) for obtaining high material removal rate. High removal rates (1 - 1.5 μm/min) are possible using B₄C (500 grit) abrasive.

8) The groove formed on the bevel of the spindle plays an important role in all the three stages of polishing. Initially, in the roughing stage, it is preferable to machine the groove, though not essential, in order to obtain high material removal rate. It is, however, necessary to maintain the groove formed at the end of the roughing stage as sphericity would not improve in the intermediate stage without this. Continuation of the groove in the semi-finishing stage results in significant improvement in the sphericity. Further, in the final finishing stage, machining the groove is necessary to significantly improve the surface finish.

7.2 FUTURE WORK

Major effort in this investigation has been devoted to the modifications of the apparatus design so that consistent and repeatable polishing runs can be obtained. The problem was that with set-up variations, parametric studies regarding sphericity and surface finish could not be made. After implementing the modifications listed in Chapter 4 (e.g. *in-situ* machining, self-alignment method, etc.), consistent and repeatable runs can now be obtained for a given set of parameters. With this done, the future work recommended for large batch magnetic float polishing includes the following:

- 1) Further apparatus considerations
- 2) More in-depth parameter studies focusing on sphericity and surface finish
- 3) Mechanism of polishing

7.2.1 Future apparatus consideration

In order to decrease the set-up variations further, the process should be partially automated. This would significantly reduce the set-up time and increase the precision and accuracy of the system, thereby allowing more consistent and repeatable results and decreasing the chances of error.

With the current apparatus, the findings from this investigation show that the results are dependent on very tight set-up tolerances. The quality of the set-up depends largely on the judgment of the individual using the machine. With automation, the set-up will be more accurate and repeatable for every run.

One further modification to the apparatus that should be considered is the installation of a cooling system. As is, due to the high speeds, loads, and friction involved, there is much heat generated in the polishing process. As a result, the level of magnetic fluid decreases throughout the run. This can degrade the sphericity considerably. Reasons for this include changes in fluid viscosity, increase in abrasive concentration, formation of chips of Si_3N_4 , and change in ball kinematics throughout the run. For these reasons and probably many others, a means of minimizing the evaporation should be made. More importantly, the magnetic fluid is expensive and need arises to minimize its loss as much as possible.

One approach is the installation of small diameter copper tubes wrapped around and brazed onto the outside perimeter of the polishing chamber. By circulating cold water, heat can be dissipated from the system efficiently. This method is easy to install and with little capital investment.

By implementing this, more uniform conditions would be maintained throughout the run in terms of ball kinematics and the cutting mechanism. Additionally, this would decrease the amount of fluid used per run (as approximately 50 to 100 ml, ~ 25%, of magnetic fluid is added to the chamber during a typical run to account for this evaporation). This would significantly reduce the cost of the process.

7.2.2 More in-depth parameter studies focusing on sphericity and surface finish

In this study, Taguchi method was used to determine the optimum polishing conditions for obtaining high material removal rate. This type of analysis could not be performed for sphericity in this study because of the set-up variables mentioned, as these variations would affect the results as much as changes in parameters. Therefore, the effects of parameters on sphericity could not be relied upon completely.

With the changes implemented in this investigation and repeatable results achievable for the given run parameters, the next step would be to use a systematic approach to determine the combination of parameters to obtain best sphericity. Similar investigation should be conducted for surface finish. The surface finish obtained in this study is ~8 nm Ra, but ASTM Grade 5 balls require a surface finish of 5 nm Ra. This should be done by investigating different types of abrasives, along with a wider range of loads, speeds, abrasive concentrations, and duration. Also, surface finish can be further improved with additional runs using CeO₂ although this would add to the total time for polishing.

7.2.3 Mechanism of polishing

In order to understand the micromechanisms of material removal and surface generation process, it is necessary to examine the finished balls as well as the debris generated using SEM, X-ray, and other characterization techniques.

REFERENCES

ANSI B 89.3.1 - 1972, "Measurement of out-of-roundness," ASME, (1972).

ANSI B 46.1 - 1978, "Surface texture," ASME, (1978).

Aramaki, H., Shoda, Y., Morishita, Y. and T. Sawamoto, "The performance of ball bearings with silicon nitride ceramic balls in high speed spindles for machine tools," Transactions of the ASME, Journal of Tribology, 110 (1988) 693-698.

ASTM F 2094-03, "Standard specification for silicon nitride bearing balls," Annual Book of ASTM Standards, 01.08 (2004) 497-504.

Bamberger, E. N., "Materials for rolling element bearings," In international conference on Bearing Design - Historical Aspects, Present Technology and Future Problems, San Francisco, 1980, 1-46 (ASME Century 2 Publication).

Baron, J. M., "Technology of abrasive machining in a magnetic field," Masinstrojenije, Leningrad (in Russian), 1975.

Bhagavatula, S., "Chemomechanical polishing of silicon nitride with chromium oxide abrasive," M.S. thesis, Mechanical and Aerospace Engineering, Oklahoma State University, (1995).

Bhagavatula, S. R. and R. Komanduri, "On chemomechanical polishing of Si_3N_4 with Cr_2O_3 ," Philosophical Magazine A, 74 (1996) 1003-1017.

Cento, P. and D. W. Dareing, "Ceramic materials in hybrid ball bearings," Tribology Transactions, 42 (1999) 707-714.

- Childs, T. H. C. and H. J. Yoon, "Magnetic fluid grinding cell design," *Annals of the CIRP*, 41 (1992) 343-346.
- Childs, T. H. C., Mahmood, S. and H. J. Yoon, "The material removal mechanism in magnetic fluid grinding of ceramic ball bearings," *Proceedings of the I Mech E Part B, Journal of Engineering Manufacture*, 208 (1994a) 47-60.
- Childs, T. H. C., Jones, D. A., Mahmood, S., Zhang, B., Kato, K. and N. Umehara, "Magnetic fluid grinding mechanics," *Wear*, 175 (1994b) 189-198.
- Childs, T. H. C., Mahmood, S. and H. J. Yoon, "Magnetic fluid grinding of ceramic balls," *Tribology International*, 28 (1995) 341-348.
- Childs, T. H. C. and D. J. Moss, "Wear and cost issues in magnetic fluid grinding," *Wear*, 249 (2001) 509-516.
- CI Staff Report, "Bearings optimize technology for machine tools," *Ceramic Industry*, 144 (1995) 31-32.
- CI Staff Report, "Ceramic bearings roll to the future," *Ceramic Industry*, 147 (1997) 12.
- Coats, H. P., "Method of and apparatus for polishing containers," US Patent No. 2196058 (1940).
- Dagnall, H., "Exploring surface texture," Rank Taylor Hobson Inc., (1980).
- Dagnall, H., "Let's talk roundness," Rank Taylor Hobson Inc., (1984).
- DeGaeta, A. M., "Method and apparatus for producing balls," US Patent No. 4216629 (1980).
- DePoorter, G. L., Brog, T. K. and M. J. Readey, "Structural ceramics," *ASM Handbook* 2 (1990) 1019-1024.

- Dezzani, M. M. and P. K. Pearson, "Hybrid ceramic bearings for difficult applications," *Journal of Engineering for Gas Turbines and Power*, 118 (1996) 449-452.
- Dock, M. L., "Electromagnetic float polishing of ceramic balls for bearing applications," M.S. thesis, Mechanical and Aerospace Engineering, Oklahoma State University, (1995).
- Feldhaus, J. F., "Magnetic cleaning," US Patent No. 3695934 (1972).
- Gardner, D., "Ceramic drive turbine technology," *Design News*, 47 (1991) 80-83.
- Hah, S. R., Fischer, T. E. and C. Burk, "Ceramic bearing development, Vo.4, Tribochemical finishing of silicon nitride," Technical Report No. WL-TR-96-4018, the Materials Directorate, Wright Patterson AFB OH, March, 1995.
- Hah, S. R., "Tribochemical polishing of silicon nitride," PhD thesis, Stevens Institute of Technology, Hoboken, NJ, 1995.
- Hou, Z. B. and R. Komanduri, "Magnetic field assisted finishing of ceramics - Part I: Thermal model," *Transactions of the ASME, Journal of Tribology*, 120 (1998a) 645-651.
- Hou, Z. B. and R. Komanduri, "Magnetic field assisted finishing of ceramics - Part II: On the thermal aspects of magnetic float polishing (MFP) of ceramic balls," *Transactions of the ASME, Journal of Tribology*, 120 (1998b) 652-659.
- Hou, Z. B. and R. Komanduri, "Magnetic field assisted finishing of ceramics - Part III: On the thermal aspects of magnetic abrasive finishing (MAF) of ceramic rollers," *Transactions of the ASME, Journal of Tribology*, 120 (1998c) 660-667.

- Indge, J. H., "Lapping: more a science, less an art form," *Ceramic Industry*, 135 (1990) 26-28.
- Jahanmir, S. (Ed.), *Ceramic Bearing Technology*, U.S Department of Commerce, NIST Special Publication 824 (1991).
- Jiang, M. and R. Komanduri, "Application of Taguchi method for optimization of finishing conditions in magnetic float polishing (MFP)," *Wear*, 213 (1997) 59-71.
- Jiang, M., Wood, N. O. and R. Komanduri, "On chemo-mechanical polishing (CMP) of silicon nitride (Si_3N_4) workmaterial with various abrasives," *Wear*, 220 (1998a) 59-71.
- Jiang, M., Wood, N. O. and R. Komanduri, "On the chemo-mechanical polishing (CMP) of Si_3N_4 bearing balls with water based CeO_2 slurry," *Transactions of the ASME, Journal of Engineering Materials and Technology*, 120 (1998b) 304-312.
- Jiang, M. and R. Komanduri, "On the finishing of Si_3N_4 balls for bearing applications," *Wear*, 215 (1998c) 267-278.
- Jiang, M., "Finishing of advanced ceramic balls for bearing applications by magnetic float polishing (MFP) involving fine polishing followed by chemo-mechanical polishing (CMP)," Ph.D. thesis, Mechanical and Aerospace Engineering, Oklahoma State University, (1998d).
- Kang, J., Hadfield, M. and R. Cundill, "The consequences of aggressive lapping processes on the surface integrity of HIPed silicon nitride bearing balls," In international conference on Tribology in Environmental Design 2000,

- Bournemouth, 2000, 227-234 (Professional Engineering Publishing Limited, Bury St Edmunds and London, UK).
- Kang, J. and M. Hadfield, "Parameter optimization by Taguchi methods for finishing advanced ceramic balls using a novel eccentric lapping machine," Proceedings of the I Mech E Part B, Journal of Engineering Manufacture, 215 (2001a) 69-78.
- Kang, J. and M. Hadfield, "A novel eccentric lapping machine for finishing advanced ceramic balls," Proceedings of the I Mech E Part B, Journal of Engineering Manufacture, 215 (2001b) 781-795.
- Katz, R. N., "Ceramic bearings: rolling along," Ceramic Industry, 149 (1999) 23-24.
- Kato, K., Umehara, N., Adachi S. and S. Sato, "Method for grinding using a magnetic fluid and an apparatus thereof," US Patent No. 4821466 (1989).
- Kelley, K. A., "Hybrid ceramic bearings boost spindle speed," Modern Machine Shop, 74 (2001) 111-114.
- Khuperkar, A. M., "Finishing of glass balls by chemical mechanical polishing (CMP) using cerium oxide – expanding the process capabilities of magnetic float polishing (MFP) technology," M.S. thesis, Mechanical and Aerospace Engineering, Oklahoma State University, (1999).
- Kinoshita, H. and E. Sato, "Ball polishing apparatus and method for the same," US Patent No. 5214884 (1993).

- Komanduri, R. and M. C. Shaw, "Scanning electron microscope study of surface characteristics of abrasive materials," Transactions of the ASME, Journal of Engineering Materials and Technology, 96 (1974) 145.
- Komanduri, R., "On material removal mechanisms in finishing of advanced ceramics and glasses," Annals of the CIRP, 45 (1996a) 509-514.
- Komanduri, R., Umehara, N. and M. Raghunandan, "On the possibility of chemo-mechanical action in magnetic float polishing of silicon nitride," Transactions of the ASME, Journal of Tribology, 118 (1996b) 721-727.
- Komanduri, R., Lucca, D. A. and Y. Tani, "Technological advances in fine abrasive processes," Annals of the CIRP, 46 (1997) 545-596.
- Komanduri, R., Hou, Z. B., Umehara, N., Raghunandan, M., Jiang, M., Bhagavatula, S. R., Noori-Khajavi, A. and N. O. Wood, "A gentle method for finishing Si₃N₄ balls for hybrid bearing applications," Tribology Letters, 7 (1999a) 39-49.
- Komanduri, R. and M. Jiang, "Magnetic float polishing processes and materials therefor," US Patent No. 5931718 (1999b).
- Komanduri, R. and M. Jiang, "Magnetic float polishing of magnetic materials," US Patent No. 5957753 (1999c).
- Lakshmanan, A., "Finishing of large diameter and large batch advanced ceramic balls (Si₃N₄) for bearing applications using magnetic float polishing," M.S. thesis, Mechanical and Aerospace Engineering, Oklahoma State University, (2000).

- Liu, M. and S. Nemat-Nasser, "Microstructure of a bearing-grade silicon nitride," *Journal of Materials Research*, 14 (1999) 4621-4629.
- London, C. L., "Apparatus for low stress polishing of spherical objects," US Patent No. 4965967 (1990).
- Lynch, T. P., "Hybrid ceramic bearings increase turbine life," *Design News*, 47 (1991) 220-221.
- Messerschmidt, S., "Ball lapping device," US Patent No. 3660942 (1972).
- Messerschmidt, K., "Device for lapping balls in continuous operation," US Patent No. 3984945 (1976).
- Niizeki, S., "Ceramic bearings for special environments," *Motion & Control*, (2000) 17-22.
- O'Brien, M. J., Presser, N. and E. Y. Robinson, "Failure analysis of three Si₃N₄ balls used in hybrid bearings," *Engineering Failure Analysis*, 10 (2003) 453-473.
- Perry, B. D., "An investigation of magnetic float polishing techniques including conventional, eccentric shaft and ultrasonic assisted polishing," M.S. thesis, Mechanical and Aerospace Engineering, Oklahoma State University, (1997).
- Raghunandan, M., "Magnetic float polishing of silicon nitride balls," Ph.D. thesis, Mechanical and Aerospace Engineering, Oklahoma State University, (1996).
- Raghunandan, M. and R. Komanduri, "Finishing of silicon nitride balls for high-speed bearing applications," *Transactions of the ASME, Journal of Manufacturing Science and Engineering*, 120 (1998) 376-386.

Rao, S., "Finishing of ceramic balls by magnetic float polishing with online vibration monitoring and control," M.S. thesis, Mechanical and Aerospace Engineering, Oklahoma State University, (1999).

Ren, C. Z., Wang, T. Y., Jin, X. M. and H. Xu, "Experimental research on the residual stress in the surface of the silicon nitride ceramic balls," *Journal of Materials Processing Technology*, 129 (2002) 446-450.

Saint-Gobain Ceramics Website (www.cerbec.com).

Sato, C., "Ball lapping machine," US Patent No. 5301470 (1994).

Shinmura, T., Takazawa, K., Hatano, E. and M. Matsunaga, "Study on magnetic abrasive finishing," *Annals of the CIRP*, 39 (1990) 325-328.

Taguchi, G., *Taguchi methods: research and development*, Quality Engineering Series, Vol. 1, 1992 (ASI Press, Dearborn, Michigan).

Taguchi, G., *Taguchi on robust technology development, Bringing quality engineering upstream*, 1993 (ASME, New York).

TalyRond 250 User's Handbook, Rank Taylor Hobson, Inc.

TalySurf 120L User's Handbook, Rank Taylor Hobson, Inc.

Tani, Y. and K. Kawata, "Development of high-efficient fine finishing process using magnetic fluid," *Annals of the CIRP*, 33 (1984) 217-220.

Tonooka, K., Nojima, H. and T. Kobayashi, "Sphere polishing machine," US Patent No. 5913717 (1999).

Umehara, N., "Research on magnetic fluid polishing," PhD thesis (in Japanese), Tohoku University, (1990).

- Umehara, N. and K. Kato, "Principles of magnetic fluid grinding of ceramic balls," *Applied Electromagnetics in Materials*, 1 (1990) 37-43.
- Umehara, N. and K. Kato, "Fundamental properties of magnetic fluid grinding with a floating polisher," *Journal of Magnetism and Magnetic Materials*, 122 (1993) 428-43.
- Umehara, N. and R. Komanduri, "Magnetic fluid grinding of HIP-Si₃N₄ rollers," *Wear*, 192 (1996) 85-93.
- Umehara, N. and K. Kato, "Magnetic fluid grinding of advanced ceramic balls," *Wear*, 200 (1996) 148-153.
- Yasunaga, N., Obara, A. and O. Imanaka, "Study of mechanochemical effect on wear and its application to surface finishing, *Journal of JSPE*, 44 (1978) 77-83 (in Japanese).
- Yeckley, R. L., "Silicon nitride bearing ball having a high rolling contact fatigue life," US Patent No. 5508241 (1996).
- Yuan, J. L., Lu, B. H., Lin, X., Zhang, L. B. and S. M. Ji, "Research on abrasives in the chemical-mechanical polishing process for silicon nitride balls," *Journal of Materials Processing Technology*, 129 (2002) 171-175.
- Wang, L., Snidle, R. W. and L. Gu, "Rolling contact silicon nitride bearing technology: a review of recent research," *Wear*, 246 (2000) 159-173.
- Ziegler, G., Heinrich, J., and G. Wotting, "Relationships between processing, microstructure and properties of dense and reaction-bonded silicon nitride," *Journal of Materials Science*, 22 (1987) 3041-3086.

VITA

Tejas Kirtane

Candidate for the Degree of

Master of Science

Thesis: FINISHING OF SILICON NITRIDE (Si_3N_4) BALLS FOR ADVANCED BEARING APPLICATIONS BY LARGE BATCH MAGNETIC FLOAT POLISHING (MFP) APPARATUS

Major Field: Mechanical Engineering

Biographical:

Personal Data: Born in Mumbai, Maharashtra, India, on August 14, 1975, the son of Dr. Shrikant K. Kirtane and Dr. Manjiri S. Kirtane

Education: Received Bachelor of Engineering degree in Mechanical Engineering from Vishwakarma Institute of Technology (University of Pune), Pune, India, in July 1997. Completed the requirements for the Master of Science degree with a major in Mechanical Engineering at Oklahoma State University, Stillwater, Oklahoma in December, 2004

Experience:

- Graduate Research Assistant in Mechanical and Aerospace Engineering Department, Oklahoma State University, Stillwater, Oklahoma, May 2003 - December 2004.
- Junior Project Engineer in Vacuum Plant and Instruments Manufacturing Company Limited, Pune, India, November 1999 - March 2001
- Graduate Trainee Engineer in Sandvik Asia Limited, Pune, India, October 1997 - September 1998